Characterization of the Role of Histone Deacetylase 7 in $CD8^+$ T Cell Dependent Anti-tumor Immune Responses and T Cell Homeostasis

Inaugural-dissertation to obtain the academic degree Doctor rerum naturalium (Dr. rer. nat)

Submitted to the Department of Biology, Chemistry, Pharmacy of Freie Universität Berlin

by

Cansu Yerinde

from Istanbul, Turkey

Berlin, 2021

This work was conducted at the Department of Gastroenterology, Rheumatology and Infectious Diseases at Charité - Universitätsmedizin Berlin, Campus Benjamin Franklin under the supervision of Prof. Dr. Britta Siegmund between January 2017 and April 2021.

1st reviewer: Prof. Dr. Britta Siegmund

2nd reviewer: Prof. Dr. Gerhard Wolber

Date of defense: 19.10.2021

1. INTRODUCTION

1.1 Immunological memory and CD8$^+$ T cells in infections and cancer

The mammalian immune system functions as a defense mechanism against bacterial and viral infections, diseases and several other undesired biological invasions. In addition, it has the capability of recognizing and tolerating “the self” to prevent potential allergic reactions and autoimmune diseases. The mammalian immune defense can be broadly categorized into two types as innate and adaptive immunity. Innate immunity is the first line of defense against pathogens and mainly mediated by dendritic cells (DCs), natural killer (NK) cells and macrophages. Adaptive immunity, mediated by B and T cells, provides immunological memory and specific immune defense due to the clonal selection of a tremendous repertoire of lymphocytes possessing antigen-specific receptors (Best et al., 2013).

The concept of adaptive immunity was known since centuries, exemplified by the famous observation of Edward Jenner that milk maids exposed to cowpox were protected against smallpox (Smith, 2011). These were the initial steps of understanding the adaptive immunity and the vaccination. By the accumulation of knowledge and the rapid development of vaccines, many devastating diseases such as polio and smallpox were successfully eliminated. Vaccine technologies depend on the generation of neutralizing antibody responses (Greenwood, 2014). However, there are several diseases including human immunodeficiency virus (HIV) and malaria, in which the approach of neutralizing antibodies has not been successful yet (Nabel, 2007; Todryk and Hill, 2007). Moreover, antigenic drift in infections like influenza virus requires yearly vaccination according to the emerging new types of the virus (Kohlmeier et al., 2006). To target this kind of diseases, vaccines were modified so that their action depends on CD8$^+$ T cell-mediated immunological memory. CD8$^+$ T cells are able to recognize and react to epitopes with less strain to strain variation as well as to pathogens that do not allow themselves to be targeted by neutralizing antibodies due to their life cycles (Brown and Kelso, 2009; Kohlmeier et al., 2006; Masopust, 2008). Therefore, CD8$^+$ T cells represent the key players of immune responses against pathogens (Cosma and Eisenlohr, 2018).

Besides the infections driven by pathogen invasion, CD8$^+$ T cells also target cancer cells for elimination. Tumor-associated antigens (TAA) represent the main trigger of CD8$^+$ T cell-mediated anti-tumor responses (Gonzalez et al., 2018). The presentation of TAAs to T cells by

either major histocompatibility complex class I (MHC I) or class II (MHC II) on antigen presenting cells induces T cell activation, subsequently promoting their clonal expansion and recruitment of other types of immune cells to attack tumors, in which $CD8^+$ T cells can destroy cancer cells by direct cytotoxicity (Pluhar et al., 2015).

Despite the presence of a complex immune response against tumor cells, the formation of very large tumors in hosts suggests, that tumors are capable of immune evasion through several mechanisms (Gonzalez et al., 2018). For instance, tumor cells can downregulate MHC molecules that block TAA presentation to T cells, thus favoring their immune escape (Cornel et al., 2020). Tumor cells can also secrete immunosuppressive cytokines including interleukin (IL)-10 (Itakura et al., 2011). Similarly, regulatory T cells (Treg) in the tumor microenvironment secrete immunosuppressive cytokines IL-10 and transforming growth factor β (TGF-β), which promote the suppression of effector T cell functions and subsequent immune evasion of tumors (Plitas and Rudensky, 2020). Tumor cells can also establish new structures and physical barriers formed by collagen and fibrin to hinder themselves from immune attack. Importantly, tumor cells upregulate the expression of several inhibitory molecules such as programmed cell death protein 1 (PD-1) and cytotoxic T-lymphocyte associated protein 4 (CTLA-4) promoting self-tolerance and downregulation of anti-tumor responses against them (Gonzalez et al., 2018).

Deregulation of T-cell dependent anti-tumor immune responses due to immune evasion in tumors have promoted intense investigations leading to novel immunotherapies of cancers including adoptive T cell transfers, chimeric-antigen receptor (CAR)-engineered T-cell and checkpoint blockade therapies (Murciano-Goroff et al., 2020). Therefore, understanding the molecular regulators of $CD8^+$ T cell responses against tumors is a crucial step to improve these cancer treatment approaches.

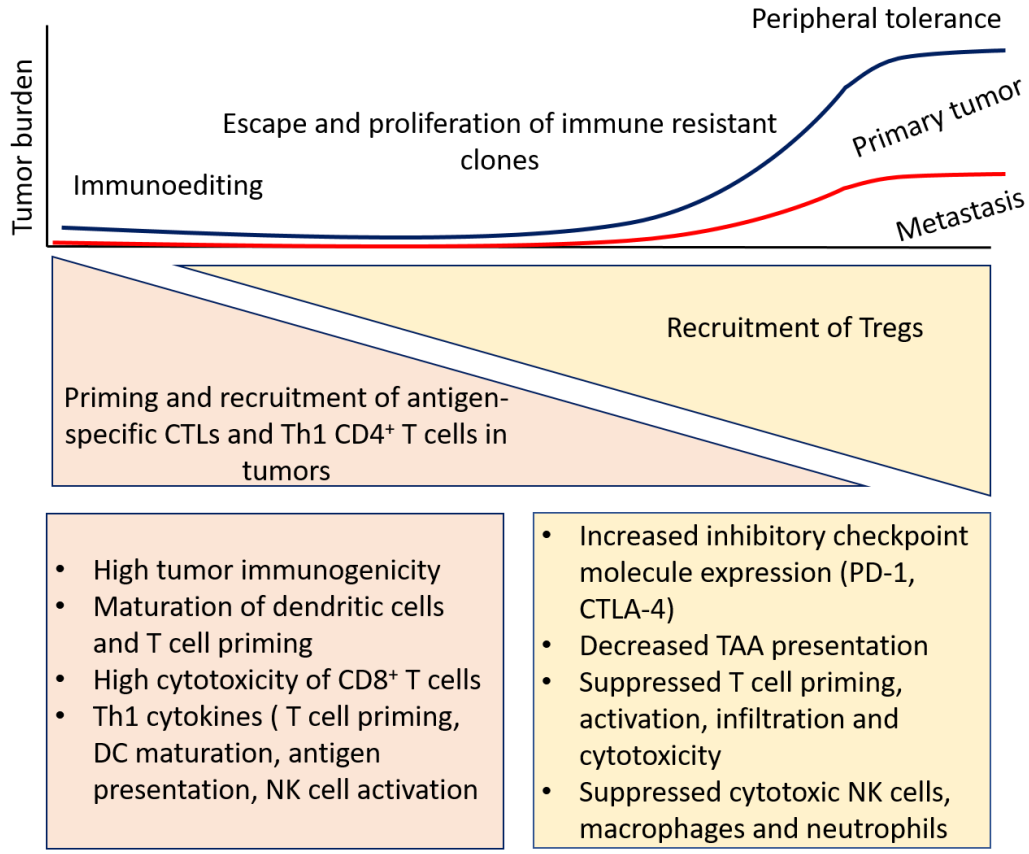

Figure 1-1 Mechanisms of immune evasion in tumors. *Tumor progression can be controlled during the early stages of tumorigenesis by different mechanisms such as the presence of cytotoxic T lymphocytes (CTLs), effector responses of Th1 cells against tumor-associated antigens (TAA), natural killer (NK) cells as well as high tumor immunogenicity. Due to the permanent selective pressure of effector responses, some tumor variants can escape resulting in their outgrowth. Multiple mechanisms such as the upregulation of checkpoint molecule expression such as programmed cell death protein-1 (PD-1) and cytotoxic T-lymphocyte associated protein-4 (CTLA-4), decreased presentation of TAA, recruitment of regulatory T cells (Tregs) and suppressed functions of NK cells contribute to the immune evasion and an uncontrolled tumor growth. Adapted from* (Gonzalez et al., 2018).

1.2 Differentiation of CD8$^+$ T cells

CD8$^+$ T cells possess unique T-cell receptors (TCR) that can recognize and bind to cognate-peptide bound MHC expressed on the surface of antigen-presenting cells such as DCs. Thanks to the vast numbers of TCRs, specific responses against numerous foreign antigens can be generated. Naïve T cells (T_N) constantly recirculate in the body and migrate to secondary lymphoid organs to meet a cognate antigen and subsequently initiate an antigen-specific response to eradicate for example pathogens (Shrikant et al., 2010). The homing process of T_N cells are facilitated via the expression of specific markers such as L-selectin (CD62L) and CC-chemokine receptor (CCR) 7. Successful retention in the secondary lymphoid organs results in the activation of CD8$^+$ T cells followed by a massive expansion of CD8$^+$ effector T cells (T_E). T_E are identified by the expression of killer cell lectin-like receptor subfamily G member 1

(KLRG1$^+$) and CD127$^-$, and they can lyse infected cells via the release of effector molecules perforin, granzyme A and B in an antigen-specific manner. In addition to these effector molecules, phagocytes and DCs produce IL-12 that facilitates the production of pro-inflammatory cytokines Interferon γ (IFNγ) and tumor necrosis factor α (TNFα) to further facilitate the eradication of the infection (Chen et al., 2018).

Once the infection is cleared, KLRG1$^+$CD127$^-$CD8$^+$ T_E cells contract, mainly regulated via apoptosis by the ratio of the expression of pro- and anti-survival proteins such as B-cell lymphoma 2 (Bcl-2), Bim and Fas, leaving behind a small population of KLRG1$^-$CD127$^+$CD8$^+$ cells, which are long-lived memory T cells (T_{mem}) that provide the immunological memory against the specific cognate antigen (Martin and Badovinac, 2018). T_{mem} are metabolically, transcriptionally and epigenetically poised to re-activation and rapid expansion in case of a secondary infection and cognate antigen re-encounter (Chen et al., 2018). Therefore, with these abilities they provide long-term protection against infections.

T_{mem} can be further categorized as central memory (T_{CM}) and effector memory (T_{EM}) CD8$^+$ T cells. T_{EM} are characterized by low expression of CD62L and CCR7 (CD62L^{lo}CCR7^{lo}), whereas T_{CM} cells are characterized by high expression of CD62L and CCR7 (CD62L^{hi}CCR7^{hi}). The expression of CD62L and CCR7 on T_{CM} cells promotes their homing into secondary lymphoid organs where they are able to rapidly expand and produce vast amounts of IL-2 against secondary infections, whereas T_{EM} express integrins and chemokine receptors providing their localization into inflammatory tissues. Thus, T_{CM} cells are specialized to control systemic infections such as lymphocytic choriomeningitis virus (LCMV) infection, whereas T_{EM} cells handle infections localized in peripheral tissues (Chen et al., 2018; Martin and Badovinac, 2018).

The effector to memory differentiation of CD8$^+$ T cells is driven by key transcription factors including T-bet and Eomesodermin (Eomes). T-bet belongs to the T-box family of transcription factors and acts as the master regulator of effector differentiation of CD8$^+$ T cells. The expression of T-bet is required for IFNγ production as well as the expression of cytolytic effector molecules such as granzyme B and perforin for the lysis of target cells (Szabo et al., 2002). T-bet also serves as a marker for short-lived effector cells characterized as KLRG1$^+$CD127$^-$ cells (Joshi et al., 2007). Eomes is similarly a member of the T-box family of transcription factors, and it has an abundant role for memory differentiation and function

(Knudson et al., 2017; Pearce et al., 2004). The expression of Eomes increases as cells differentiate into a KLRG1$^-$CD127$^+$ long-lived memory state (Takemoto et al., 2020). Both transcription factors were shown to be possess crucial roles by mediating the expression of CD122 (IL-15Rβ), which keeps CD8$^+$ T cells responsive against IL-15 that is a critical cytokine for memory differentiation. The expression of T-bet and Eomes in CD8$^+$ T cells is inversely correlated, and the sustained expression of these transcription factors governs the transcriptional programs maintaining the effector and memory phenotypes of CD8$^+$ T cells (Intlekofer et al., 2005).

1.3 Other regulators of CD8$^+$ T cell differentiation

1.3.1 Cellular metabolism

Apart from transcriptional and epigenetic programs, cell continuously regulate their metabolism in order to adapt to altered conditions and environments, therefore metabolic regulation of CD8$^+$ T cells are also tightly regulated (Metallo and Heiden, 2013). Catabolic and anabolic reactions are used to break down or synthesize macromolecules, respectively, to meet the cellular energy demands supplied in the form of adenosine triphosphate (ATP) as well as the metabolic intermediates that are dispensable for cellular growth. Two molecules of ATP and pyruvate are generated through glycolysis pathway. Under conditions in which oxygen is enriched, pyruvate enters the tricarboxylic acid (TCA) cycle. Pyruvate is metabolized further via TCA cycle and oxidative phosphorylation resulting in the generation of 38 ATP, the maximal number of ATP molecules. Substrates that are metabolized through the TCA cycle are not limited to pyruvate. Similarly, fatty acids are oxidized and converted into acetyl-coenzyme A (acetyl-CoA) via TCA cycle. Similarly, amino acids that are catabolized into 4- and 5- carbon substrates can enter this cycle (Metallo and Heiden, 2013).

The metabolic requirements of a CD8$^+$ T cell differ with respect to their differentiation state. Naïve CD8$^+$ T cells are metabolically quiescent, and they mainly harness oxidative phosphorylation. Once they are activated via their antigens, they immediately switch to glycolysis pathway which can supply the anabolic intermediates that are necessary for their rapid growth and proliferation as well as effector responses (Buck et al., 2015; Chang et al., 2013). On the contrary, memory CD8$^+$ T cells depend on oxidative phosphorylation along with an increased spare respiratory capacity that provides the high energy demand necessary for

rapid response and proliferation in case of antigen reencounter (Buck et al., 2015, 2016; Windt et al., 2011).

Besides glycolysis and fatty acid oxidation (FAO), amino acid metabolism is crucial for immune responses of T cells (Ren et al., 2017). For instance, activated T cells harness glutamine to produce cellular energy and as a nitrogen source as well as for the production of many metabolic intermediates (Howie et al., 2014). Amino acid transporters are critical for the regulation of peripheral naïve T-cell hemostasis, activation and differentiation into memory $CD8^+$ T cells (Ren et al., 2017). The effects of amino acid transporters and metabolism might be through mammalian target of rapamycin (mTOR) signaling and the regulation of autophagy (Howie et al., 2014; Jin et al., 2015; Nakaya et al., 2014; Rebsamen et al., 2016). Therefore, the manipulation of amino acid transporter-mTOR pathway could improve the treatments of inflammatory and autoimmune diseases as well as cancers associated with T-cell-mediated immune responses.

1.3.2 Mammalian Target of Rapamycin

mTOR is a kinase regulating the metabolism, cell survival and energy status of the cells. It has a central role to sense nutrient availability and energy status of the cells, subsequently regulating their survival and growth (Jones and Pearce, 2017). The crucial role of the mTOR pathway with regard to differentiation and function of several types of immune cells including $CD8^+$ T cells has been recently characterized (Pollizzi and Powell, 2015).

The role of mTOR with regard to differentiation and function of $CD8^+$ T cells has been intensively studied in terms of its connection to the cellular metabolism and memory differentiation of $CD8^+$ T cells (Jones and Pearce, 2017). For instance, mTOR inhibition in $CD8^+$ T cells by rapamycin treatment promotes central memory differentiation of $CD8^+$ T cells (Pearce et al., 2009; Xu et al., 2014). This switch of $CD8^+$ T cells into memory state was attributed to the catabolic FAO and autophagy. In line with these observations, deletion of tuberous sclerosis 2 (TSC2), which results in constitutively active mTOR, promotes the differentiation of $CD8^+$ T cells into effector phenotype as well as a failure in memory differentiation that is marked by increased glycolysis (Pollizzi et al., 2015). Conversely, the genetic deletion of Ras homolog enriched in brain (Rheb), which blocks the activity of mTOR, interferes with effector differentiation of $CD8^+$ T cells and promotes their memory

differentiation. However, these memory cells were not capable of differentiating into secondary effector cells upon antigen reencounter (Pollizzi et al., 2015).

mTOR is present in cells within two different complexes, namely, mTORC1 and mTORC2. The interaction partners of mTOR determine these complexes. Within the mTORC1 complex, mTOR interacts with Raptor, whereas it interacts with Rictor in the mTORC2 complex (Zoncu et al., 2011). To understand the role of mTOR in the differentiation of memory $CD8^+$ T cells, mTORC1 and mTORC2 should be studied separately since they act through different intracellular pathways. For instance, the inhibition of mTORC2 activity through the genetic deletion of Rictor promotes long-lived cells which have more potent memory characteristics than conventional memory $CD8^+$ T cells (Pollizzi et al., 2015). This phenotype results from the increased expression of the rate limiting enzyme carnitine palmitoyltransferase 1a (CPT1A) in FAO as well as the spare respiratory capacity, which are the metabolic characteristics of memory $CD8^+$ T cells (Windt et al., 2011). However, the effects of genetic ablation of mTORC2 can be attributed to its function to block the forkhead box (FOXO)-mediated expression of IL-15 that is dispensable for memory differentiation by promoting FAO. These results offer that inhibitors which can specifically block mTORC2 hold potential to improve memory responses of $CD8^+$ T cells without any impairment in their effector functions.

1.3.3 Store-Operated Calcium Entry

Calcium release-activated channels (CRAC) are the main mediators of cellular calcium influx and have fundamental roles in several non-excitable cell types including T cells (Bergmeier et al., 2013). CRAC are mainly activated through Store-Operated Calcium Entry (SOCE). The TCR stimulation of T cells results in the activation of phospholipase Cγ and Cβ, respectively and the subsequent release of the second messenger inositol-1-4-5-triphosphate ($InsP_3$). $InsP_3$ binds its receptor, located on the membrane of endoplasmic reticulum (ER) resulting in its opening and depletion of the Ca^{2+} stores. Stromal interaction molecule (STIM) 1 and STIM2 are single-pass transmembrane proteins and are located on the ER membrane (Liou et al., 2005; Roos et al., 2004). They are capable of sensing the reduction of Ca^{2+} levels in ER through their paired N-terminal EF-hand Ca^{2+} binding domain positioning in ER luminal. The dissociation of Ca^{2+} from EF-hand domains of STIM1 leads to its subsequent oligomerization and translocation to ER plasma membrane junctions where they establish large clusters of STIM1 puncta (Luik et al., 2006). Later, Orai1 calcium release-activated calcium modulator 1 (ORAI1) proteins are

recruited via STIM1 proteins to these puncta followed by opening of CRAC and subsequent Ca^{2+} influx into the cell (Prakriya et al., 2006; Yeromin et al., 2006). Although STIM2, the homolog of STIM1, mediates this process similarly, the activation of STIM2 is slower in terms of kinetics which results in weaker depletion of ER Ca^{2+} stores (Brandman et al., 2007). Therefore, despite the presence of several mediators of CRAC channels, STIM1 and ORAI1 can be considered as the key molecular regulators of SOCE and subsequent CRAC function.

The observation that patients with severe immunodeficiency syndromes harbor mutations in the main components of SOCE such as *ORAI1* and *STIM1* genes highlighted the critical role of this Ca^{2+} influx pathway for the immune cell function (Feske, 2011, 2009). Patients with impaired SOCE signaling were more susceptible to chronic and recurrent infections such as cytomegalovirus (CMV), Epstein Barr virus (EBV) and human herpes virus (Byun et al., 2010). Both adaptive and innate immunity of the patients were impaired due to *ORAI1* and *STIM1* mutations. Until now, several mutations were characterized in *ORAI1* and *STIM1*, all of which result in T cell dysfunction. Since *ORAI1*- and *STIM1*-mutant patients suffer from a similar form of immunodeficiency, this syndrome was called “CRAC channelopathy” further emphasizing the critical role of deterred SOCE pathway in the pathogenesis of the disease. The phenotypes of these patients demonstrated that SOCE is dispensable for the activation of T cells as well as their survival and resistance to activation-induced cell death (AICD).

In addition to the CRAC channelopathy patients, studies using transgenic mice also allowed to characterize the role of SOCE in T cell function in more detail. For instance, mice with T cell specific deletion of *Stim1* were more prone to develop acute and chronic tuberculosis upon challenge with *Mycobacterium tuberculosis* (Mtb) since mice with defective SOCE signaling were characterized by higher bacterial burden and pulmonary infection eventually reduced survival compared to wild type (wt) mice (Desvignes et al., 2015). During the chronic phase of infection, *Stim1*-deficient $CD4^+$ and $CD8^+$ T cells were shown to have impaired AICD upon stimulation with repeated TCR engagement resulting in increased pulmonary lymphocytosis and hyperinflammation (Desvignes et al., 2015). Therefore, SOCE has crucial roles to handle bacterial infections consistent with the phenotypes of immunodeficient CRAC channelopathy patients.

Similarly, simultaneous conditional deletion of *Stim1* and *Stim2* in T cells in mice proved that SOCE controls immunity against acute LCMV infection as well as the maintenance of virus-

specific memory $CD8^+$ T cells since abolished SOCE resulted in the impaired formation of $KLRG1^-CD127^+$ long-lived memory $CD8^+$ T cells promoting higher viral load in SOCE-deficient mice (Shaw et al., 2014). The cytotoxic capacities, survival as well as the pro-inflammatory cytokine production of LCMV-specific SOCE-deficient $CD8^+$ T cells were also impaired as assessed by *in vitro* and adoptive T cell transfer experiments (Shaw et al., 2014).

The crucial roles of SOCE in T cells during bacterial and viral infections suggested that SOCE could also be important for tumor immune surveillance. Thus, conditional deletion of *Stim1* and its homologue *Stim2* in murine T cells resulted in impaired tumor growth of melanoma and adenocarcinoma tumors (Weidinger et al., 2013). Adoptive $CD8^+$ T cell transfer experiments showed that pharmacologic inhibition of SOCE by CRAC channel inhibitor BTP2 treatment did not interfere with the homing capacities of $CD8^+$ cytotoxic T lymphocytes (CTLs) into tumors or tumor draining lymph nodes. However, simultaneous transfer of wt or double knockout (DKO) CTLs and B16-Ova melanoma cells into congenically marked mice showed that SOCE was essential for the prevention of tumor engraftment in the mice since the transfer of DKO CTLs could not rescue the mice from tumor formation. Both genetic deletion and pharmacologic inhibition of SOCE impaired the cytotoxic killing capacities of CTLs as assessed by *in vitro* co-culture experiments with tumor cells. SOCE-deficient CTLs have impaired degranulation and pro-inflammatory cytokine production including IFNγ and TNFα, thus deterred anti-tumor immunity (Weidinger et al., 2013).

The calmodulin-regulated phosphatase calcineurin is the target of immunosuppressant drugs such as cyclosporin A and FK506, which inhibit the proliferation and pro-inflammatory cytokine production of T cells (Müller and Rao, 2010). The main regulator of calcineurin activity is free cytosolic Ca^{2+} which is mainly provided by SOCE signaling in T cells. However, how SOCE and its downstream targets calcineurin and nuclear factor of activated T-cells (NFAT) pathway contribute to T cell proliferation was not clearly known until recently. Vaeth et al. showed that SOCE and calcineurin control T cell proliferation by regulating their cellular metabolism (Vaeth et al., 2017). More specifically, genetic deletion of *Stim1* and *Stim2* in T cells and subsequent inactivation of calcineurin and NFAT activities result in impaired aerobic glycolysis of T cells by the deregulated expression of glucose transporter molecules Glut1 and Glut3 interfering with glucose uptake by these cells (Vaeth et al., 2017). They also showed that SOCE was required for TCR-induced AKT-mTOR pathway and the blockade of SOCE signaling

results in defective metabolism and proliferation of T cells (Vaeth et al., 2017). Therefore, SOCE does not only control metabolism and proliferation of T cells through calcineurin and NFAT signaling, but it also regulates additional mechanisms such as mTOR pathway meaning that SOCE is a central regulator of T cell function, proliferation and metabolism. The critical roles of SOCE during bacterial and viral infections as well as anti-tumor immunity suggest that understanding the regulators of SOCE is crucial to develop new therapies of immune diseases and cancer.

1.4 $CD8^+$ T cells in tumor microenvironment

Tumor microenvironment represents a highly complex ecosystem in terms of the presence of many different cell types. Apart from tumor cells themselves, tumor microenvironment is composed of stromal cells and extracellular matrix, endothelial cells and tumor vasculature as well as several types of immune cells (Giraldo et al., 2019). Immune cell population of tumor microenvironment includes $CD8^+$ T cells and NK cells with anti-tumor functions, DCs and B cells that prime and educate T cells, as well as anti-inflammatory M2 macrophages, myeloid-derived suppressor cells (MDSC) and Treg which promote tumor proliferation and growth, immunosuppression and angiogenesis, and therefore the tumor metastasis (Giraldo et al., 2019; Gonzalez et al., 2018).

$CD8^+$ T cells are the key players of immunity against tumor cells by recognizing tumor-specific or TAA and the subsequent release of cytotoxic molecules or pro-inflammatory cytokines. Therefore, before $CD8^+$ T cells exert their effects against tumor cells, they have to be primed and educated with tumor-specific or TAA presented by DCs (Giraldo et al., 2019). Although it was traditionally known that the activation of $CD8^+$ T cells is taking place in secondary lymphoid organs, it has recently been appreciated that within tumors the priming of $CD8^+$ T cells by antigen-presenting cells occurs within tertiary lymphoid structures (TLS) present in the tumors (Engelhard et al., 2020). TLS are specialized regions that are protected from immunomodulatory effects of tumor-stromal or other anti-inflammatory cell types. Moreover, TLS regions are enriched for T cell activating cytokines, thus anti-tumor functions of $CD8^+$ T cells in the tumor microenvironment are regulated within these regions. T cell infiltration as well as the presence of TLS regions within tumors correlate with better disease outcome and better prognosis of many solid tumor cancers including colorectal cancer, melanoma as well as ovarian cancers.

1.5 The fate of CD8$^+$ T cells in tumor microenvironment: CD8$^+$ T cell dysfunction and exhaustion

CD8$^+$ T cells that represent an abundant population of immune cell infiltrates in tumors, are present as naïve, effector and memory cells in this microenvironment. As naïve CD8$^+$ T cells meet their specific tumor-expressed antigens, they are activated, and gain effector functions followed by the contraction and formation of tumor-specific memory cells. However, there exists several confounding factors that interfere with this process resulting in the impairment of CD8$^+$ T cell functions within tumor microenvironment. T cell dysfunction and exhaustion in tumor microenvironment was defined as a unique feature of many cancers, thus several hallmarks of T cell dysfunction and exhaustion were defined. In tumor microenvironment, continuous antigen exposure of CD8$^+$ T cells to either tumor-specific antigens or TAA results in an anergic phenotype of these cells (Schietinger and Greenberg, 2014). Dysfunctional CD8$^+$ T cells in tumors are characterized by the loss of their main functions such as effector responses, pro-inflammatory cytokine and effector molecule production, thus cytotoxic function as well as their proper proliferation. Besides, CD8$^+$ T cells in tumor microenvironment with dysfunctional or exhausted phenotype express sustained and high levels of several inhibitory receptors including PD-1, T cell immunoglobulin and mucin-domain containing-3 (Tim-3), CTLA-4, lymphocyte-activation gene 3 (Lag-3) and T cell immunoreceptor with Ig and ITIM domain (Tigit). Furthermore, dysfunctional and exhausted CD8$^+$ T cells have deregulated transcriptional, epigenetic as well as metabolic programs (Schietinger and Greenberg, 2014; Yerinde et al., 2019; Zhang et al., 2020).

With the increasing knowledge on tumor microenvironment composition and the crucial role of immune infiltrates to handle tumorigenesis, there were several attempts to treat cancer with immunotherapy approaches. These immunotherapy strategies are not restricted to, but include the adoptive transfer of TILs, adoptive transfer of peripheral blood derived T cells, CAR-engineered T cells as well as TCR-engineered T cells (Schietinger and Greenberg, 2014; Yerinde et al., 2019; Zhang et al., 2020). However, the success of such immunotherapy methods was limited since durable responses could not been achieved due to the fact that T cell dysfunction and exhaustion interrupt their expected responses and functions in the tumor microenvironment. Nevertheless, recent checkpoint blockade therapies, which aim to hinder inhibitory receptors that are highly expressed by exhausted CD8$^+$ T cells including anti-PD-1/-

PD-L1, anti-CTLA-4 or their combination have been more effective against cancers (Dougan et al., 2019). Hence, understanding the mechanism and the regulators of T cell dysfunction and exhaustion in tumors is a very important step to improve current therapies and overcome their limitations.

1.6 Histone deacetylases with a focus on class IIa

1.6.1 Lysine acetylation of histones and non-histone proteins

Post-translational acetylation of lysine residues on proteins represents one of the essential mechanisms in eukaryotic cells to control numerous cellular processes. Although lysine acetylation was initially discovered as a specific modification of histones (Strahl and Allis, 2000; Struhl, 1998), nonhistone proteins are similarly acetylated in almost every cellular compartment. Therefore, lysine acetylation is a major post-translational modification crucial for gene regulation, cell signaling as well as metabolic regulation (Choudhary et al., 2014; Duan and Walther, 2015). Thus, the deregulation of this crucial posttranslational modification causes the development of several diseases.

More specifically, lysine acetylation is the transfer of an acetyl group to the primary amine in the ε-position of the lysine side chain of a protein, which leads to the neutralization of positive electrostatic charge at the specific acetylated position. Acetyl-CoA, which is a central metabolite and signal transducer, is the only source for acetyl groups in cells (Pietrocola et al., 2015).

Although acetylation can also occur via nonenzymatic processes (Santo-Domingo and Demaurex, 2012), it mainly takes place via the counteracting balance of enzymatic activities. Therefore, histone acetyltransferases (HATs) mark the proteins with acetylation, while histone deacetylases (HDACs) reverse these marks by removing acetyl groups. These codes regulated by HATs and HDACs are recognized by so called “reader” proteins which possess specific acetyl-lysine binding domains that are mainly bromodomains. Hence, the complex co-action of writers, erasers and readers of lysine acetylation represents one of the key cellular mechanisms for the regulation of epigenomic and metabolic processes as well as other critical cellular functions (Ali et al., 2018).

Histone acetylation is the best characterized acetylation event. Nucleosomes that are wrapped with DNA represent the basic subunit of chromatin. Core nucleosomes compromise

histone variants as H2A, H2B, H3 and H4. Acetylation occurs mainly on the lysine residues of N-terminal tails of histones protruding from nucleosomes. The sites for acetylation on histones are well conserved among species compared to the other post-translational events such as methylation, thus representing a universal mechanism for the regulation of gene expression in mammalian cells (Marmorstein and Zhou, 2014). Thereby, lysine acetylation on histone tails disrupts the electrostatic interaction between negatively charged phosphodiester backbone of DNA and nucleosomes making them loose and more available for the DNA transcription machinery and increased gene expression at the target sites of lysine acetylation. Hence, along with other posttranslational modifications of histones, lysine acetylation of histone tails contributes to the "histone code" which is a very dynamic mechanism for the regulation of mammalian gene expression (Marmorstein and Zhou, 2014).

Although enzymes mediating lysine acetylation are called "histone" acetyltransferases and deacetylases since histones were their first target that were discovered, lysine acetylation can also target other types of nuclear proteins including well known transcription factors p53, nuclear factor-κB (NF-κB) and signal transducer and activator of transcription 3 (STAT3) (Roy, 2005; Brooks and Gu, 2011; Chen et al., 2001; Wang et al., 2016; Zhuang, 2013). Acetylation of transcription factors can mediate their nuclear translocation, stabilization, prevention of ubiquitination by hindering acetylation sites as well as changing the composition of molecular complexes they are in. Similar to transcription factors, RNA polymerase complex II and the basal transcription machinery can also be acetylated although little is known about this mechanism (Boija et al., 2017; Choudhary et al., 2009; Muth et al., 2001). In addition to the nuclear proteins, cytoplasmic proteins can be similarly acetylated contributing to their stability and aggregation in the cytoplasm. For instance, tubulin is the first protein identified as a cytoplasmic protein that is acetylated (Hubbert et al., 2002; North et al., 2003). Heat shock protein 90 (HSP90) as well as microtubule-associated proteins are other well-characterized cytoplasmic targets of lysine acetylation (Jiménez-Canino et al., 2016; Kovacs et al., 2005). Similarly, mitochondrial proteins are also acetylated contributing to the regulation of cellular metabolism (Ali et al., 2018).

Acetylation of lysine residues are catalyzed by 21 different putative acetyl transferases. Depending on their homologies to yeast proteins and their biochemical functions, the well-characterized catalyzers of lysine acetylation are grouped into three main families as GCN5-

related N-acetyltransferases (GNAT), p300/CREB binding protein (p300/CBP) and MOZ, Ybf2, Sas2 and Tip60 (MYST) families. TBF-associated factor 250 kd (TAFII250, KAT4), α-tubulin acetyltransferase (αTAT1), circadian locomotor output cycles protein kaput CLOCK (KAT13D) as well as nuclear receptor coactivator 1 (NCoA-1) are the other proteins with acetyltransferase activity, however they are not members of the acetyltransferase families mentioned above (Marmorstein and Zhou, 2014).

1.6.2 Histone deacetylases

HDACs can be grouped according to their homology to yeast homologs as zinc-dependent Rpd3/Hda1 and NAD^+-dependent silent information regulator 2 (Sir-2) or Sir2-like protein (Sirtuin) family of HDACs (Yang and Seto, 2008). Zinc-dependent Rpd3/Hda1 family represents the classical family of HDACs, and it contains 11 members which can be further subdivided into three groups as class I, class II and class IV depending on their sequence similarity as well as phylogenetic analysis. Class II HDACs are further categorized as class IIa and class IIb (De Ruijter et al., 2003).

With the rapidly increasing knowledge in the chromatin field and the dispensable roles of HDACs in chromatin organization as well as their dual functions for regulating non-histone proteins and transcription factors, HDAC research expanded tremendously since their discovery. Moreover, HDAC inhibitors hold promise for the treatment of oncological as well as non-oncological diseases.

1.6.2.1 Classification of histone deacetylases

Class I HDACs

Class I family of HDACs is composed of HDAC1, HDAC2, HDAC3 and HDAC8. HDAC1 is the first HDAC that was discovered, therefore class I HDACs represent the founding members of HDACs. Class I HDACs possess an N-terminal catalytic domain with deacetylase activity, and a C-terminal domain both of which are highly conserved in eukaryotic cells (Marmorstein and Zhou, 2014; Sengupta and Seto, 2004). Besides the conserved and almost identical N-terminal catalytic domain, HDAC1 and HDAC2 are homologous for their C-terminal tail possessing tandem casein kinase 2 (CK2) phosphorylation sites. HDAC3 is slightly different from HDAC1 and HDAC2 since it harbors only one CK2 phosphorylation site on C-terminus (Zhang et al., 2005), while HDAC8 has conserved motifs for protein kinase A (PKA) phosphorylation on its C-

terminal tail which negatively regulates its catalytic activity (Lee et al., 2004; Vannini et al., 2004).

All class I members, except HDAC8, can function as the catalytic subunits of multiprotein complexes, thus HDAC1 and HDAC2 interact with each other and forms the catalytic subunits of complexes including mammalian Sin3, nucleosome remodeling deacetylase (NuRD) and corepressor of RE-1 silencing transcription factor (CoREST) (Grozinger and Schreiber, 2002). Multiprotein complexes with the core deacetylase activities can interact with sequence-specific transcription factors leading to the suppression of gene expression at the target site as well as shaping the epigenetic landscapes by cooperating with other chromatin-modifying enzymes. Similarly, some subunits of these multiprotein complexes can bind to chromatin directly resulting in its remodeling. Therefore, deacetylase activities of HDAC1 and HDAC2 are synergistic with additional chromatin modification mechanisms further contributing to the regulation of epigenetic programs (Grozinger and Schreiber, 2002).

Class IIa HDACs

Class IIa HDACs comprise HDAC4, HDAC5, HDAC7 and HDAC9, which differ from class I HDACs in several aspects. Class IIa HDACs harbor unique motifs for myocyte enhancer factor 2 (MEF2) and 14-3-3 binding on their N-terminal tail (Verdin et al., 2003). Class IIa HDACs can localize in nucleus as well as cytoplasm depending on the cellular context since they possess intrinsic nuclear localization and nuclear export signals providing a dynamic nucleocytoplasmic shuttling. This feature of class IIa HDACs allows for their interaction with different cytoplasmic and nuclear partners contributing to their diverse roles in the cellular processes and defining them as crucial signal transducers (Nurd, 2001).

Another distinguishing feature of class IIa HDACs is that they have minimal or no catalytic activity compared to class I HDACs due to the substitution of tyrosine, which stabilizes the transition state of the deacetylase activity, to histidine (Y976H) within their catalytic domain (Lahm et al., 2007; Moreth et al., 2007). Consistently, mutant HDAC4 with H976Y mutation promotes a rescue of catalytic activity which shows comparable deacetylase activity with class I HDACs. Since class IIa HDACs do not possess deacetylase activity, they rather represent acetyl lysine readers and perform their transcriptional repressor functions through large multiprotein complexes. Thus, they take place in multiprotein complexes such as HDAC3 and

N-CoR/SMRT and shape the chromatin structure via the catalytic functions of other HDACs (Fischle et al., 2002).

Class IIb HDACs

The nuclear roles of class IIa HDACs are well established, although little is known about their cytoplasmic functions. However, the role of HDAC6, which is a class IIb HDAC member, in the regulation of the functions of cytoplasmic proteins has been studied in detail. HDAC6 is predominantly found in the cytoplasm, suggesting that its main function is not related to histone acetylation and gene regulation (Boyault et al., 2007). For instance, HDAC6 regulates cell motility by deacetylating α-tubulin, cortactin and HSP90 as well as cell adhesion, immune synapse formation and cilia assembly (Boyault et al., 2007; Gao et al., 2007; Kovacs et al., 2005, 2005b). HDAC6 also plays a role in cellular processes including aggresome formation, stress response and autophagy through its ubiquitin Zn-finger binding domain (ZnF) (Kawaguchi et al., 2003).

Class IV HDACs

HDAC11, which is the only member of class IV HDACs, shows sequence similarity to both class I and class II HDACs. It is a highly conserved HDAC whose function and regulation have not been intensively studied. However, it has been shown that HDAC11 regulates IL-10 expression and immune tolerance in antigen presenting cells (Villagra et al., 2009).

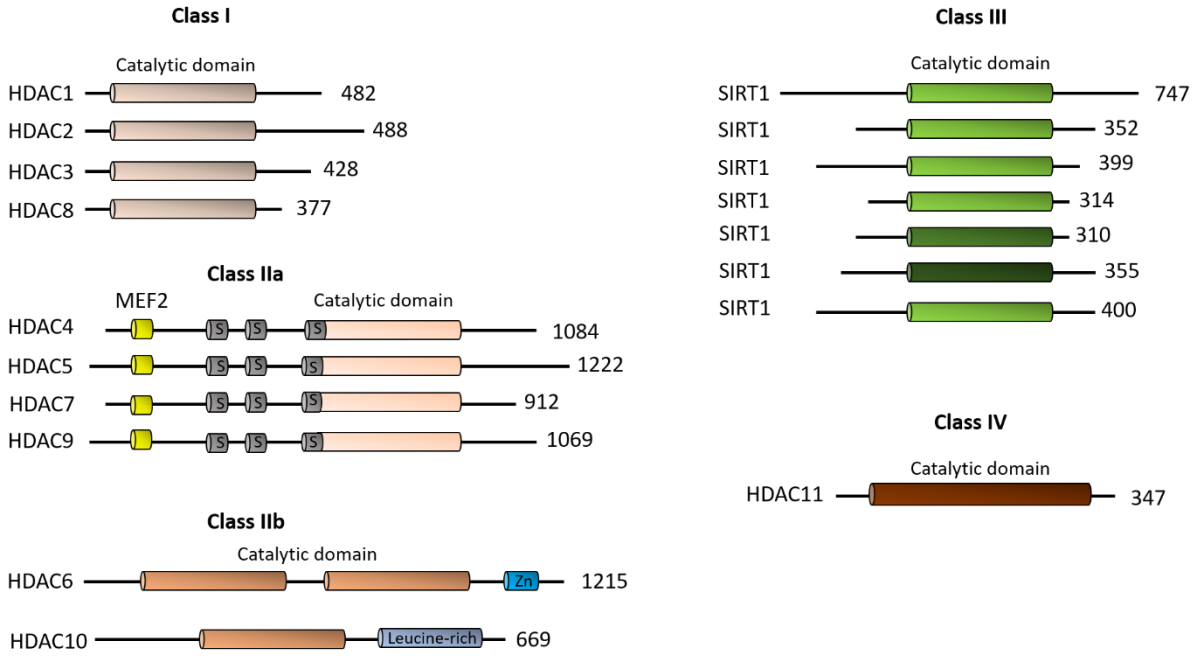

Figure 1-2 Classification of human histone deacetylases and their domain organization*. Histone deacetylases (HDACs) are grouped into four main classes as class I, class II, class II and class IV. Class II HDACs are further sub-grouped into class IIa and class IIb. Zn-dependent class I, class II and class IV HDACs represent the classical HDAC families with their homology to yeast Rpd3/Hda deacetylases, while NAD^+-dependent class III are non-classical HDACs with their homology to yeast Sirtuin. Class IIa HDACs harbor conserved serine residues as phosphorylation sites as well as myocyte enhancer factor 2 (MEF2) binding site on their N-terminus, while their catalytic domains with deacetylase activity are located on their C-terminal tail. Numbers on the right of each scheme represent the amino acid numbers of each HDAC member. Adapted from* (Park and Kim, 2020)

1.6.3 Control of class IIa HDAC functions

Subcellular localization

The functions of class IIa HDACs are controlled at multiple layers. The regulation of their subcellular localization represents one of the mechanisms controlling their activity (Di Giorgio and Brancolini, 2016). Due to this feature of class IIa HDACs, they have the ability to quickly respond to changing cellular conditions and environment by the regulation of their redistribution within the cells. Class IIa HDACs accumulate in the nucleus upon dephosphorylation which allow them to associate and form a multiprotein complex with HDAC3 and N-CoR/SMRT with deacetylase activity resulting in chromatin remodeling (Di Giorgio and Brancolini, 2016).

Phosphorylation is the key event that regulates the subcellular localization of class IIa HDACs. This post-translational modification determines the availability of the nuclear localization signal for importin-α as well as nuclear exclusion signal from chromosomal maintenance 1 (CRM1) (Di Giorgio and Brancolini, 2016). Although calcium/calmodulin-dependent kinase (CaMK) II is the first kinase that was discovered regulating the nuclear exclusion of class IIa

HDACs, several additional kinases were identified facilitating the same process (McKinsey et al., 2000). Kinases that phosphorylate class IIa HDACs can be grouped into CaMKs, protein kinase D (PKD), salt-inducible kinases (SIK), checkpoint kinase-1 (CHK1) and microtubule affinity regulating kinases (Backs et al., 2008; Dequiedt et al., 2005; Walkinshaw et al., 2013). However, the regulation of subcellular distribution of class IIa HDACs is a more complex mechanism since several phosphatases including protein phosphatase 1 (PP1) and protein phosphatase 2A (PP2A) induce their nuclear import (Kozhemyakina et al., 2009; Martin et al., 2008). Three different conserved serine residues are present on the N-terminal tail of class IIa HDACs, with the exception of HDAC7 which has four residues. Once these sites are phosphorylated, they allow the association of class IIa HDACs with the dimers of 14-3-3 chaperons resulting in nuclear exclusion. 14-3-3 binding is able to facilitate nuclear exclusion by different ways. It can either hinder the nuclear localization signal which block the nuclear import or making nuclear exclusion signal more available for a direct interaction with CRM1 (Grozinger and Schreiber, 2000; Kozhemyakina et al., 2009; Nishino et al., 2008).

The tight regulation of subcellular localization of class IIa HDACs contributes to important physiological processes. From an immunological point of view, PKD, which is a serine/threonine kinase activated by PKC, is related to lymphocyte maturation and thymic selection as well as B-lymphocyte activation upon B cell receptor (BCR) stimulation (Dequiedt et al., 2005; Matthews et al., 2006; Parra et al., 2005). For instance, MEF2-mediated epigenetic program is blocked in resting double positive $CD4^{+}CD8^{+}$ thymocytes due to the nuclear accumulation of HDAC7. TCR activation upon antigen stimulation results in the activation of PKD1 kinase, which in turn phosphorylates HDAC7 and its subsequent nuclear export. Thereby, MEF2 is relieved from its co-repressor and induces the expression of its direct target the proapoptotic nuclear receptor *Nur77*, leading to the negative selection of double positive thymocytes via apoptosis (Dequiedt et al., 2005).

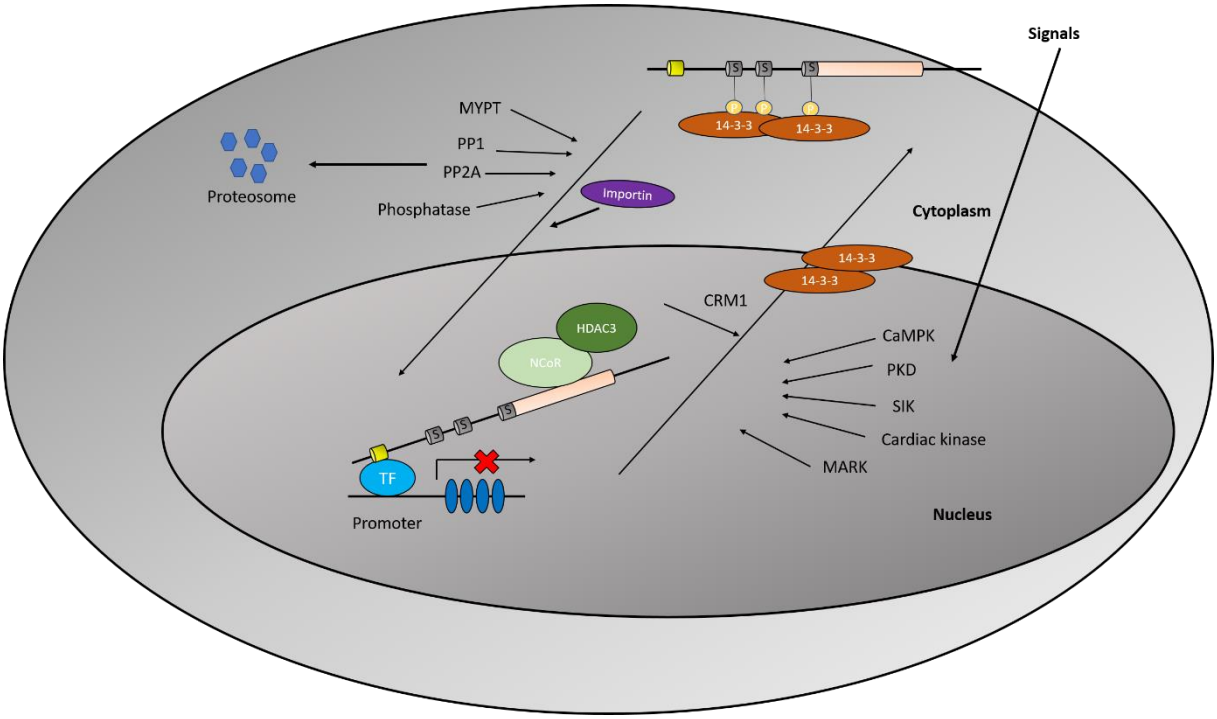

Figure 1-3 Class II HDAC regulation*. Several intra- or extracellular signals induce the serine residue-phosphorylation of class IIa HDAC on its adaptor domain by various kinases such as cyclic AMP receptor kinase (cAMPK), protein kinase D (PKD), salt-inducible kinase (SIK), cardiac kinases and microtubule associated protein (MAP)-microtubule regulating protein kinase (MARK). Phosphorylation events leads to the dissociation of class IIa HDAC from its co-repressor complex and its subsequent cytoplasmic localization via a chromosomal maintenance 1 (CRM1)-dependent pathway by facilitating its association with 14-3-3 dimers resulting in the expression of its target genes. In the cytoplasm, class II HDAC dissociates from 14-3-3 dimers by unknown mechanisms and dephosphorylated by several phosphatases including protein phosphatase (PP)-1, PP2A and the myosin phosphatase targeting (MYPT) protein. Dephosphorylated class IIa HDAC might be more prone to degradation in proteasome. Nuclear import of class IIa HDAC results in its re-association with its-corepressor complex and subsequent suppression of the target gene expression. Adapted from* (Martin et al., 2007)

Transcriptional control

Although the regulation of subcellular localization of class IIa HDACs is a key and dispensable mechanism mediating their diverse functions, it does not represent the only mechanism controlling their actions.

Class IIa HDACs are well characterized for their tissue-specific expression and their important roles during development. However, very little is known about their transcriptional regulation. Class IIa HDACs possess multiple transcriptional variants (Di Giorgio and Brancolini, 2016). Concerning HDAC7, two different isoforms have been characterized as a non-spliced isoform retaining the first intron following the first start codon and the most common and spliced isoform containing 25 exons. It was shown that these two isoforms of HDAC7 differentially regulate cellular proliferation. The generation of these two HDAC7 isoforms is tightly regulated during the differentiation of vascular smooth muscle cells (Margariti et al., 2009; Zhou et al., 2011a).

Mithramycin is an antibiotic with anti-neoplastic properties interfering with RNA synthesis by binding to GC-rich sequences and it can inhibit the expression of HDAC4 by removing the specificity protein (Sp) family of transcription factors (Sleiman et al., 2011). Indeed, electro mobility shift assays (EMSA) and chromatin immunoprecipitations (ChIP) proved that Sp1 and Sp2 transcription factors directly bind to the promoter of HDAC4 and control its mRNA expression, further supported by experiments in which Sp1 and Sp2 expression was genetically manipulated (Theos et al., 2005). Similar to HDAC4, Sp1 also controls the expression of HDAC7 by inducing its expression during platelet-defined growth factor BB monomer (PDGF-BB)-driven differentiation of murine embryonic stem cells into smooth as well as vascular smooth muscle cells (Zhang et al., 2010; Zhou et al., 2011b). Another example of HDAC7 mRNA regulation is during the differentiation of pre-B cells into macrophages (Barneda-Zahonero et al., 2013). While HDAC7 is expressed at high levels in pre-B cells, its expression is profoundly reduced in macrophages (Barneda-Zahonero et al., 2013). Although the role of HDAC7 for repressing the MEF2-target genes, which are dispensable for the functions of macrophages, is well characterized, it is still an open question how HDAC7 expression is regulated through this differentiation process.

During muscle differentiation, the expression of class IIa HDACs are upregulated which acts a negative-feedback loop determining the rate of differentiation. Interestingly, the upregulation of HDAC9 is induced by different isoforms of MEF2 transcription factors including MEF2A, MEF2C and MEF2D where they directly bind to the promoter of HDAC9 promoting its expression (Haberland et al., 2007). Nevertheless, the potential role of MEF2 transcription factors for inducing the expression of the other class IIa HDACs has not been proven yet. It is also proposed that MEF2-dependent upregulation of class IIa HDACs can contribute to certain compensatory mechanisms. In different cell lines, the depletion of one class IIa HDAC promotes the increased expression of another class IIa member. This redundancy is suggested to be the result of a MEF2-driven mechanism since once MEF2 is relieved from its co-repressor, it subsequently induces the expression of another HDAC by directly binding to the regulatory regions such as distal promoter for HDAC5 and HDAC9 or enhancers for HDAC4 and HDAC7 (Clocchiatti et al., 2015, 2013; Mihaylova et al., 2011).

Even though we still lack the complete knowledge on the transcriptional control of class IIa HDAC expression, the ENCODE project which provides ChIP-seq data on different cell lines can

provide insights about potential transcription factors and epigenetic regulators playing a role in class IIa HDAC expression (Di Giorgio and Brancolini, 2016). As mentioned above, ChIP-seq data retrieved from the ENCODE project confirm the binding of MEF2 to HDAC5 and HDAC9 promoters. Both proximal and distal promoters of HDAC4 and HDAC7 are occupied by several transcription factors and epigenetic regulatory proteins, suggesting that the expression of these two class IIa HDAC members is tightly controlled. On the contrary, promoters of HDAC5 and HDAC9 are not under such a high supervision (Di Giorgio and Brancolini, 2016). Consistent with the previous role of HDAC4 and HDAC7 during oncogenic transformation, transcription factors with proto-oncogenic functions control cell cycle progression including Fos proto-oncogene (FOS), Myc proto-oncogene (MYC), Jun proto-oncogene (JUN) bind to the proximal promoters of these class IIa HDAC members. According to ENCODE ChIP-seq data, six different transcriptional regulators bind to the promoters of all class IIa HDACs. While three of them (Pol2, TAF1, TBP) are related to general transcriptional machinery, the others are SP1, Myc-associated factor X (MAX) and yin and yang 1 (YY1) (Di Giorgio and Brancolini, 2016). YY1 is known to bind to promoters near transcription start sites of highly expressed genes. ChIP-seq data further confirmed the binding of SP1 as described in previous studies. The binding of MAX and YY1, which are interaction partners of MYC, to promoters of class IIa HDACs suggest their involvement in the Myc transcription network (Vella et al., 2012).

Proteolysis and massive degradation

The activities of class IIa HDACs can also be regulated through their selective proteolytic processing. For example, during apoptosis HDAC4 and HDAC7 are cleaved by caspase 3 and caspase 8, respectively, resulting in an increased apoptosis rate and thus representing another mechanism controlling class II HDAC functions (Paroni et al., 2004; Scott et al., 2008).

Similarly, class IIa HDAC activities are controlled via ubiquitin proteasome system (UPS) by regulating their protein levels. Treatment of HEK 293 cells with proteasome inhibitors ALLN and MG132, which are broad proteasome inhibitors, leads to the increase of HDAC4, HDAC5 and HDAC7 protein levels (Li et al., 2004). Specifically, cytoplasmic HDAC7 protein levels are controlled via UPS degradation once HDAC7 is shuttled from the nucleus to the cytoplasm by phosphorylation-mediated export (Li et al., 2004). Moreover, UPS-mediated cytoplasmic degradation of HDAC7 induces β-actin expression, which is a vital step in endochondral ossification (Bradley et al., 2015).

1.6.4 Immunological roles of class IIa HDACs: HDAC7 as a regulator of T cell development

Among other class IIa HDACs, HDAC7 plays a crucial role in immune cells. The comparison of multiple tissues for mRNA expression levels of HDAC7 revealed the thymus with the highest expression (Dequiedt et al., 2003). In thymus, HDAC7 is expressed in double positive ($CD4^+CD8^+$) thymocytes. Moreover, transcriptional activity of *Nur77* upon TCR activation was repressed via histone acetylation mediated through HDAC7, and interaction of MEF2D and HDAC7 is necessary for this suppression of *Nur77* expression (Dequiedt et al., 2003). If the three serine phosphorylation sites on the amino terminal-tail of HDAC7 are mutated, HDAC7 is trapped in the nucleus since its nucleocytoplasmic shuttling is impaired. The ectopic expression of this triple mutant HDAC7 (HDAC7-ΔP) resulted in suppression of *Nur77* induction in response to TCR activation suggesting that HDAC7 is necessary for the modulation of thymocyte apoptosis rates after TCR activation (Dequiedt et al., 2003). Indeed, RNA-interference-mediated knockdown of *Hdac7* resulted in increased apoptosis in thymocytes during TCR activation. Therefore, this study characterized HDAC7 as the key regulator of *Nur77* transcription and TCR-mediated apoptosis in thymocytes.

In a follow-up study, constitutively active HDAC7 fused with the activation domain VP16 (HDAC7-VP16) and nuclear trapped HDAC7-ΔP were separately expressed in thymocytes and subsequently were compared via microarrays to characterize the putative HDAC7 gene targets with differential expression during positive and negative selection of thymocytes (Kasler and Verdin, 2007). HDAC7 was found to regulate several genes differentially expressed during positive and negative selection of thymocytes. These genes mainly regulate the coupling between TCR engagement and its subsequent downstream signaling cascades (Kasler and Verdin, 2007). Therefore, HDAC7 was further confirmed as a key player for the regulation of thymocyte survival and their positive and negative selection.

In a conditional mouse model, in which *Hdac7* is deleted specifically in thymocytes, it was shown that HDAC7 deletion interferes with T cell maturation at the double positive stage (Kasler et al., 2011). HDAC7 is not important for regulating the TCR affinity thresholds for positive selection or β-selection, but is rather essential for the regulation of apoptosis and survival during positive selection of thymocytes, since *Hdac7*-deficient thymocytes have a reduced lifespan *in vivo*. *Hdac7*-deficient thymocytes have altered expression programs for several crucial mediators and modulators of TCR-engagement response resulting in sustained

mitogen-activated protein kinase (MAPK) activity, which partially leads to impaired survival in *Hdac7*-deficient thymocytes (Kasler et al., 2011). Similarly, *Hdac7*-deficient thymocytes feature an increased activity of PKD, which is essential for the nuclear export of HDAC7 upon TCR activation. Therefore, cytoplasmic localization of HDAC7 through its nuclear export controls an auto-excitatory loop and a feed-forward mechanism in which HDAC7 regulates its own state (Kasler et al., 2011). A transgenic mouse model that expresses phosphorylation-defective HDAC7-ΔP, which cannot localize to the cytoplasm in thymocytes, showed that the negative selection of thymocytes was completely blocked resulting in the subsequent escape of autoreactive T cells to the periphery, thus driving a lethal autoimmune phenotype in mice. In the same study, it was shown that a phosphorylation defective mutant HDAC7 impairs the gene expression program related to negative selection of thymocytes as assessed by gene expression profiling via microarrays (Kasler et al., 2012). Interestingly, the *Hdac7* gene resides in a risk locus for primary sclerosing cholangitis (PSC) that is an autoimmune liver disease (Raf, 2013).

Recently, HDAC7 was also shown to govern effector programming of natural killer T (NKT) cells in thymus (Kasler et al., 2018). The expression of HDAC7-ΔP mutant in thymocytes resulted in inhibition of negative selection as well as NKT cell development diverting Vα14/Jα18 TCR into a conventional T cell-like lineage. In addition, conditional deletion of *Hdac7* in thymocytes led to the reduced survival of NKT cells and their apoptosis as well as simultaneous increase of innate effector cells. Mechanistically, these processes were modulated through the binding of HDAC7 to PLZF and regulating PLZF-dependent transcriptional programs (Kasler et al., 2018). Moreover, the analysis of genome-wide association studies (GWAS) in inflammatory bowel disease (IBD) and PSC and its intersection with HDAC7-regulated genes in spleen and thymus revealed that most of the HDAC7 target genes are in risk loci for these diseases consistent with the autoimmune phenotype that is observed in HDAC7-ΔP transgenic mice (Kasler et al., 2018). These findings are in line with the previous observations related to the role of HDAC7 in thymocyte selection and survival as well as the development of autoimmune diseases and its potential link to human autoimmunity.

Although the functions of HDAC7 during thymocyte development and survival have been better characterized, little is known about its role in peripheral adult T cells. Serine-threonine phosphoproteome profiling of CTLs via high-resolution mass spectrometry revealed about 500

events mediated by TCR activation and signaling (Navarro et al., 2011). Among chromatin regulators, HDAC7 has a very high expression, and it constitutively localizes to the cytoplasm due to its phosphorylation-dependent nuclear export. The nuclear accumulation of HDAC7 via dephosphorylation caused the suppression of key effector cytokine-coding genes, cytokine receptors as well as cell adhesion molecules which are essential regulators of CTL function (Navarro et al., 2011). Therefore, besides its crucial roles in thymocytes, HDAC7 is a key determinant for effector functions of CTLs. However, its role in peripheral T cells is not fully understood yet.

Apart from T cells, HDAC7 has also a critical role for the differentiation of pre-B cells into macrophages (Barneda-Zahonero et al., 2013). During this differentiation process, the expression of HDAC7 is downregulated. If HDAC7 is ectopically expressed during this re-programming, it interferes with the gain of macrophage functions as well as myeloid gene transcriptional program. Mechanistically, HDAC7 recruits MEF2C to the promoters of macrophage-related genes in pre-B cells and suppresses their expression. If HDAC7 is downregulated via small interfering RNA (siRNA)-mediated knockdown, myeloid genes are expressed in pre-B cells (Barneda-Zahonero et al., 2013). Therefore, HDAC7 is a crucial regulator of transcriptional repression in lymphoid cells which determines essential steps of T cell and B cell development and differentiation as well as their functions.

1.7 Histone deacetylase inhibitors

Deregulation of histone acetylation contributes to the pathogenesis of several diseases including cancer. As a result, targeting HDACs for cancer treatment has emerged as a research field. HDAC inhibitors (HDACi) can be either generated from natural compounds or synthesized. They can be divided into four main groups with respect to their structures as hydroxamic acids, benzamides, cyclic peptides and short-chain fatty acids. Until now, the hydroxamic acids suberoylanilide hydroxamic acid (SAHA), belinostat and panobinostat received FDA approval as anti-cancer drugs. They are pan-HDAC inhibitors blocking all class I, class II and class IV HDACs. Cyclic peptide FK228 has also been approved by FDA and it has been reported to specifically target class I HDACs (Suraweera et al., 2018a). The HDACi SAHA and FK228 have been used to treat the cutaneous T cell lymphoma. More recently, belinostat and panobinostat have been approved for the treatment of peripheral T cell lymphoma and multiple myeloma, respectively (Suraweera et al., 2018a). Although the treatments of these

cancer types with HDACi is promising, the success of HDACi treatment for solid tumors is still limited. Moreover, HDACi treatment is restrained by its dose-limiting toxicity as well as adverse effects such as thrombocytopenia, nausea, neutropenia, vomiting, diarrhea, fatigue, cardiac toxicity as well as ventricular arrhythmia as the most relevant side effect (Poligone, 2011; Sciences, 2017; Suraweera et al., 2018b). Most pan-HDACi target the C-terminal catalytic domains of HDACs, which are well conserved between different isoforms. Thus, pan-HDACi are also disadvantageous in terms of their target specificities and off-target effects. Another approach to inhibit HDACs is to target their catalytic activities through Zn-binding sites on the C-terminus by metal-chelating inhibitors that interfere with the metal-dependent hydrolysis of the acetylated substrate. However, Zn-binding sites are highly conserved in metalloenzymes meaning that HDACi targeting these sites can cause cross reactivity. Therefore, the structure and the nature of Zn-binding sites and nearby interaction pockets should be better understood to improve metal-chelating-mediated HDAC inhibition (Day and Cohen, 2013; Suraweera et al., 2018a).

The N-terminal domain of class IIa HDACs interacts with transcriptional co-repressors and co-activators. Interaction partners of class IIa HDACs mediate the posttranslational modifications, which function as regulatory signals. This is a unique feature of the class IIa HDAC family discriminating them from class I HDACs (Verdin et al., 2003). Therefore, targeting the N-terminal domain of class IIa HDACs represents an approach to improve the target specificity for the treatment of diseases in which class IIa HDACs and their downstream pathways are deregulated. Class IIa HDACs have minimal or no catalytic activity against acetylated histones and non-histone proteins, but they act as scaffold proteins to form large multiprotein complexes with repressor activity. They have tissue specific expression and are crucial regulators of specific developmental and differentiation processes such as skeletal muscle formation, cardiac hypertrophy, neuronal development, bone formation and T cell development. The control of several critical cellular processes by class IIa HDACs suggests that targeting their inhibition has potential to treat various human pathologies. Therefore, to enhance the generation of class IIa HDAC-specific inhibitors, more research is required to understand the regulation of class IIa HDACs, and their downstream targets regulated through their N-terminal domain, especially MEF2-regulated genes.

1.7.1 HDAC inhibitors for the treatment of inflammatory diseases

Besides oncological diseases, the influences of HDACi have been studied in the inflammatory context. However, the effects of HDACi on the immune responses were controversial. For instance, treatment of mice with trichostatin A (TSA) during a model of systemic lupus erythematosus (SLE) caused diminished mRNA expression of pro-inflammatory cytokines including IFNγ, IL-6, IL-2 as well as the anti-inflammatory IL-10 (Mishra et al., 2003). Although a similar effect for IL-10 was observed in peripheral T cells of SLE patients who received HDACi treatment, an increase in IFNγ production was present in the same cells which is partially controversial with the observations in murine models of SLE (Mishra et al., 2001). Similarly, anti-inflammatory effects of HDAC inhibition with TSA, phenylbutyrate or FK228 were observed in mouse models of rheumatoid arthritis assessed by decreased production of the pro-inflammatory cytokine TNFα (Chung et al., 2003; Nishida et al., 2004). Anti-inflammatory effects of HDACi have been well-established since these effects of HDACi could be validated in several studies using either patient samples or mouse models of inflammatory conditions or autoimmune diseases (Adcock, 2007; Glauben et al., 2006). At the same time, it seems that the anti-inflammatory effects of HDACi is dose dependent (Leoni et al., 2002; Hull et al., 2016). For instance, higher doses of SAHA (1-5 μM) are needed to exert its anti-tumor effects, whereas its much lower doses (50-200 nM) are sufficient to drive their anti-inflammatory responses resulting in decreased production of pro-inflammatory cytokines (Leoni et al., 2002; Cantley et al., 2015; Hull et al., 2016). Although dose-dependent effects of HDACi have been confirmed in multiple additional studies, this observation is not valid for all types of HDACi suggesting that careful study design in terms of cell type and dosage is necessary to interpret the anti-inflammatory functions of HDACi (Cantley et al., 2015; Hull et al., 2016).

The anti-inflammatory effects of HDACi encouraged the initiation of clinical trials for the treatment of chronic inflammatory diseases. For instance, in vitro treatment of pancreatic β cells with SAHA or TSA interfered with the cytokine-mediated destruction of these cells mediated by NF-κB signaling suggesting that HDAC inhibitor treatment holds promise for the treatment of type I diabetes, which is a metabolic disease coupled with a massive inflammatory component (Larsen et al., 2007). Similarly, TSA treatment led to diminished pro-inflammatory cytokine production as well as relieving the pathological destruction of myelin in a mouse model of multiple sclerosis (Faraco et al., 2011). On the contrary, another pan-

HDAC inhibitor sodium butyrate resulted in the increase of matrix metalloproteinase 9 (MMP-9) which has been positively correlated with pro-inflammatory responses in murine models of multiple sclerosis (Fiorino and Zvibel, 1996). Therefore, a deeper characterization of HDACi is necessary to better understand how they affect pro- and anti-inflammatory responses in chronic inflammatory diseases.

1.8 Myocyte enhancer factor 2 transcription factors

MEF2 plays a crucial role in cell differentiation and development including the skeletal, cardiac, neuronal, vascular, blood and immune system (Potthoff and Olson, 2007). They converge extracellular or intracellular signals on their downstream targets to regulate epigenetic and transcriptional responses. MEF2 transcription factors also play key roles for the regulation of apoptosis. For instance, MEF2C activity inhibits apoptosis in endothelial cells (Hayashi et al., 2004). Furthermore, MEF2A, MEF2C and MEF2D inhibit MAPK-induced apoptosis in developing neurons (Li et al., 2001; Mao et al., 1999). On the contrary, MEF2C and MEF2D activities trigger the apoptosis in T cells upon TCR signaling through the activation of pro-apoptotic *Nur77* expression (Dequiedt et al., 2003; Youn and Jun, 2000; Youn, 2000).

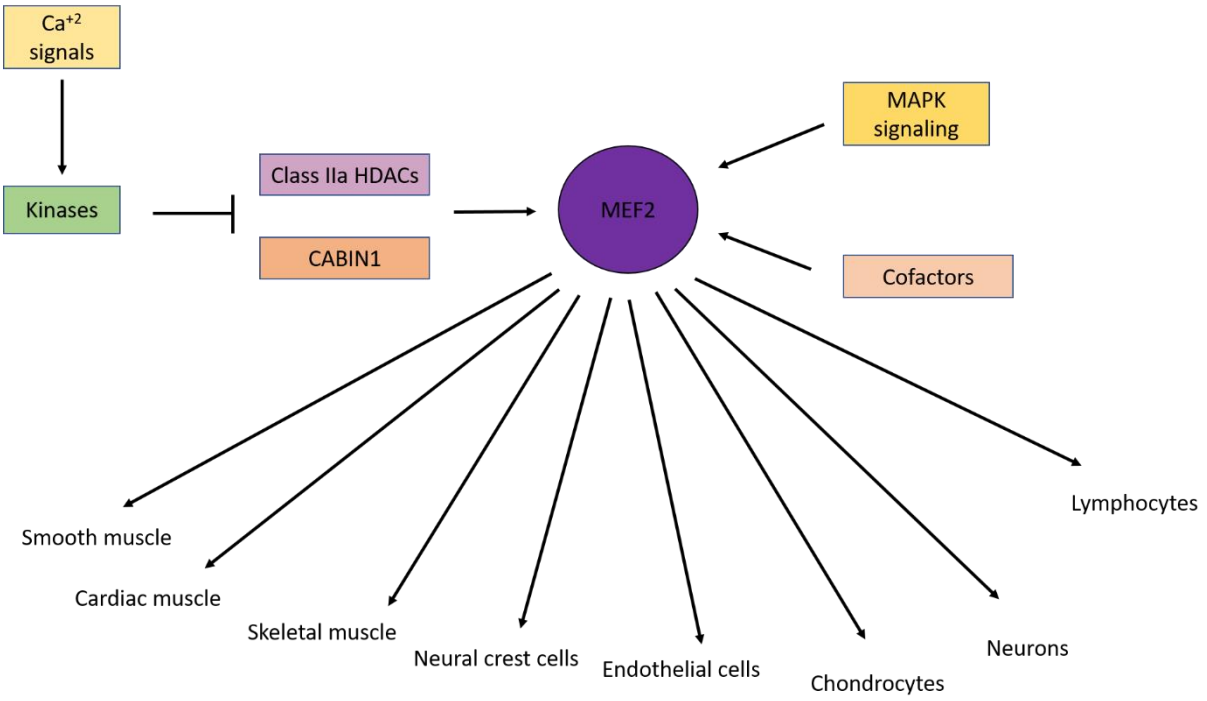

Figure 1-4 MEF2 transcription factors have diverse functions in different cell types. *The activity of MEF2 transcription factors is regulated by multiple factors including Ca^{2+} induced kinases, class IIa HDACs, calcineurin binding protein 1 (CABIN 1) as well as mitogen activated protein kinase (MAPK) signaling. MEF2 has important roles in several tissue types including smooth, cardiac, skeletal muscles as well as neural crest cells, endothelial cells, chondrocytes, neurons and lymphocytes. Adapted from* (Potthoff and Olson, 2007)

MEF2 transcription factors are members of the evolutionary conserved MADS transcription factor family. The MEF2 family is composed of four members in vertebrates including MEF2A, MEF2B, MEF2C and MEF2D. Structurally, all MEF2 family members harbor an N-terminal DNA binding MADS domain, a MEF2 domain in the center and a C-terminal transactivation domain (Pon and Marra, 2016; Potthoff and Olson, 2007). Although MEF2 and MADS domains are more homologous and conserved across different MEF2 members, the transactivation domain on the C-terminus is less conserved possessing only 6% homology in terms of amino acid sequence between MEF2A and the most divergent member MEF2B (Potthoff and Olson, 2007).

The MADS domain located on the N-terminus of MEF2 consists of 56 amino acids with a highly conserved amino acid sequence, while the central MEF2 domain has 29 amino acids which are specific to each MEF2 family member (Od and Ion, 1995; Shore and Sharrocks, 1995). Importantly, both the MADS and MEF2 domains are equally essential for the DNA binding activity (Molkentin et al., 1996). MEF2 transcription factors bind to DNA as dimers and MADS and MEF2 domains are dispensable for the dimerization of MEF2 proteins. Moreover, the DNA binding of MEF2 transcription factors occur via their homo-dimerization and hetero-dimerization. Although the DNA binding motifs of MEF2 family members are quite conserved, their DNA-binding affinities diverge which contributes further to their differential transcriptional activator capacities (Molkentin et al., 1996).

Another important layer of control for the transcriptional regulator activity of MEF2 is its association with co-activators and co-repressors through the central MEF2 domain (Dev, 1982; Miska et al., 1999; Youn et al., 2000). Among others, class IIa HDACs HDAC4, HDAC5, HDAC7 and HDAC9 are well characterized interaction partners of MEF2 transcription factors mediating the suppression of the target gene expression. Class IIa HDACs lack deacetylase activity, thus they promote gene repression via the recruitment of other co-repressors including C-terminal binding protein 1 (CtBP), heterochromatin protein 1 (HP1) and class I HDACs (Fischle et al., 2002; Lahm et al., 2007; Zhang et al., 2001). Another co-repressor partner of MEF2 is calcineurin binding protein 1 (CABIN1) (Han et al., 2003). Similarly, CABIN1 has been shown to associate with class I HDACs as well as H3K9 methyltransferase SUV39H1 resulting in inhibition of target gene expression (Jang et al., 2007). Indeed, MEF2 transcription factors also interact with well characterized transcriptional activators including p300 and

CREBBP through their MEF2 domains (He et al., 2011; Lundblad et al., 1995; Slepak et al., 2001). In line with its interaction partners, MEF2 proteins modulate gene expression via inducing changes in the histone modifications such as acetylation and deacetylation. Moreover, MEF2 proteins themselves are deacetylated by class II HDACs or p300. For example, HDAC4 deacetylates MEF2D resulting in its subsequent sumoylation which blocks its transcriptional activator function (Zhao et al., 2005). Furthermore, the acetylation of MEF2C by p300 result in its increased transcriptional activator activity (Ma et al., 2005). P300 also functions as an adaptor protein linking MEF2 to the core transcriptional machinery such as RNA polymerase II as well as other transcription factors since p300 itself is able to interact with them (Cohen et al., 2011).

Since the binding sites on MEF2 for co-repressors and co-activators overlap, it is expected that a competition for binding to the MEF2 transcription factors exist. In line with this expectation, decreased CABIN1 binding to MEF2D promotes an enhanced interaction between MEF2D and p300 (Youn and Jun, 2000). The interaction between MEF2D and class IIa HDACs as well as CABIN1 can be disrupted through increased calcium levels in the cell. Since high calcium levels induce calcium-dependent kinases such as PKD, class IIa HDACs and CABIN1 are phosphorylated promoting their nuclear export via association with 14-3-3 proteins and via sequestering into complexes with calcium-calmodulin (Youn and Jun, 2000). Indeed, calcium-dependent nucleocytoplasmic shuttling of class IIa HDACs and CABIN1 is consistent with the presence of calcium-sensitive genes as targets of MEF2D and *Nur77* is a well-known example of such mechanism (Dequiedt et al., 2003; Youn and Jun, 2000).

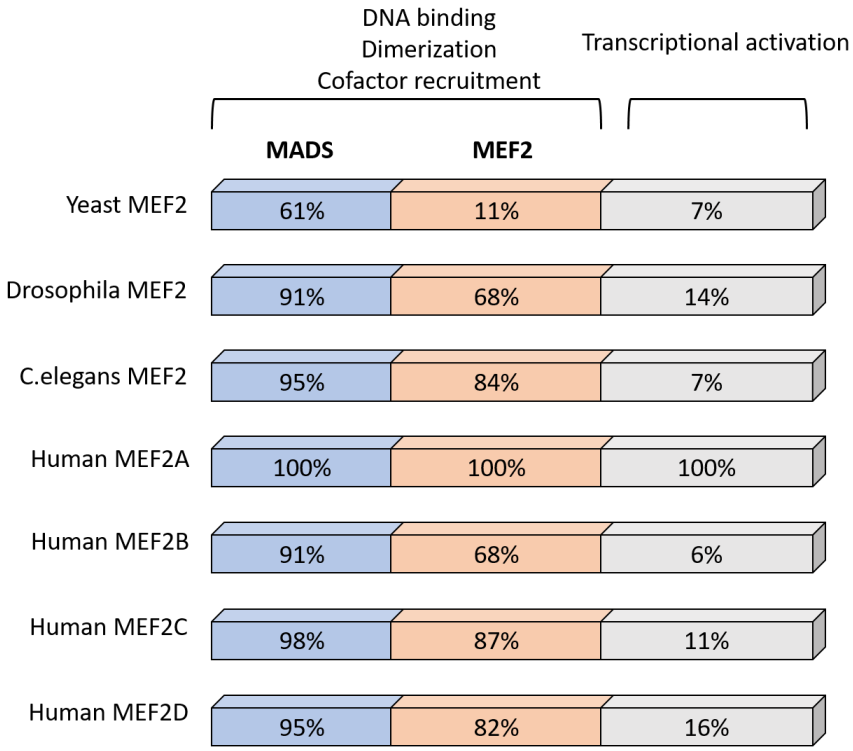

Figure 1-5 The structure of MEF2 transcription factors, isoforms of human MEF2 proteins and their amino acid sequence similarity to different organisms. *MADS and myocyte enhancer factor 2 (MEF2) domains are important for the DNA binding, dimerization as well as cofactor recruitment activities of MEF2 proteins. C-terminus of MEF2 is important for their transcriptional activation. Adapted from* (Potthoff and Olson, 2007)

Although the functions of MADS and MEF2D domains of MEF2 transcription factors are clear, how the transactivation domains promote the target gene expression is not fully understood. Co-immunoprecipitation experiments revealed that MEF2C, MEF2D and MEF2A interact with the positive transcription elongation factor b (P-TEFb) through their transactivation domains, which hyper-phosphorylates RNA polymerase II to induce transcription (Johnson, 2014; Taube et al., 2002). Transcriptional activator domains of MEF2 are also hot spots for several posttranslational modifications providing the integration of regulatory signals. There exist phosphorylation sites for p38, BMK1 and PKA (Cox et al., 2003; Du et al., 2008; Kato et al., 2000; Zhao et al., 1999). Phosphorylation of transactivation domain of MEF2 also results in sumoylation of close residues that triggers decreased MEF2-induced transcription. Another posttranslational modification induced by phosphorylation of MEF2 transactivation domain is the ubiquitination. For instance, if MEF2D is phosphorylated on S98 and S110 via CDK4/cyclin D1, it interacts with SKP2 which is an E3 ligase promoting ubiquitination of MEF2D and its subsequent degradation, thus resulting in blockade of transition into S phase of cell cycle (Giorgio et al., 2015). Therefore, along with MADS and MEF2 domains, posttranslational

modifications on the transactivation domain of MEF2 proteins represent important regulators of their transcriptional activities.

The profiling of genome-wide downstream targets of MEF2 proteins revealed that different MEF2 family members in different cell types have completely different sets of target genes in neurons, cardiomyocytes and osteoclasts (Fai et al., 2015; Flavell et al., 2008; Johnson et al., 2014). Similarly, downstream targets of each MEF2 transcription factor were compared by their knockdown in murine myoblasts revealed that the number of candidate target genes ranged between 110 for MEF2D with the fewest and 4020 for MEF2A with the highest number of target genes (Estrella et al., 2015). Also, 10 to 80% of the target genes characterized did not overlap with the targets of the other MEF2 proteins. Only 21 genes were identified as the target genes of all MEF2 family members, which are enriched for NOS and integrin signaling as well as amyloid processing and focal adhesion kinase (FAK) signaling (Estrella et al., 2015).

Studies aimed to identify the direct gene targets of MEF2 were restricted to a few cell types. Especially, little is known about the roles of MEF2 transcription factors in adult peripheral T cells. Therefore, characterization of the signaling pathways regulating MEF2 proteins and their downstream targets holds potential to understand the relevance of this transcription factor family to human inflammatory diseases.

2 MATERIALS and METHODS

2.1 Materials

2.1.1 Instruments

Table 1 Instruments used in this study

Instrument	Company
Agarose gel electrophoresis chambers	Peqlab, Erlangen, Germany
Centrifuge 5810 R	Eppendorf, Hamburg, Germany
CO_2 cell culture incubators	Thermofisher Scientific, Waltham, MA
FACS Canto II	BD, Franklin Lakes, NY
Heraeus FRESCO 21 Centrifuge	Thermofischer Scientific
HERAsafe Biological Safety Cabinet	Thermofischer Scientific
HLC Heating Thermomixer	Ditabis, Phorzheim, Germany
IKA KS 4000 i (orbital shaker)	IKA, Staufen, Germany
LAS-4000 Mini Fluorescence Image Analyzer	Fujifilm, Tokyo, Japan
Mini Protean System for Western Blot	Biorad, Feldkirchen, Germany
Primovert light microscope	Zeiss, Oberkochen, Germany
Seahorse XF 96 Extracellular Flux Analyzer	Agilent, Santa Clara, CA
SonoPULS GM70 Ultrasonic Homogenizer	Bandelin, Berlin, Germany
SpectraMax (Fluorescence 96-well plate reader)	Molecular Devices, Silicon Valley, CA
StepOne Plus Real Time PCR System	Agilent, Santa Clara, CA

T 3000 Thermocycler	Biometra, Göttingen, Germany
Trans-illuminator	Peqlab

2.1.2 Antibodies

Table 2 Antibodies used in flow cytometric analyses

Antigen anti-	Clone	Fluorochrome	Company	Catalog no.	Dilution
IFNγ	XMG1.2	APC-Cy7	BD, Franklin Lakes, NY	561479	1:200
Annexin V		Pacific Blue	Biolegend, San Diego, CA	640918	1:100
CD127	A7R34	PerCP-Cy5.5	eBioscience, Waltham, MA	45-127182	1:100
CD178 (FasL)	MFL3	APC-Efluor780	eBioscience	47-5911-82	1:100
CD279 (PD-1)	J.43	EF450	ebioscience	48-9985-82	1:100
CD3	145-2C11	APC	eBioscience	17-0031-82	1:100
CD3	145-2C11	PerCpCy5	BD	551163	1:300
CD366 (Tim-3)	RMT3-23	PeCy7	Biolegend	119716	1:100
CD4	GK1.5	FITC	BD	553729	1:200
CD4	GK1.5	APC-eF780	eBioscience	47-0041-80	1:300
CD8	53-6.7	PerCpCy5	Biolegend	100733	1:200
CD8	53-6.7	APC	eBioscience	17-0081-81	1:500
CD8a	53-6.7	FITC	Biolegend	100706	1:200
CD90.1 (Thy1.1)	OX-7	PE	Biolegend	202524	1:1000
CD90.2 (Thy1.2)	30-H12	FITC	Biolegend	105306	1:200
Eomes	Dan11mag	Efluor450	Invitrogen, Waltham, MA	48-4875-82	1:100
IFNγ	XMG1.2	APC	BD	554413	1:200
KLRG1	2F11	APC-Efluor780	eBioscience	47-5893-80	1:100
TNFα	MP6_XT22	PeCy7	BD	557644	1:200

Table 3 Antibodies used in Western blot

Antigen anti-	Host	Clone	Company	catalog #	Dilution
acetyl-Histone 3-lysine 9/14	rabbit	polyclonal	Cell Signaling Technology, Frankfurt am Main, Germany	9677S	1:1000
β-actin	mouse	AC-74	Sigma-Aldrich, St. Louis, USA	A2228	1:2000
HDAC7	rabbit	D4E1L	Cell Signaling Technology	33418S	1:1000

MEF2D	rabbit	polyclonal	Abcam, Cambridge, UK	ab32845	1:1000 1:100 for IP
phospho-mTOR-Ser2448	rabbit	polyclonal	Cell Signaling Technology	2971S	1:1000
phospho-mTOR-Ser2481	rabbit	polyclonal	Cell Signaling Technology	2974S	1:1000
total mTOR	rabbit	polyclonal	Cell Signaling Technology	2972	1:1000

2.1.3 Buffers

Buffers used in flow cytometry

Magnetic-activated cell sorting (MACS) buffer (10X)

- 5 g bovine serum albumin (BSA) (Fraction V) (Sigma-Aldrich, St. Louis, USA)
- 100 ml phosphate-buffered saline (PBS) (1X) (Gibco, Darmstadt, Germany)

Erythrocyte lysis buffer (pH 7.3)

- 8.9 g NH_4Cl (Merck, Darmstadt, Germany)
- 1 g $KHCO_3$ (Merck)
- 0.038 g ethylenediaminetetraacetic acid (EDTA) (Sigma-Aldrich)
- 1 L distilled water

Buffers used in Western blot

Sodium dodecyl sulfate (SDS) running gel (8%, 10 ml)

- 40% acrylamide mix (2 ml) (Biorad, Feldkirchen, Germany)
- 1.5 mM Tris base pH 8.8 (2.5 ml) (Carl Roth, Karlsruhe, Germany)
- 10% SDS (0.1 ml) (Carl Roth)
- 10% ammonium persulfate (APS) (0.1 ml) (Sigma-Aldrich)
- tetramethylethylenediamine (TEMED) (0.01 ml) (Biorad)
- distilled water (5.3 ml)

Stacking gel (5%, 3 ml)

- 40% acrylamide mix (0.38 ml) (Biorad)
- 1.0 M Tris base pH 6.8 (0.28 ml) (Carl Roth)

- 10% SDS (0.03 ml) (Carl Roth)
- 10% APS (0.03 ml) (Sigma-Aldrich)
- TEMED (0.003 ml) (Carl Roth)

Protein lysis buffer

- Complete protease inhibitor cocktail (Merck)
- 1 mM NaF (Sigma-Aldrich)
- 1 mM Na_3VO_4 (Merck)
- Phosphatase inhibitor cocktail (Sigma-Aldrich)
- Radioimmunoprecipitation assay (RIPA) buffer (Sigma-Aldrich)

Laemmli buffer (6X)

- 60 mM Tris-HCl pH 6.8 (Carl Roth)
- 12% SDS (Carl Roth)
- 47% glycerol (Carl Roth)
- 0.06% bromophenol blue (Merck)
- 12.5% β-mercaptoethanol (Sigma-Aldrich)

Electrophoresis buffer (10X)

- 144 g glycine (Carl Roth)
- 30 g Tris base (Carl Roth)
- 10 g SDS (Carl Roth)
- 1 L distilled water

Transfer buffer (10X)

- 30.3 g Tris base (Carl Roth)
- 144 g glycine (Carl Roth)
- 1 L distilled water

Transfer buffer (1X)

- 100 ml transfer buffer (10X)
- 200 ml 100% methanol (Merck)
- 700 ml distilled water

Tris-Buffered Saline (TBS) pH 7.6 (10X)

- 24 g Tris base (Carl Roth)
- 88 g NaCl (Carl Roth)
- 1 L distilled water

Tris-Buffered Saline-Tween20 (TBS-T) (1X)

- 100 ml TBS pH 7.6 (10X)
- 1 ml Tween (Carl Roth)
- 900 ml distilled water

Blocking buffer (5 %)

- 2.5 g BSA (Fraction V) (Sigma-Aldrich)
- 50 ml TBS-T (1X)

Stripping buffer (stock)

- 10 ml 20% SDS (Carl Roth)
- 3.085 ml Tris base (2 M) (Carl Roth)
- 87 ml distilled water

Stripping buffer (fresh)

- 10 ml stripping buffer (stock)
- 87.25 µl β-mercaptoethanol (Sigma-Aldrich)

Buffers used in Co-immunoprecipitation

Co-immunoprecipitation (Co-IP) lysis buffer

- 150 mM NaCl (Carl Roth)
- 50 mM Tris base pH 7.5 (Carl Roth)
- 1% octylphenoxypolyethoxyethanol IGPAL-CA-630 (Sigma-Aldrich)
- 5% glycerol (Carl Roth)
- protease inhibitor cocktail (Sigma-Aldrich)
- NaF (Sigma-Aldrich)
- Na_3VO_4 (Merck)

Co-IP wash buffer (low salt)

- 20 mM Tris-HCl pH 8.0 (Carl Roth)
- 150 mM NaCl (Carl Roth)
- 2 mM EDTA (Sigma-Aldrich)
- 0.1% SDS (Carl Roth)
- 1% Triton X-100 (Sigma-Aldrich)
- protease inhibitor cocktail (Sigma-Aldrich)
- NaF (Sigma-Aldrich)
- Na_3VO_4 (Merck)

Co-IP elution buffer

- 1X Laemmli buffer

Buffers used in Chromatin Immunoprecipitation

ChIP lysis buffer

- 50 mM Tris base pH 8.0 (Carl Roth)
- 10 mM EDTA (Sigma-Aldrich)
- 1% SDS (Carl Roth)
- protease inhibitor cocktail (Sigma-Aldrich)
- NaF (Sigma-Aldrich)
- Na_3VO_4 (Merck)

ChIP dilution buffer

- 16.7 mM Tris-HCl pH 8.0 (Carl Roth)
- 167 mM NaCl (Carl Roth)
- 1.2 mM EDTA (Sigma-Aldrich)
- 0.01% SDS (Carl Roth)
- 1.1% Triton X-100 (Sigma-Aldrich)
- protease inhibitor cocktail (Sigma-Aldrich)
- NaF (5 mM) (Sigma-Aldrich)
- Na_3VO_4 (Merck)

Low-salt wash buffer

- 20 mM Tris-HCl pH 8.0 (Carl Roth)
- 150 mM NaCl (Carl Roth)
- 2 mM EDTA (Sigma-Aldrich)
- 0.1% SDS (Carl Roth)
- 1% Triton X-100 (Sigma-Aldrich)
- protease inhibitor cocktail (Sigma-Aldrich)
- 5 mM NaF (Sigma-Aldrich)
- Na_3VO_4 (Merck)

High-salt wash buffer

- 20 mM Tris-HCl pH 8.0 (Carl Roth)
- 500 mM NaCl (Carl Roth)
- 2 mM EDTA (Sigma-Aldrich)
- 0.1% SDS (Carl Roth)
- 1% Triton X-100 (Sigma-Aldrich)
- protease inhibitor cocktail (Sigma Aldrich)
- 5 mM NaF (Sigma-Aldrich)
- Na_3VO_4 (Merck)

ChIP elution buffer

- 100 mM $NaHCO_3$ (Merck)
- 1% SDS (Carl Roth)

Buffers used in intracellular calcium influx measurement

Ringer solution (0 mM Ca^{+2})

- 155 mM NaCl (Carl Roth)
- 4.5 mM KCl (Calbiochem, Darmstadt, Germany)
- 3 mM $MgCl_2$ (Carl Roth)
- 10 mM D-glucose (Carl Roth)
- 5 mM Na-HEPES (Carl Roth)

2.1.4 Primers

RT-qPCR primers

All RT-qPCR primers used in this study were purchased from TIB MOLBIOL (Berlin, Germany).

Table 4 Primers used for RT-qPCR

Primer name	Primer sequence (5′-3′)
Hdac7-forward	TGTCACCGACCTTGCCTTCAAA
Hdac7-reverse	ATCTTGCTGGCTTTGCCGTGT T
Pdcd1-forward	ACCCTGGTCATTCACTTGGG
Pdcd1-reverse	GTAAGAATGCCTATCTGCCCTG
Havcr2-forward	GTAAGAATGCCTATCTGCCCTG
Havcr2-reverse	GCAACTCGTTGGTACACTGTGA
Tigit-forward	CCACAGCAGGCACGATAGATA
Tigit-reverse	CATGCCACCCCAGGTCAAC
Ctla4-forward	CATGGTGTCGCCAGCTTTC
Ctla4-reverse	GGTAATCTAGGAAGCCCACTGTA
Lag3-forward	CCTCGATGATTGCTAGTCCCT
Lag3-reverse	GTAGACAGGCACTCGGTTCTG

Genotyping primers

All genotyping primers used in this study were purchased from TIB MOLBIOL (Berlin, Germany).

Table 5 Primers used for genotyping

Mouse strain	Primer target	Primer sequence (5′-3′)
Hdac7$^{fl/fl}$CD4-Cre **Hdac7$^{fl/fl}$CD4-Cre-OT1-Thy1.1**	Flox-Forward	CCAGTGGACGAGCATTCTGGAGAAAGGC
Hdac7$^{fl/fl}$CD4-Cre **Hdac7$^{fl/fl}$CD4-Cre-OT1-Thy1.1**	Flox-reverse	GTTGCAGGGTCAGCAGCGCAGGCTCTG
Hdac7$^{fl/fl}$CD4-Cre **Hdac7$^{fl/fl}$CD4-Cre-OT1-Thy1.1**	Cre-1	ATCAAGGTCCTGAGGAAGAG
Hdac7$^{fl/fl}$CD4-Cre **Hdac7$^{fl/fl}$CD4-Cre-OT1-Thy1.1**	Cre-2	ACCTCATCACTCGTTGCATC
Hdac7$^{fl/fl}$CD4-Cre **Hdac7$^{fl/fl}$CD4-Cre-OT1-Thy1.1**	Cre-3	CTAGGAGTTGTGCTGCACAG
Hdac7$^{fl/fl}$CD4-Cre-OT1-Thy1.1	OT1-forward	CAGCAGCAGGTGAGACAAAGT
Hdac7$^{fl/fl}$CD4-Cre-OT1-Thy1.1	OT1-reverse	GGCTTTATAATTAGCTTGGTCC
Hdac7$^{fl/fl}$E8I-Cre	E8I-Cre-Forward	CGATGCAACGAGTGATGAGG
Hdac7$^{fl/fl}$E8I-Cre	E8I-Cre-Reverse	GCATTGCTGTCACTTGGTCCT

ChIP-qPCR primers

All ChIP-qPCR primers used in this study were purchased from TIB MOLBIOL (Berlin, Germany).

Table 6 ChIP-qPCR primer sequences

Primer name	Primer sequence **(5′-3′)**
mFasL-Region 1-Forward	AGGAACAGCCTGAGATTGC
mFasL-Region 1-Reverse	ACCTTTTTGGCAGACTCTACAT
mFasL-Region 2-Forward	TGTTTTGGCATAGGTGAGAG
mFasL-Region 2-Reverse	CACACCATTTATGTCTAATAACC
mFasL-Region 3-Forward	GTAAATGTTGAATAATGTTTTAGTA
mFasL-Region 3-Reverse	CCCTATCCATCCCACTTC

2.2 Methods

2.2.1 Cell culture

EL-4 and EG7-Ova cells were purchased from ATCC (Manassas, VA). B16-Ova cells were kindly provided by Gerald Willimsky (Charité - Universitätsmedizin Berlin, Germany). EL-4 and EG.7-Ova cells were cultured in RPMI 1640 (Gibco, Darmstadt, Germany) medium supplemented with 10% FCS and 100 μg/ml penicillin-streptomycin (Gibco) 500 μM β-mercaptoethanol (Sigma Aldrich, St. Louis, USA). B16-Ova cells were cultured in DMEM (Gibco) medium with 10% fetal bovine serum (FCS) and 100 μg/ml penicillin-streptomycin. For stable expression of ovalbumin (Ova), EG7-Ova and B16-Ova cells were cultured in the presence of 50 μg/ml G418 (Sigma-Aldrich).

2.2.2 Mouse strains

Twelve to 20-week-old animals were used for experiments. *Hdac7$^{flox/flox}$Cd4-Cre, Hdac7$^{flox/flox}$E8I-Cre* or *Hdac7$^{flox/flox}$Cd4-Cre-OTI-Thy1.1* mice were bred at the Charité animal facility under specific pathogen free (SPF) conditions. For subsequent single cell analyses, mice were anesthetized with isoflurane followed by cervical dislocation and organ harvest. All

animal protocols were approved by the regional animal study committee of Berlin (LaGeSo, Berlin, Germany) and conducted accordingly.

2.2.3 Genotyping

Ear biopsies from mice were digested in 100 µl DirectPCR Lysis reagent Ear (Invivogen, San Diego, CA) supplemented with 20 µg/ml proteinase K (Sigma-Aldrich) for 3 h or overnight at 55°C by shaking at 800 rpm followed by inactivation for 45 min at 85°C at 300 rpm. Samples were directly used in the polymerase chain reaction (PCR) for genotyping.

2.2.4 In vitro differentiation of murine cytotoxic T cells

$CD8^+$ T cells were isolated from splenocytes by negative magnetic enrichment using Easysep Mouse $CD8^+$ T cell isolation kit (Stemcell, Cologne, Germany) according to manufacturer's instructions. One million cells were cultured into 12-well cell culture plates coated with 2 µg/ml anti-CD3 (Biolegend, San Diego, CA) and anti-CD28 (Biolegend) antibodies in complete RPMI 1640 medium supplemented with 10% FCS, 100 µg/ml penicillin-streptomycin solution, β-mercaptoethanol and 40 ng/ml recombinant murine IL-2 (Peprotech, New Jersey, NY). After 48 h, cells were harvested, washed and cultured in the presence of 20 ng/ml murine IL-2 and expanded for 5 days. IL-2-containing medium was refreshed every two days.

2.2.5 Tumor allografts and isolation of tumor-infiltrating lymphocytes

For in vivo tumor experiments, $1x10^6$ EG7-Ova or $1x10^5$ B16-Ova cells were intradermally injected into the flank of mice. Tumor measurement was performed every other day by using an in-situ caliper.

For the isolation of tumor-infiltrating lymphocytes, mice were sacrificed after 14 days and tumors were excised. Tumors were washed thoroughly with PBS and cut into very small pieces using surgical scalpel followed by digestion in complete RPMI 1640 (Gibco) medium supplemented with 200 U/L collagenase D (Sigma-Aldrich) and 20 µg/ml DNase I (Sigma-Aldrich) at 37°C for 40 minutes on a shaker. Digested tumors were passed through 70 µm cell strainer (Thermofisher Scientific). Filtered cells were washed with PBS by centrifugation at 400 g for 7 min at 4°C and processed for subsequent experiments.

2.2.6 Adoptive T cell transfer

For rescue experiments, EG.7-Ova cells were intradermally injected into *Hdac7$^{flox/flox}$Cd4-Cre* (Thy1.2) mice. Seven days later, 8x10^6 *in vitro* differentiated Thy1.1$^+$ wt-Ot1 or *Hdac7^{ko}*-Ot1 CTLs were transferred into tumor-bearing mice via intravenous (i.v.) injections and tumor growth was monitored every other day. Mice were sacrificed seven days after adoptive CTL transfer and tumors, tumor draining lymph nodes (TDLN) and spleens were harvested and the frequencies of Thy1.1$^+$ wt or *Hdac7^{ko}* cells were determined. Thy1.1$^+$ cells were further analyzed to assess their survival, expression of protein markers related to cellular exhaustion or memory formation via flow cytometry.

For homing experiments, wt mice were similarly injected with B16-Ova cells and ten days later, B16-Ova tumor-bearing mice were transferred with wt or *Hdac7^{ko}* CTLs. Two hours after CTL transfer, mice were sacrificed and tumors, spleens and TDLN were harvested to determine the frequency and homing of Thy1.1$^+$ cells.

2.2.7 Immunocytochemistry

EG7-Ova tumors were excised from mice and rinsed, fixed overnight in 4% formalin and later embedded in histosec (Merck, Darmstadt, Germany). One to 2 μm sections were cut, dewaxed and subjected to a heat-induced epitope retrieval step prior to incubation with anti-Foxp3 (clone FJK-16s, eBiosciences, San Diego, CA) antibody followed by secondary anti-rabbit antibody incubations (Diavona). Envision$^+$ System-HRP Labeled Polymer Anti-Rabbit (Agilent, Santa Clara, USA) was used for detection. To visualize horseradish peroxidase (HRP), diaminobenzidine (DAB, Agilent) was used. Proteins were deactivated by incubation at 116^{o}C for 5 min in acidic buffer (1.8 bar), and then sections were incubated with anti-CD4 (clone 4SM95, eBiosciences) followed by incubation with biotinylated secondary rabbit anti-rat antibody (Diavona). In order to detect biotin, sections were incubated with alkaline phosphatase (AP)-labeled streptavidin (Agilent) followed by visualization of AP by chromogen RED (Agilent). Subsequently, proteins were inactivated, and sections were incubated with anti-CD8 (clone 4SM15, Thermofisher Scientific) followed by incubation with biotinylated secondary rabbit anti-rat antibody and sections were similarly incubated with AP-labeled streptavidin (Agilent). To visualize AP HIGHDEF blue IHC chromogen (Enzo Life Sciences, Lörrach, Germany) was used. All incubation steps with primary and secondary antibodies were performed for 30 min at room temperature. Hematoxylin was used to counterstain nuclei and

slides were cover-slipped with glycerol gelatin (Merck). Primary antibodies were omitted to perform negative controls. Endogenous AP and HRP were blocked by peroxidase and AP Blocking Reagent (Agilent). All images were acquired by using an AxioImager Z1 microscope (Carl Zeiss MicroImaging Inc.). After staining steps, positive cells were quantified in 10 high power fields (field of vision x400 original magnification). All evaluations were performed in a blinded manner.

2.2.8 Flow cytometric analysis of murine CD8$^+$ T cells

Single cell suspensions were obtained by filtering through 70 and 40 μm cell strainers (Thermofisher Scientific). Erythrocytes were lysed in Erylysis buffer for 2 min at room temperature. Cells were first stained with live/dead marker according to manufacturer's instructions. Surface markers were stained in MACS buffer for 15 min at room temperature at the indicated dilutions of the corresponding antibodies. For the measurement of intracellular cytokines, cells were stimulated with 0.01 μg/ml phorbol myristate acetate (PMA) (Sigma-Aldrich) and 1 μg/ml ionomycin (Sigma-Aldrich) or 1 μg/ml Ova peptide (SIINFEKL) (Sigma-Aldrich) in the presence of 0.01 mg/ml Brefeldin A for 6 h.

For the intracellular staining of cytokines and transcription factors, FoxP3 intracellular staining kit (Thermofisher Scientific, USA) was used, and staining was performed at 4^{o}C for 30 min. All fluorochrome-labeled cells were analyzed by FacsCanto II (BD Biosciences, Franklin Lakes, NY) and FlowJo V10.1(FlowJo, LLC, Ashland, USA). All antibody dilutions and additional information on fluorochrome-labeled antibodies are shown in Table 2.

2.2.9 Annexin V-propidium iodide staining of CD8$^+$ T cells

Cells were harvested and surface staining of CD8 was performed as described. Cells were washed twice with 1X annexin V binding buffer (Thermofisher Scientific) and stained with annexin V diluted in the same buffer followed by incubation at room temperature for 5 min. Cells were stained with propidium iodide (PI) and directly measured by flow cytometry.

2.2.10 In vitro killing assay

To determine the cytotoxic capacities of *in vitro* differentiated wt-OT1 or *Hdac7^{ko}*-OT1 CTLs, they were co-cultured with carboxyfluorescein diacetate succinimidyl ester (CFSE)-labeled EG.7-Ova cells at different target to effector cell ratios and incubated for 2 h followed by

annexin V staining of cells. The percentage of Annexin V^+ CFSE-labeled target EG.7-Ova cells was measured by flow cytometry as a readout for the killing capacities of CTLs.

2.2.11 In vitro T cell exhaustion assay

Murine $CD8^+$ T cells were isolated from splenocytes as described and activated with 1 µg/ml anti-CD3 (Biolegend) and 1 µg/ml anti-CD28 (Biolegend) in the presence of 20 ng/ml recombinant murine IL-2 (Peprotech). After 48 h, cells were collected, washed with centrifugation and subsequently divided into two groups. One million cells in 2 ml medium were cultured into 1 µg/ml anti-CD3 and anti-CD28 antibody coated 12-well plates without any recombinant IL-2 for restimulation. The second group was cultured only in the presence of recombinant IL-2 (20 ng/ml) into uncoated wells as control without restimulation. Cells were restimulated for 48 h followed by the second and the third restimulations. Exhaustion markers were analyzed every other day by flow cytometry.

2.2.12 Intracellular calcium influx measurement

In vitro differentiated CTLs were labeled with 2 µM Fura-2-AM (Invitrogen, Karlsruhe, Germany) for 20 min at room temperature, washed and re-suspended in RPMI 1640 medium (Gibco). Subsequently, $4x10^5$ cells were cultured in poly-L-lysine (Sigma, Netherlands) coated 96-well plates and the Fura-2 emission ratio (340/380 nm) was measured using a FlexStation microplate reader. Baseline intracellular $Ca2^+$ ($[Ca^{2+}]_i$) was acquired in 0 mM Ca^{2+} Ringer solution for 300 s as previously described. Subsequently, cells were stimulated with 1 µM thapsigargin (EMD Millipore, Billerica, MA). After 600 s, Ca^{2+} containing Ringer solution (2 mM $CaCl_2$) was added to the cells (final $[Ca^{2+}]_o$ 1 mM). Cells were excited at 340 and 380 nm and fluorescence emission measured at 510 nm every 5 s. The Ca^{2+} influx rate ($\Delta R/\Delta t$) was calculated 20 s (t_{20}) after re-addition of Ca^{2+} (t_0) using the equation $(R[t_{20}] - R[t_0])/(t_{20} - t_0)$, with R being the Fura-2 emission ratio 340/380 nm. Graphs were plotted using Prism 6 software (Graphpad Software, La Jolla, CA).

2.2.13 CFSE dilution assay

$CD8^+$ T cells were stained with 0.5 µM CFSE for 5 min at 37°C followed by washing and re-suspension in complete RPMI 1640 medium. CFSE labeled cells were *in vitro* activated with 1 µg/ml anti-CD3 (Biolegend) and 1 µg/ml (Biolegend) anti-CD28 and 40 ng/ml recombinant

murine IL-2 (Peprotech) as described before and cells were analyzed by flow cytometry three days later. Cell division was analyzed using the FlowJo software (BD Biosciences).

2.2.14 Metabolic flux analyses

Cellular oxygen consumption rate (OCR) and extracellular acidification rate (ECAR) were measured using the Seahorse XFe96 Analyzer (Agilent). Briefly, 300.000 cells/well were cultured in corresponding assay media. For OCR measurement, XF RPMI Assay medium (Agilent) was supplemented with 1 mM pyruvate (Sigma-Aldrich), 2 mM glutamine (Sigma-Aldrich) and 10 mM glucose (Carl Roth). For ECAR measurement, XF RPMI Assay Medium was supplemented with 1 mM glutamine. Cells were cultured into Seahorse XF96 Cell Culture Microplate (Agilent), which was pre-coated with 10fold diluted poly-L-lysine (Sigma-Aldrich). Cells were centrifuged for their complete attachment and incubated in a non-CO_2 incubator at 37°C for 60 min. OCR was measured under basal conditions in response to 2 µM oligomycin (Sigma-Aldrich), 1 µM fluorocarbonyl cyanide phenylhydrazone (FCCP) (Sigma-Aldrich) and 0.5 µM rotenone + antimycin A (Sigma-Aldrich). Glutamine uptake was measured in response to stimulation with 4 mM glutamine. For glycolysis, ECAR was measured in response to 10 mM glucose, 1 µM oligomycin and 50 mM 2-deoxy-D-glucose (2-DG).

2.2.15 Chromatin Immunoprecipitation

Cells were harvested in complete growth medium and fixed by adding formaldehyde solution at a final concentration of 1% followed by incubation at room temperature for 5 min by gentle shaking. Fixed cells were washed with ice-cold PBS three times with centrifugation. Cell pellet was resuspended in cold ChIP lysis buffer including protease and phosphatase inhibitors and incubated at 4^{o}C for 10 min. After cell lysis, chromatin sonication was performed with 2/4 power and 30 cycles of 10 seconds sonication and 20 seconds rest on ice. Lysed and sonicated samples were centrifuged at 14.000 g for 20 min to discard the debris. Two % of the samples were stored as input controls and the rest was 4fold diluted with ChIP dilution buffer supplemented with protease and phosphatase inhibitors. Sonicated samples were subsequently pre-cleared with salmon sperm blocked protein A agarose beads (Sigma-Aldrich) by rotating for 1 h at 4^{o}C. Samples were centrifuged at 100 g for 2 min and supernatant was incubated with protein A beads and primary antibodies or control IgG. Next day, protein A agarose beads were washed with low- and high-salt buffers followed by DNA elution by incubation at 30^{o}C for 15 min. To reverse-crosslink ChIP DNA, elutes were incubated overnight

in ChIP elution buffer supplemented with RNase A. Next day, DNA was purified by column purification according to manufacturer's instructions for high SDS containing samples (Macharey Nagel, Düren, Germany).

The concentration of ChIP DNA was measured by Qubit device using Qubit High Sensitivity DS kit (Thermofisher Scientific) to selectively determine the concentration of double stranded DNA. The quality and the fragment size of DNA was assessed by agarose gel electrophoresis or Cell Free DNA Screen Tape Analysis (Agilent) according to manufacturer's instructions.

2.2.16 ChIP-qPCR

Input DNA, mock and ChIP samples were 8fold diluted. Quantitative PCR (qPCR) was performed with Sybr green master mix (Applied Biosystems, Foster City, CA) according to manufacturer's instructions. qPCR was analyzed by StepOnePlus real time PCR system (Agilent). For the analysis of ChIP-qPCR data, fold enrichment of ChIP DNA over mock was calculated by using the formula $2^{-\Delta Ct(ChIP\text{-}mock)}$. The enrichment of ChIP DNA over input DNA was calculated using the formula $100*2^{\Delta Ct((Ct\ input\text{-}log50)\text{-}Ct\ mock\ or\ ChIP))}$. Primers used for specific regions of gene promoters are listed in Table 6.

2.2.17 Immunoblotting

For immunoblotting of mTOR, phospho-mTOR-Ser2448, phospho-mTOR-ser2481, HDAC7, acetyl-Histone 3 Lysine9/Lysine14 and β-actin, CTLs were lysed in RIPA buffer including complete protease inhibitors (Roche, Basel, Switzerland) and phosphatase inhibitor cocktail (Sigma-Aldrich). Thirty μg of whole cell lysates was run in 8% SDS-PAGE gels. For acetylated-Histone 3, 15% SDS-PAGE was used. Proteins were transferred to polyvinylidene fluoride (PVDF) membranes at 250 mA for 1-2 h. Membranes were blocked with 5% BSA-Tris-buffered saline with Tween20 (TBST) solution and incubated overnight with primary antibodies at 4°C on a rotator. All primary antibodies were diluted 1:1000 in 5% BSA-TBST solution. On the consecutive day, membranes were washed with 1X TBST solution and incubated with 1:2000 diluted HRP-linked secondary antibodies (Dako, Denmark) in 2.5% BSA-TBST solution for 1 h at room temperature. The detection was performed on luminescent image analyzer LAS-4000 mini using the Western blot detection ECL reagent (GE Healthcare, Chicago, IL). Densitometric analysis was performed using the ImageJ (1.48V) software (National Institute of Health, USA).

2.2.18 Statistical analysis

Statistical differences were determined by using student's t test. For correlation analysis, Spearman correlation coefficient was calculated for the respective experiments. All statistical analysis was performed by using Graphpad Prism Software Version 8 (Graphpad Software, La Jolla, CA).

3 AIM OF THE STUDY

$CD8^+$ T cells are the essential components of anti-viral and anti-tumor immunity since they can eliminate the infected or tumor cells by their antigen specific cytotoxicity. Besides their direct killing capacities, $CD8^+$ T cells provide long-term immunity against infections and tumors by generating a pool of memory $CD8^+$ T cells which are poised to reactivation by virus- or tumor-specific antigens in case of reencounter during life, thus providing an immunological memory. In recent years, $CD8^+$ T cell-based immunotherapy methods such as adoptive T cell transfer, CAR T-cell and checkpoint blockade therapies were shown to be successful for the treatment of several cancer types. Therefore, understanding the regulators of anti-tumor responses of $CD8^+$ T cells is not only essential for the development of novel immunotherapeutic approaches, but also to eliminate the limitations of current cancer immunotherapies such as immune surveillance and the cellular exhaustion of $CD8^+$ T cells within the immunosuppressive tumor microenvironment.

Little is known about the roles of several epigenetic regulators including histone deacetylases (HDAC) for the regulation of anti-tumor immune responses of $CD8^+$ T cells. Among other HDACs, HDAC7 has emerged as a prominent candidate as potential epigenetic regulator of $CD8^+$ T cells since HDAC7 has a crucial role during the thymic development of T cells by regulating their survival at the transcriptional level. The nucleocytoplasmic shuttling of HDAC7 is also regulated in $CD8^+$ T cells during TCR stimulation. However, the role of HDAC7 in the anti-tumor immune responses of adult $CD8^+$ T cells is still unknown. Given that several HDAC inhibitors are currently being used in the clinics for the treatment of cancers or under clinical trials for the treatment of infectious and autoimmune diseases, understanding the role of HDAC7 in $CD8^+$ T cells is clinically relevant. Therefore, in this PhD project we aimed to understand the role of HDAC7 in the anti-tumor immune responses of $CD8^+$ T cells as well as T cell homeostasis by using conditional deletion of *Hdac7* in mice, by *in vitro* experiments using primary murine $CD8^+$ T cells, by tumor models in mice as well as transcriptomic and genomic approaches to characterize the downstream targets of HDAC7 at the molecular level.

4 RESULTS

4.1 HDAC7 is the main Class II HDAC expressed in CD8⁺ T cells during their differentiation into cytotoxic T cells

To compare the expression of class II HDACs, CD8⁺ T cells were isolated from the splenocytes of wt mice and differentiated into CTLs by *in vitro* anti-CD3 and anti-CD28 activation for 48 h followed by stimulation with recombinant murine IL-2 (20 ng/ml) for an additional five days. RNA samples were collected every 48 h and the mRNA expression of class II HDACs HDAC4, HDAC5, HDAC6, HDAC7, HDAC9 and HDAC10 were measured by qPCR. We observed that HDAC7 has the highest expression among other class II HDACs for all timepoints during *in vitro* differentiation of CD8⁺ T cells into CTLs suggesting that HDAC7 might have a key role in this cell type **(Figure 4-1)**.

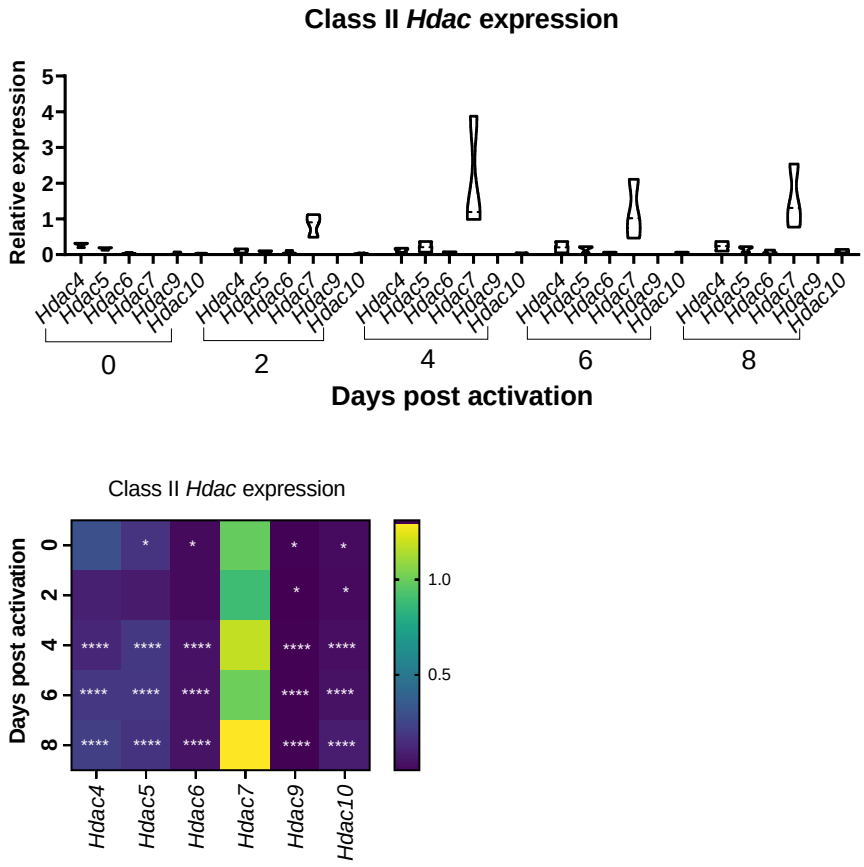

Figure 4-1 HDAC7 is the main class II HDAC expressed in CD8⁺ T cells during cytotoxic T lymphocyte (CTL) differentiation. *Wild type (wt) CD8⁺ T cells were activated with anti-CD3 and anti-CD28 antibodies for 48 h and cultured in the presence of recombinant IL-2 (20 ng/ml) over a 6-day time period for CTL differentiation. The mRNA expression of indicated class II histone deacetylases (HDACs) were measured by qPCR. The expressions were normalized to housekeeping gene 36b4. $2^{-\Delta Ct}$ values were plotted. Two-way Anova test, n=4, *p<0.05,****p<0.0001*

4.2 Generation of mouse models for conditional deletion of *Hdac7* in T cells

In order to investigate the role of HDAC7 in anti-tumor responses in CD8$^+$ T cells, three different mouse strains were used in this study. *Hdac7$^{fl/fl}$-CD4-Cre* mice harbor conditional deletion of *Hdac7* in all T cells, whereas *Hdac7* is exclusively deleted in CD8$^+$ T cells in *HDAC7$^{fl/fl}$-E8I-Cre* strain. HDAC7$^{fl/fl}$-CD4-Cre-OT1-Thy1.1$^+$ strain was also generated by crossing wt-OT1 mice with *Hdac7$^{fl/fl}$-CD4-Cre* mice. To assess the deletion efficiency of *Hdac7* in each mouse strain, qPCR was performed after RNA isolation and cDNA synthesis from sorted CD4$^+$ and CD8$^+$ T cells from splenocytes. qPCR experiments showed that *Hdac7* was efficiently deleted in both CD4$^+$ and CD8$^+$ T cells of *Hdac7$^{fl/fl}$-CD4-Cre* strain, while *Hdac7* was only deleted in CD8$^+$ T cells of *HDAC7$^{fl/fl}$-E8I-Cre* mice **(Figure 4-2)**.

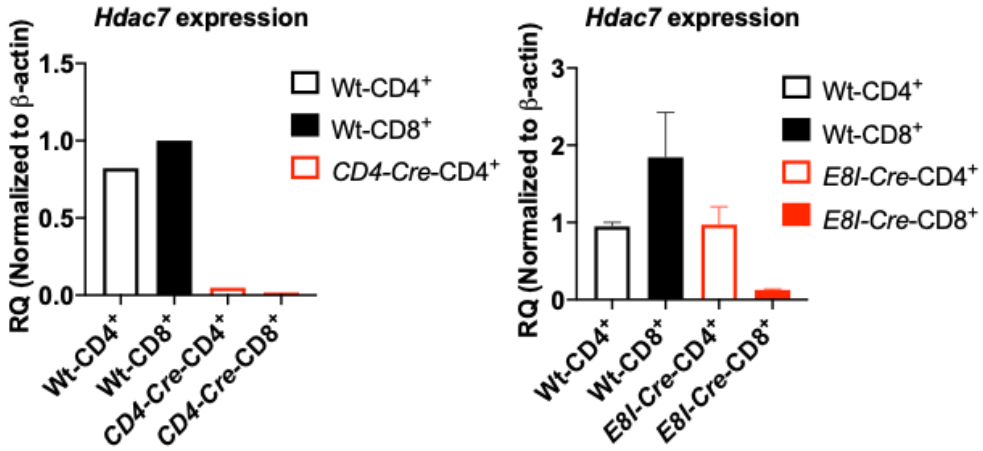

Figure 4-2 The deletion efficiency of Hdac7 in Hdac7$^{fl/fl}$-CD4-Cre* and *HDAC7$^{fl/fl}$-E8I-Cre* mouse strains. *CD4$^+$ and CD8$^+$ T cells were sorted from the splenocytes from Hdac7$^{fl/fl}$-CD4-Cre or HDAC7$^{fl/fl}$-E8I-Cre mice or wild type (wt) littermates followed by RNA extraction, cDNA synthesis and qPCR. Relative quantification (RQ) of Hdac7 expression was calculated by normalization to β-actin expression.*

4.3 *Hdac7* deletion results in decreased frequency and a preactivated phenotype of CD8$^+$ T cells under steady state conditions

To analyze whether the lack of *Hdac7* affects the phenotype of T cells under steady state conditions, splenocytes were isolated from *Hdac7$^{fl/fl}$-E8I-Cre* mice and wt littermates. Splenocytes were then stained with anti-CD3, anti-CD4 and anti-CD8 antibodies to discriminate CD4$^+$ and CD8$^+$ T cells as well as with anti-CD44 anti-CD62L antibodies to analyze effector, naïve and central memory T cells. The flow cytometry analysis showed that the frequency of CD8$^+$ T cells were significantly lower in *Hdac7$^{fl/fl}$-E8I-Cre* mice compared to wt littermates in line with an increase in the frequency of CD4$^+$ T cells **(Figure 4-3)**. The frequency of CD44$^+$CD62L$^-$ effector CD8$^+$ T cells is not different between *Hdac7$^{fl/fl}$-E8I-Cre* and wt mice.

Interestingly, the frequency of $CD44^{-}CD62L^{+}$ naïve $CD8^{+}$ T cells was significantly lower in *Hdac7*$^{fl/fl}$*-E8I-Cre* mice compared to wt littermates, and the frequency of $CD44^{+}CD62L^{+}$ central memory $CD8^{+}$ T cells was significantly higher in *Hdac7*$^{fl/fl}$*-E8I-Cre*. However, $CD4^{+}$ effector, naïve and central memory T cells remained unchanged in *Hdac7*$^{fl/fl}$*-E8I-Cre* compared to wt mice **(Figure 4-3)**. These results suggested that *Hdac7* deletion in $CD8^{+}$ T cells results in their reduced frequency as well as a pre-activated phenotype under steady state conditions.

Similarly, cytokine production in $CD4^{+}$ and $CD8^{+}$ T cells from *Hdac7*$^{fl/fl}$*-E8I-Cre* and wt littermates were analyzed upon PMA/ionomycin stimulation **(Figure 4-4)**. For $CD8^{+}$ T cells, no statistically significant difference was observed for the production of IFNγ and TNFα between wt and *Hdac7*$^{fl/fl}$*-E8I-Cre* mice. $CD8^{+}$ T cells from *Hdac7*$^{fl/fl}$*-E8I-Cre* mice produced significantly less IL-2 compared to wt mice. No difference was observed in the production of IL-2, while IFNγ production was lower in $CD4^{+}$ T cells **(Figure 4-4)**. In line with the pre-activated phenotype of $CD8^{+}$ T cells, the expression of CD40L, which is a marker for T cell activation, was significantly higher in $CD8^{+}$ T cells from *Hdac7*$^{fl/fl}$*-E8I-Cre* mice compared to wt littermates. For $CD4^{+}$ T cells, the expression of CD40L remained unchanged **(Figure 4-4)**. Therefore, the lack of *Hdac7* in $CD8^{+}$ T cells results in reduced frequencies of $CD8^{+}$ T cells as well as a pre-activated phenotype suggesting that *Hdac7*-deficient $CD8^{+}$ T cells might display deterred anti-tumor responses.

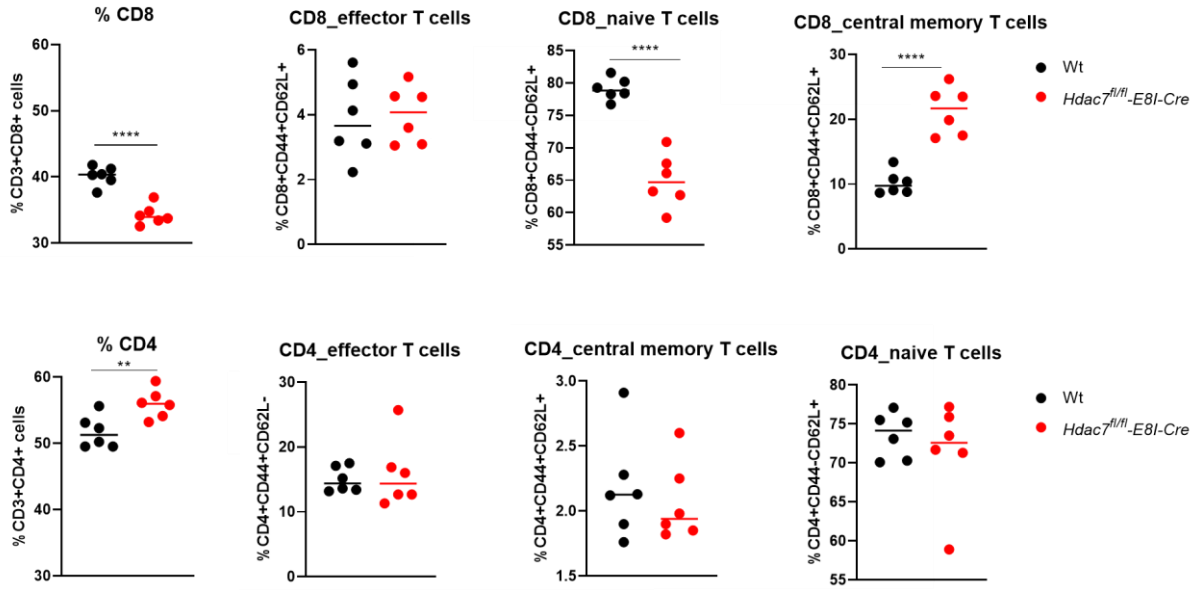

Figure 4-3 Hdac7 deletion in CD8⁺ T cells results in their decreased frequency and pre-activated phenotype. *The frequencies of CD8⁺ T cells, effector, naïve and central memory CD8⁺ T cells (upper panel). The frequencies of CD4⁺ T cells, effector, naïve and central memory CD8⁺ T cells (lower panel). n=6, multiple t test, **p<0.01, ****p<0.0001*

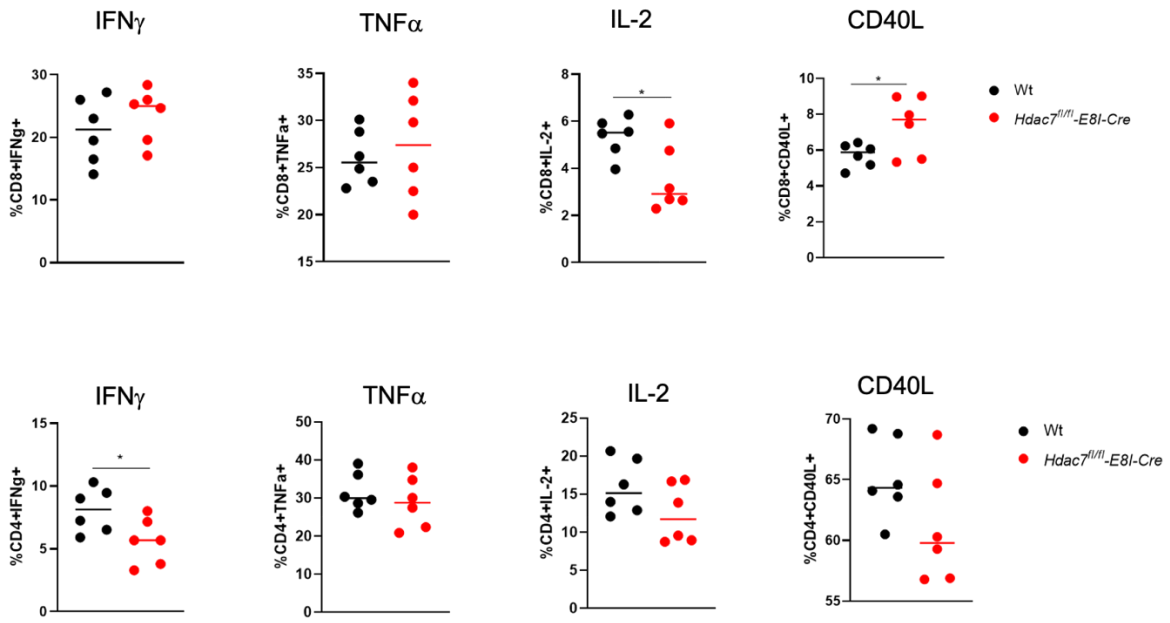

Figure 4-4 Hdac7 deletion in CD8⁺ T cells results in decreased IL-2 production and increased CD40L expression. *Interferon γ (IFNγ), tumor necrosis factor α (TNFα), interleukin 2 (IL-2) production and CD40 ligand (CD40L) expression in CD8⁺ T cells (upper panel) and CD4⁺ T cells (lower panel) upon PMA/ionomycin stimulation in the presence of brefeldin A for 6 h. n=6, multiple t test, *p<0.05*

4.4 *Hdac7* deletion in CD8⁺ T cells results in decreased cell growth due to impaired survival

To understand which pathways could be affected by the lack of *Hdac7* in CD8⁺ T cells, we analyzed comparative bulk RNA-seq data from in vitro activated wt and *Hdac7*^{ko} CD8⁺ T cells. Our analysis revealed that pathways related to cellular amino acid metabolism and apoptosis were enriched in activated *Hdac7*^{ko} CD8⁺ T cells compared to wt CD8⁺ T cells **(Figure 4-5)**.

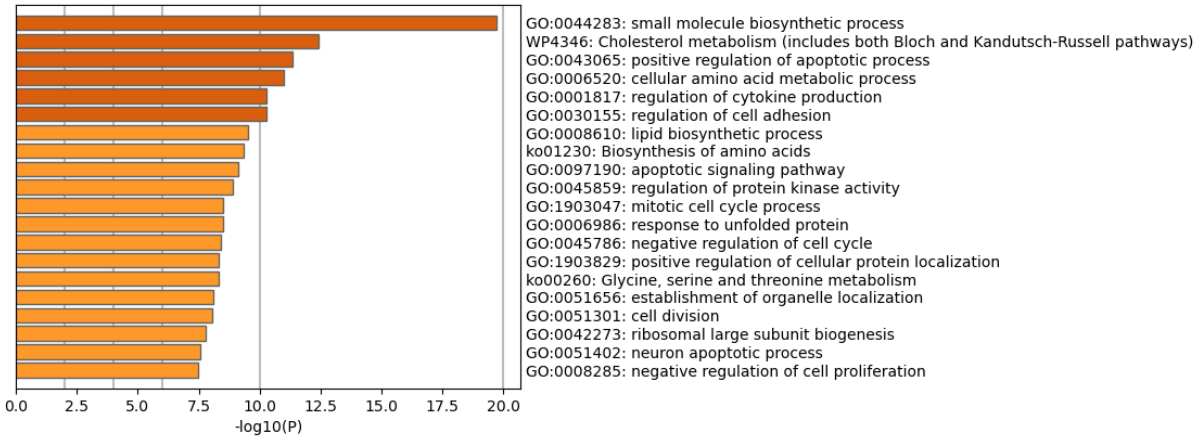

Figure 4.5 RNA-seq pathway analysis. *Naïve wild type (wt) and Hdac7^{ko} CD8⁺T cells were in vitro activated with anti-CD3 and anti-CD28 antibodies for 48 h and RNA samples were prepared for bulk RNA sequencing. Pathway analysis was performed. Bar graph shows -log$_{10}$(P value) of significantly enriched pathways in Hdac7^{ko} CD8⁺ T cells compared to wt.*

To investigate the role of HDAC7 in CD8$^+$ CTL, we established an in vitro CTL differentiation protocol. Briefly, CD8$^+$ T cells were isolated from the splenocytes of *Hdac7$^{fl/fl}$-CD4-Cre-OT1* (*Hdac7^{ko}*) mice or wt littermates by negative selection and in vitro activated with plate-bound anti-CD3 and anti-CD28 antibodies in the presence of recombinant murine IL-2. After 48 hours, antibodies were washed away, and cells were continued to grow in the presence of IL-2 for an additional five days to allow their differentiation into CTL. On day 7, in vitro experiments to investigate the role of HDAC7 in CTLs were performed.

To assess if *Hdac7* deletion affect the cellular growth of CD8$^+$ T cells during CTL differentiation, cells were counted every other day. It was observed that *Hdac7^{ko}* CD8$^+$ T cells had impaired cell growth as assessed by cell numbers **(Figure 4-6)**. We proposed that the reduced numbers of *Hdac7^{ko}* CD8$^+$ T cells might result from their reduced proliferative capacity and/or survival due to increased apoptosis. To determine whether *Hdac7*-deficiency leads to a defective proliferation, a CFSE dilution assay was performed which did not reveal any difference between proliferative capacity when comparing wt and *Hdac7^{ko}* CD8$^+$ T cells as assessed by percentage of divided cells and proliferation index **(Figure 4-6)**.

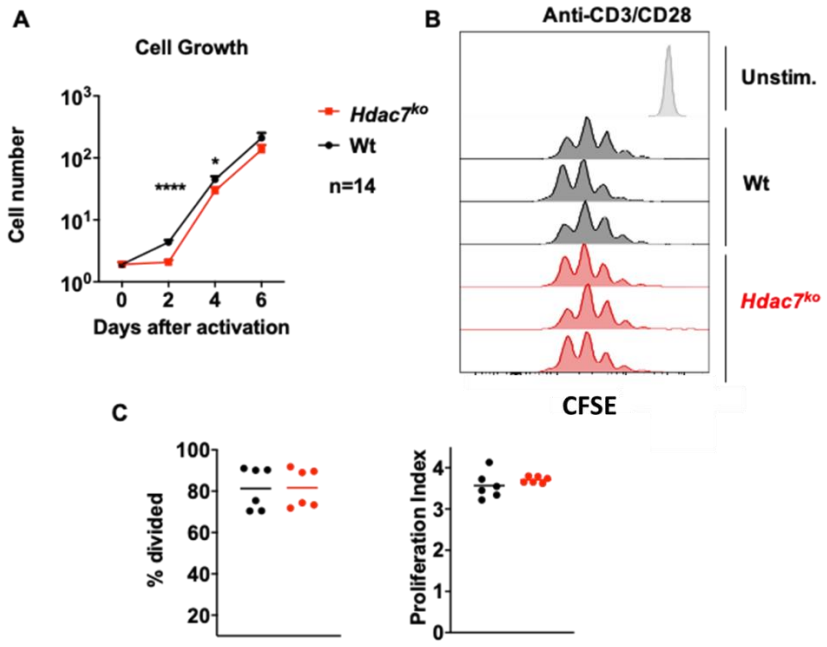

Figure 4-6 Hdac7 deletion results in impaired cell growth despite unchanged proliferative capacity in CD8$^+$ T cells. (A) *Cell growth as assessed by numbers of wild type (wt) and Hdac7^{ko} CD8$^+$ T cells during cytotoxic T lymphocyte (CTL) differentiation. Cells were counted every 48 h. (Four independent experiments, n=14).* ***(B)*** *Primary FACS plots for carboxyfluorescein diacetate succinimidyl ester (CFSE) dilution assay to examine proliferation of wt and Hdac7^{ko} CD8$^+$ T cells. CFSE labeled wt and Hdac7^{ko} CD8$^+$ T cells were activated with anti-CD3 and anti-CD28 antibodies and after 3 days, CFSE signals were analyzed by flow cytometry.* ***(C)*** *percentage of divided cells (left) and proliferation index calculated by FlowJo software according to CFSE signals. Two independent experiments, n=6. Multiple t test, ****p<0.0001, *p<0.05*

RNA-sequencing data from in vitro activated wt and *Hdac7*^{ko} CD8$^+$ T cells showed that several pro-apoptotic genes were significantly upregulated in the absence of HDAC7 **(Figure 4-7)**. Among other pro-apoptotic genes, *Fasl* popped up as the top hit in the transcriptome of activated *Hdac7*^{ko} CD8$^+$ T cells and we could validate this upregulation at the protein level by flow cytometry **(Figure 4-7)**. To compare the survival of wt and *Hdac7*^{ko} CD8$^+$ T cells, cells were stained with annexin V and PI and analyzed by flow cytometry. Thereby, the percentage of annexin V$^+$ and PI$^+$ cells was significantly higher in *Hdac7*^{ko} CD8$^+$ T compared to wt cells suggesting a role of HDAC7 for the survival of CD8$^+$ T cells.

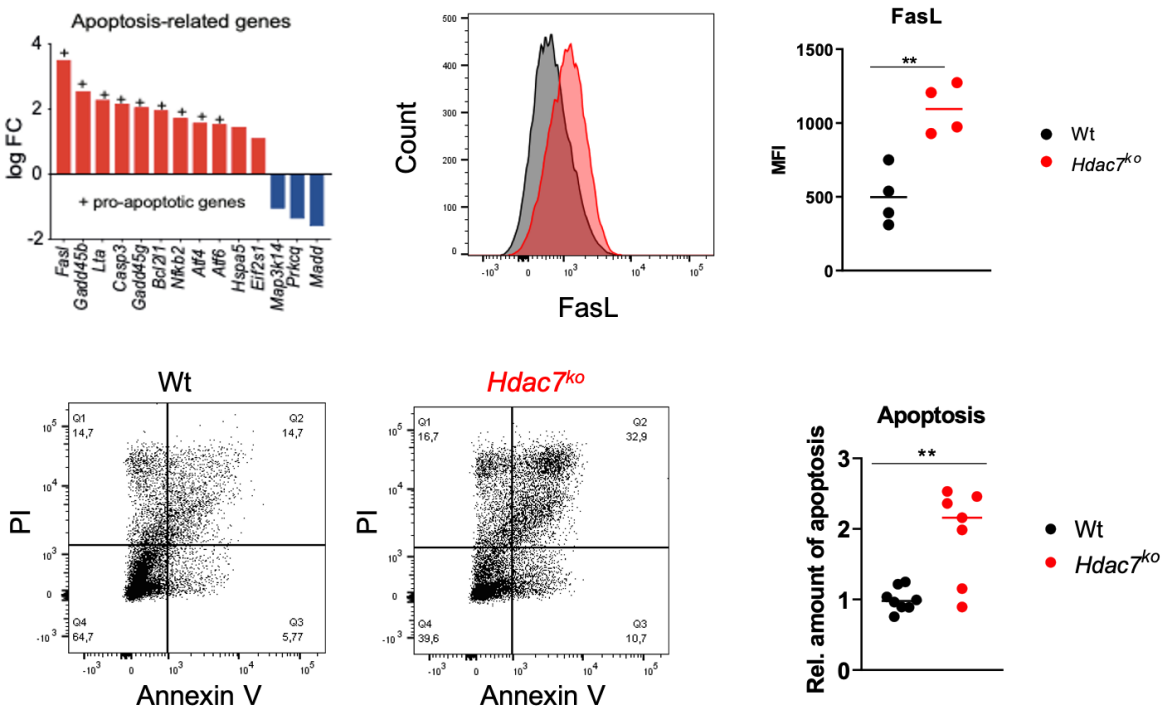

Figure 4-7 Hdac7^{ko} CTLs have increased apoptosis. *(Upper panel) Fold change expression of selected pro-apoptotic genes from RNA-seq of naïve CD8$^+$ T cells that were in vitro activated with anti-CD3 and anti-CD28 antibodies for 48 h. The upregulation of the top hit Fasl gene was confirmed at the protein level by flow cytometry, n=4, multiple t test (lower panel) CD8$^+$ T cells isolated from wt and Hdac7^{ko} mice were differentiated into CTLs for seven days as described. Apoptosis in wt and Hdac7^{ko} were measured by annexin V PI staining followed by flow cytometry analysis. Representative primary FACS plots depicting the percentages of annexin V$^+$PI$^+$ cells (left) and relative amount of apoptosis as determined by annexin V$^+$PI$^+$ population (right). The percentage of annexin V$^+$PI$^+$ cells was normalized to the mean of wt. Three independent experiments, n=7-8. Multiple t test, **p<0.01*

4.5 *Hdac7* deletion in CD8$^+$ T cells does not affect their cytotoxicity

Since CTL clear their targets such as virus infected cells or tumor cells through direct cytotoxicity, an *in vitro* co-culture method was established to investigate if *Hdac7*-deficiency has any effect on the direct killing capacity of CTLs. Briefly, *in vitro* differentiated wt-OT1 and *Hdac7*^{ko}-OT1 CD8$^+$ T cells isolated from *Hdac7*$^{fl/fl}$*CD4-Cre-OT1-Thy1.1* mice and wt littermates,

and subsequently differentiated into antigen-specific CTLs which can recognize chicken ovalbumin (Ova) peptide. Then, wt-OT1 or *Hdac7*^{ko}-OT1 CTLs were co-cultured with CFSE-labeled EG.7-Ova cells, which express chicken Ova and represent a widely used tool to study the antigen-specific responses of CD8$^+$ T cells. After 2 h of incubation, cells were stained with annexin V to determine the apoptosis in target EG.7-Ova cells induced by the cytotoxicity of wt or *Hdac7*^{ko} CTLs. However, no difference was observed between the killing capacities of wt and *Hdac7*^{ko} CTLs as the amount of apoptosis induced in target EG.7-Ova cells was not significantly different, suggesting that *Hdac7*-deletion in CD8$^+$ T cells is not required for their cytotoxicity against tumor cells **(Figure 4-8)**.

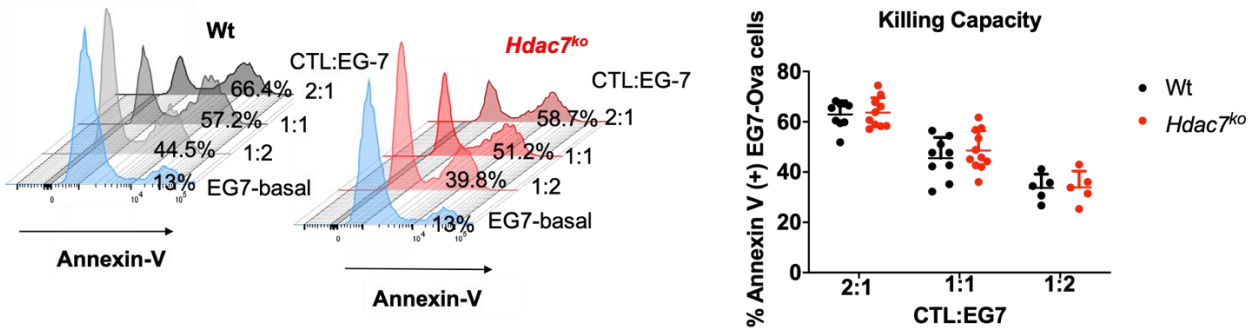

Figure 4-8 Hdac7-deficiency in CTLs does not affect their cytotoxicity. *Wild type (wt)-OT1 and Hdac7*^{ko}*-OT1 CD8*$^+$ *T cells were differentiated into cytotoxic T lymphocytes (CTLs) for 7 days and co-cultured with carboxyfluorescein diacetate succinimidyl ester (CFSE)-labeled EG.7-Ova cells at different CTL:EG.7-Ova ratios for 2 h. Cells were stained with annexin V and analyzed by flow cytometry to measure the apoptosis in EG.7-Ova cells induced by the direct cytotoxicity of wt-OT1 and Hdac7*^{ko}*-OT1 CTLs. Primary FACS plots showing the percentage of annexin V*$^+$ *EG.7-Ova cells for different CTL:EG.7-Ova ratios (left). Dot plots depicting the killing capacity of wt-OT1 and Hdac7*^{ko}*-OT1 as the percentage of annexin V*$^+$ *EG.7-Ova cells for different CTL:EG.7-Ova ratios (right). Four independent experiments, n=9-11 for 2:1 and 1:1 ratio, n=5 for 1:2 ratio.*

4.6 HDAC7 regulates amino acid metabolism in CD8$^+$ T cells and mTOR signaling

Metabolism of CD8$^+$ T cells is tightly regulated during their differentiation states and essential for their proper immune responses including cytotoxicity against tumor cells as well as their memory function. For instance, activated and effector CD8$^+$ T cells mainly depend on glycolysis, whereas memory CD8$^+$ T cells switch to mitochondrial metabolism and FAO. Therefore, metabolic states of wt and *Hdac7*^{ko} CTLs were compared by using Seahorse extracellular efflux measurements, which allows for real-time tracing of the cellular metabolism upon manipulations via drugs or inhibitors. By using this technology, glycolysis and mitochondrial metabolism as well as glutamine uptake of wt and *Hdac7*^{ko} CTLs were measured. While no difference between glycolysis and mitochondrial metabolism in wt and

Hdac7^{ko} CD8^{+} T cells was observed, *Hdac7*^{ko} CTLs had significantly higher glutamine uptake when they were pulsed with glutamine after starvation **(Figure 4-9)**. These results were also consistent with the RNA-sequencing data which showed the upregulation of several amino acid metabolism-related genes in *in vitro* anti-CD3 and anti-CD28 activated *Hdac7*^{ko} compared to wt CD8^{+} T cells. Hence, HDAC7 is not required for glycolysis and mitochondrial metabolism of CD8^{+} T cells, but it is an important factor for the regulation of amino acid metabolism in CD8^{+} T cells **(Figure 4-9)**.

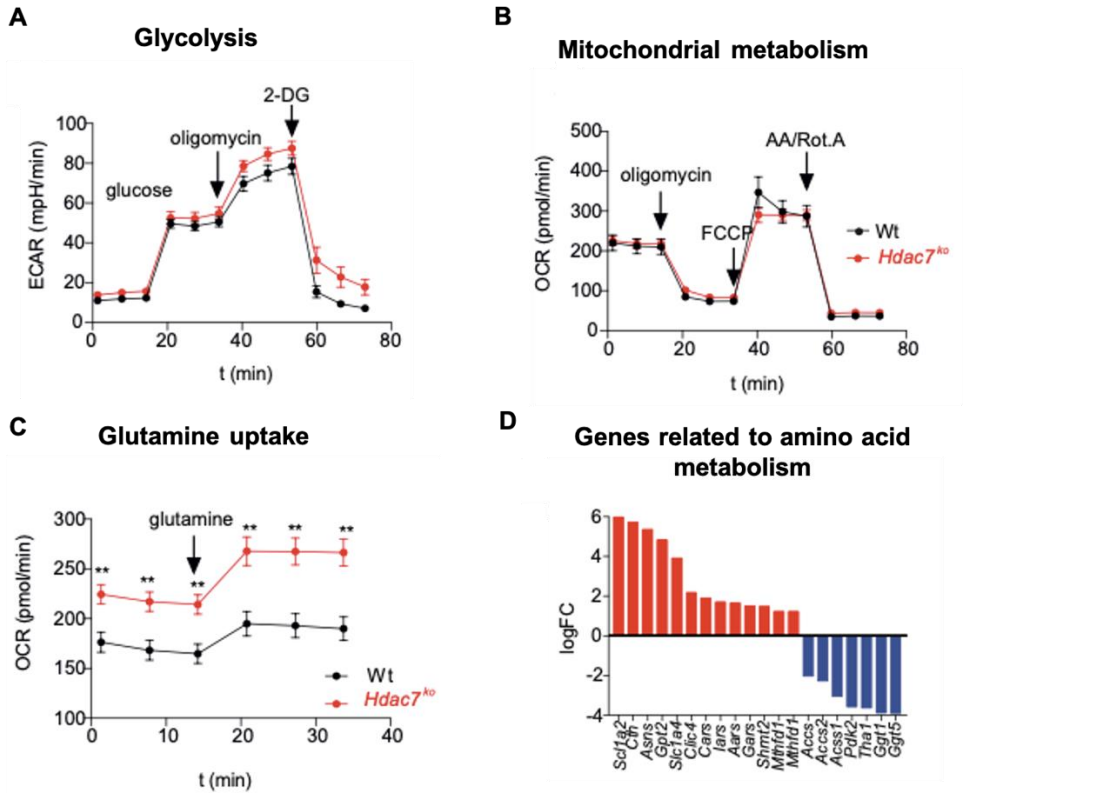

Figure 4-9 HDAC7 regulates amino acid metabolism in CTLs. *Metabolic Seahorse flux measurements of wild type (wt) and Hdac7*^{ko} *cytotoxic T lymphocytes (CTLs) 7 days post activation.* ***(A)*** *Glycolysis levels as assessed by extracellular acidification rate (ECAR) values measured in response to 10 mM glucose, 1 µM oligomycin and 50 mM 2-deoxy-D-glucose (2-DG) treatment (n=3, biologically independent samples).* ***(B)*** *Mitochondrial respiration levels assessed by oxygen consumption rate (OCR) values measured in response to 2 µM oligomycin, 1 µM fluorocarbonyl cyanide phenylhydrazone (FCCP) and 0.5 µM rotenone/antimycin A (RotA/AA) treatment (n=3, biologically independent samples).* ***(C)*** *Glutamine uptake assessed by OCR levels measured in response to 4 mM glutamine treatment. Error bars indicate mean ± SEM.* ***(D)*** *Fold change expression of amino acid metabolism related genes in Hdac7*^{ko} *CD8*$^{+}$ *T compared to wt cells from RNA-sequencing.*

Since mTOR signaling is a very central pathway which regulates the amino acid metabolism as well as the survival of T cells, mTOR protein levels between wt and *Hdac7*^{ko} CTLs were compared by immunoblotting. Here total mTOR protein was significantly decreased in *Hdac7*^{ko} CTLs compared to wt CTLs **(Figure 4-10)**. Similar reductions were observed for mTORC1 and mTORC2 proteins which were distinguished by phosphorylation at serine residues 2481 and

2448, respectively **(Figure 4-10)**. These results suggested that mTOR signaling was impaired in *Hdac7*^{ko} CTLs in line with their impaired survival and altered amino acid metabolism.

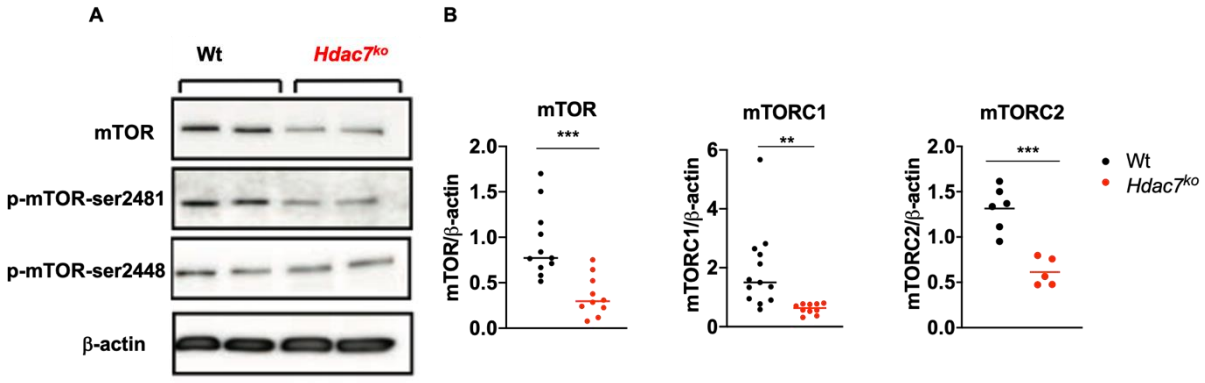

Figure 4-10 Hdac7 deletion results in impaired mTOR signaling in CTLs. (A) *Immunoblot analysis of total mammalian target of rapamycin (mTOR), phospho-mTOR-ser-2481 (mTORC2), phospho-mTOR-ser-2448 (mTORC1) and β-actin in cytotoxic T lymphocytes (CTLs) on day 7, representative of 3 independent experiments.* ***(B)*** *Fold-change expression of total mTOR, mTORC1 and mTORC2 in wild type (wt) and Hdac7*^{ko} *CTLs (right). ImageJ software (National Institutes of Health, USA) was used for the calculation of the intensity of the protein bands. Values were normalized to the intensity of the corresponding β-actin bands and then the mean of wt. Three independent experiments, n=10-11 for total mTOR and mTORC1, n=5-6- for mTORC2. Multiple t test, **p<0.01, ***p<0.0001*

4.7 HDAC7 regulates SOCE signaling and IFNγ production in CD8$^+$ T cells

Store-Operated Calcium Entry (SOCE) signaling is a crucial calcium influx pathway in T cells and it regulates cellular metabolism as well as the key functions of T cells including their effector functions and cytokine production. Recently, SOCE was shown to be an upstream regulator of mTOR signaling (Vaeth et al., 2017). Therefore, the signaling strength of SOCE pathway was compared between wt and *Hdac7*^{ko} CTLs. Briefly, the basal levels of calcium influx in wt and *Hdac7*^{ko} CTLs was measured followed by a second measurement after the treatment of cells with Thapsigargin to deplete the ER-calcium stores to induce SOCE signaling. The third measurement was performed in the presence of a higher calcium concentration to better determine the signaling strength of SOCE in these cells. According to these measurements, *Hdac7*^{ko} CTLs displayed significantly reduced SOCE-dependent calcium influx compared to wt CTLs suggesting a role of HDAC7 for the regulation of SOCE in CTLs **(Figure 4-11)**. RNA-sequencing of *in vitro* anti-CD3 and anti-CD28 activated CD8$^+$ T cells also showed that SOCE-related genes including *Stim2* and *Orai2* which are among the main components of SOCE were downregulated in *Hdac7*^{ko} CD8$^+$ T cells compared to wt further pointing to a role of HDAC7 for the regulation of SOCE in CD8$^+$ T cells **(Figure 4-11)**.

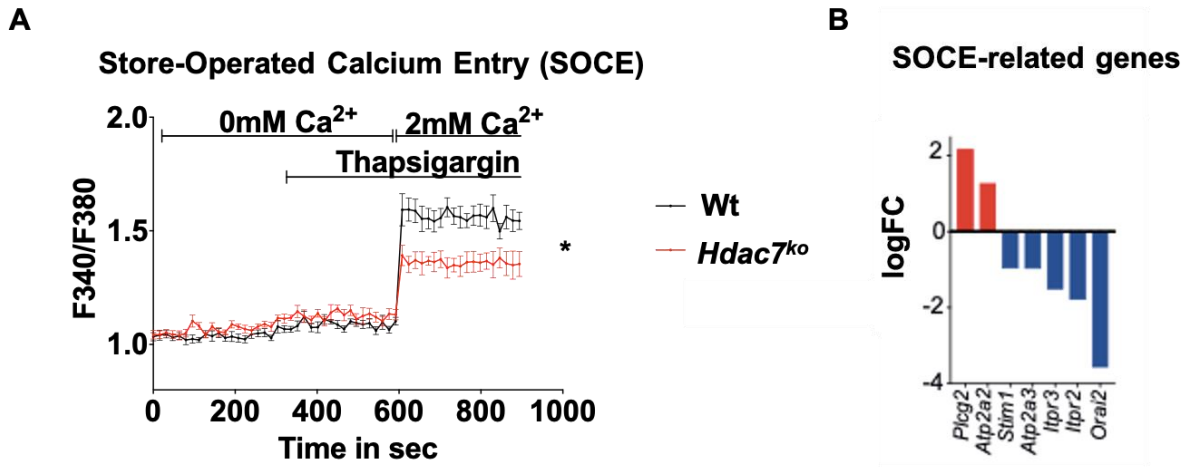

Figure 4-11 HDAC7 regulates SOCE signaling in CD8⁺ T cells. (A) *Calcium influx in wild type (wt) and Hdac7^{ko} CTLs, mean ± SEM of Ca^{2+} influx rates. n=3 independent experiments, performed in duplicates. Multiple t test*p<0.05.* ***(B)*** *Fold-change expression of store-operated calcium entry (SOCE)-component genes from comparative RNA-sequencing (for all p<0.05, n=3 biologically independent samples per group).*

Since SOCE is a central regulator of cytokine production and the effector functions of CD8$^+$ T cells, IFNγ production in wt-OT1 and *Hdac7^{ko}*-OT1 CTLs were measured in response to either Ovalbumin (Ova peptide) as well as PMA/ionomycin stimulation. Subsequently, cells were intracellularly stained for IFNγ and analyzed by flow cytometry. It was observed that the frequency of IFNγ producing *Hdac7^{ko}* CTLs were significantly lower compared to wt CTLs under both Ova peptide and PMA/ionomycin stimulation conditions **(Figure 4-12)**. These results suggested that *Hdac7* deletion in CD8$^+$ T cells might impair SOCE signaling, thus the IFNγ production, which represents the key cytokine necessary for anti-tumor immune functions of CD8$^+$ T cells.

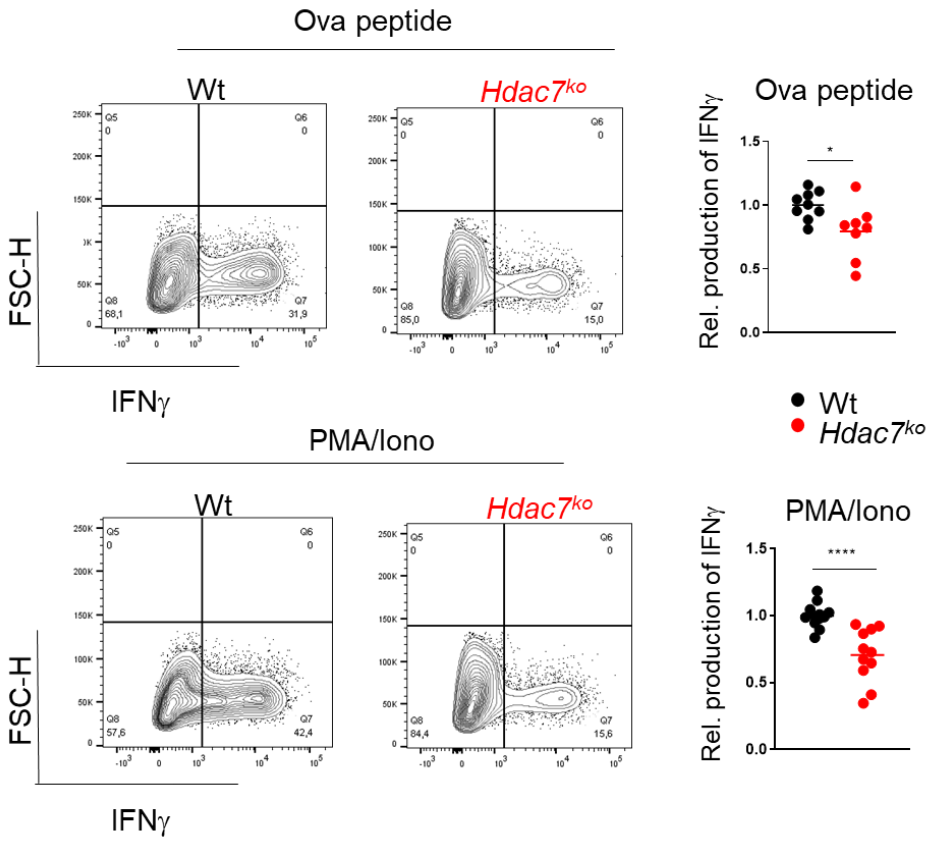

Figure 4-12 The lack of Hdac7 in CD8⁺ T cells impairs IFNγ production. *Wild type (wt) or Hdac7^{ko} cytotoxic T lymphocytes (CTLs) were stimulated with Ova peptide (upper panel) or PMA/ionomycin (lower panel). Representative primary FACS plots showing the frequency of interferon γ (IFNγ) producing CTLs (left) and dot plots comparing the relative IFNγ production in wt and Hdac7^{ko} CTLs. Values were normalized to the mean of wt CTLs. n=8-9 for Ova peptide and n=10-11 for PMA/ionomycin. Multiple t test, *p<0.05, ****p<0.0001.*

4.8 *Hdac7^{ko}* mice have uncontrolled tumor growth due to impaired anti-tumor responses of CD8⁺ T cells

Taking into consideration that *Hdac7*-deficiency in CD8⁺ T cells leads to impaired survival, amino acid metabolism as well as deregulated SOCE and mTOR signaling, we investigated if anti-tumor immune responses of CD8⁺ T cells were also affected in *Hdac7^{ko}* mice. To test this hypothesis, we challenged *Hdac7^{ko}* mice and wt littermates with EG.7-Ova lymphoma cells by intradermal injections and followed the tumor growth over time by measuring tumor volumes every other day. After two weeks, all mice were sacrificed to directly measure the tumor weights allowing a more accurate comparison of tumor sizes between wt and *Hdac7^{ko}* mice. While most of the wt mice presented with either small or rejected tumors, tumors with significantly higher volumes were observed in *Hdac7^{ko}* mice, suggesting a role of HDAC7 in CD8⁺ T cells for their proper anti-tumor immune functions **(Figure 4-13)**.

Since *Hdac7*^{ko} mice (*Hdac7*$^{fl/fl}$*CD4-Cre*) mice harbor deletion of *Hdac7* in both CD4^{+} and CD8^{+} T cells, we investigated whether the effects of HDAC7 on the tumor growth control was CD8^{+} T cell intrinsic. For this purpose, we similarly injected *Hdac7*$^{fl/fl}$*E8I-Cre* mice, in which *Hdac7* is exclusively deleted in CD8^{+} T cells, with EG.7-Ova cells and measured tumor growth every other day to eliminate the possible contribution of CD4^{+} T cells to this phenotype. Similar to *Hdac7*$^{fl/fl}$*CD4-Cre* mice, *Hdac7*$^{fl/fl}$*E8I-Cre* mice had tumors with significantly higher volumes compared to wt littermates **(Figure 4-13)**. Thus, the role of HDAC7 for the proper anti-tumor immune response was restricted to CD8^{+} T cells.

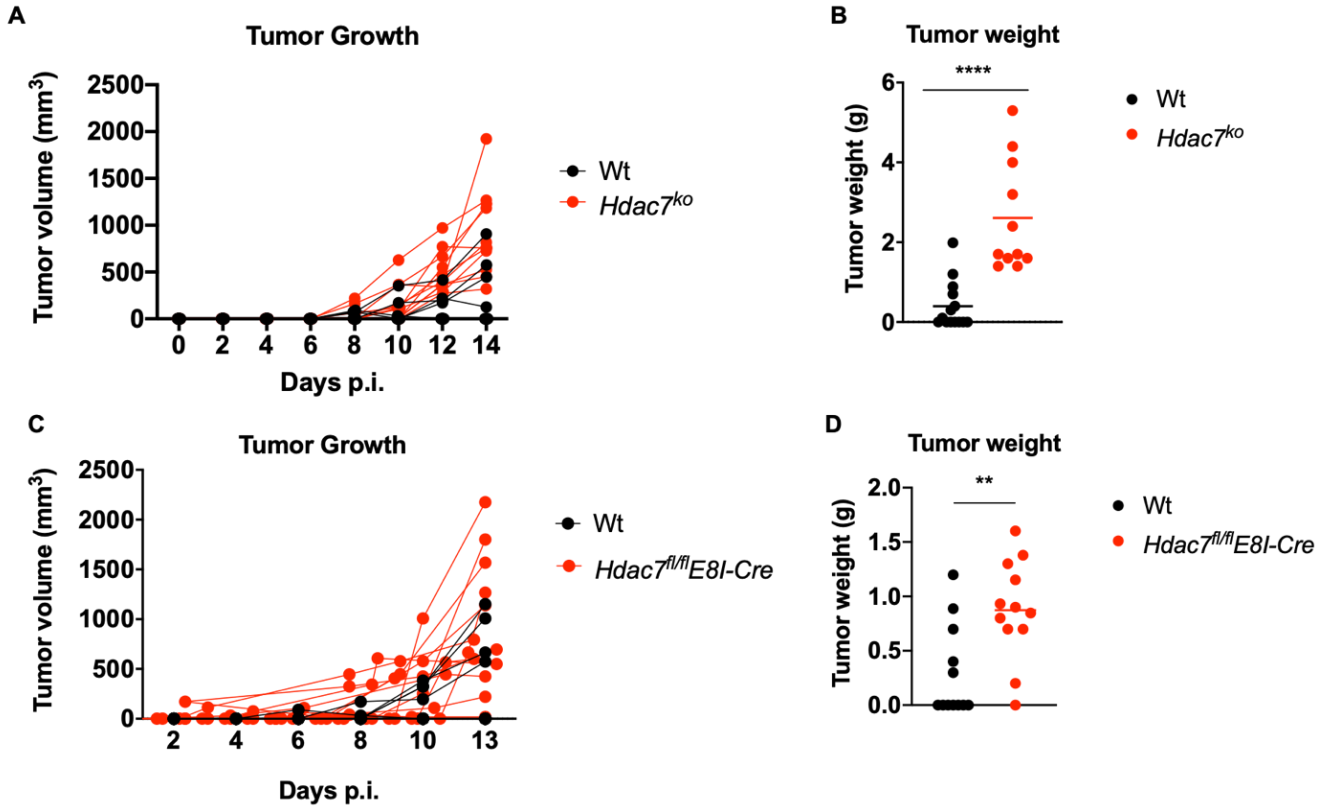

Figure 4-13 Hdac7^{ko} mice have uncontrolled tumor growth when challenged with EG.7-Ova cells. *Wild type (wt) and Hdac7$^{fl/fl}$Cd4-Cre (Hdac7^{ko}) mice were intradermally (i.d.) injected with 1x10^{6} EG.7-Ova cells. Tumor growth was followed for 14 days.* ***(A)*** *Tumor growth in wt and Hdac7^{ko} mice shown as increase in tumor volumes (n=12-14 mice per group).* ***(B)*** *Tumor weight in wt and Hdac7^{ko} mice on day 14 after tumor inoculation (n=12-14 animals per group).* ***(C)*** *Tumor growth in wt and Hdac7$^{fl/fl}$E8ICre mice (n=12-14).* ***(D)*** *Tumor weight in wt and Hdac7$^{fl/fl}$E8ICre mice on day 14 after tumor inoculation (n=12-14 mice per group). 3 independent experiments. Multiple t test, **p<0.01, ****p<0.0001*

To investigate the mechanism that led to the impaired tumor growth in *Hdac7*^{ko} mice, we performed histologic analysis of EG.7-Ova tumor tissues from both wt and *Hdac7*^{ko} mice. Tumors from *Hdac7*^{ko} mice displayed lower numbers of tumor infiltrating CD8^{+} T cells compared to tumors from wt mice, suggesting a mechanism for increased tumor growth in *Hdac7*^{ko} mice **(Figure 4-14)**.

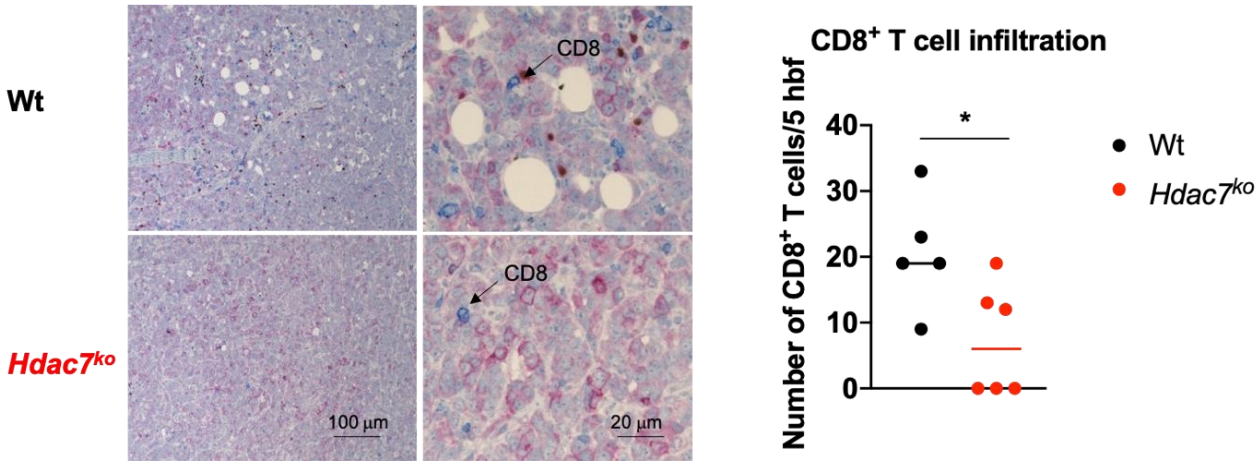

Figure 4-14 Hdac7^{ko} mice have reduced CD8^{+} T ell infiltration into tumors. *Representative images from histological analysis of EG.7-Ova tumors in wild type (wt) (above) and Hdac7^{ko} (below) mice (CD8= blue, CD4=red, Foxp3=brown) and number of tumor-infiltrating CD8^{+} T cells per 5 high power fields (hpf) in EG.7-Ova tumors in wt and Hdac7^{ko} mice 14 days p.i. n=5-6 mice per group. Multiple t test, *p<0.05*

We postulated that reduced CD8^{+} T cell infiltration into the tumors in *Hdac7^{ko}* mice could result from a homing deficiency of *Hdac7*-deficient CD8^{+} T cells into the tumors or a reflection of reduced CD8^{+} T cells in *Hdac7^{ko}* mice. To test whether the deletion of *Hdac7* in CD8^{+} T cells interferes with their homing capacity, an *in vivo* homing experiment was performed. For this purpose, tumors were established in wt mice by intradermal injection of chicken Ova expressing melanoma cell line B16-Ova. Tumor-bearing mice were adoptively transferred with *in vitro* differentiated CFSE-labeled wt-OT1 or *Hdac7^{ko}*-OT1 CTLs by intravenous injection. After 2 h, all mice were sacrificed, tumor infiltrating CTLs were isolated as described and the frequencies of wt-OT1 and *Hdac7^{ko}*-OT1 CTLs within the tumors as well as TDLN were determined by flow cytometry analysis as a readout for the homing capacities of antigen-specific transferred CTLs. There were no significant differences in the frequencies of wt and *Hdac7^{ko}* CTLs mice within B16-Ova tumors as well as TDLN after the adoptive transfer suggesting that HDAC7 deficiency in CTLs does not have any effect in their homing functions **(Figure 4-15)**. Therefore, other mechanisms should be responsible for the reduced CD8^{+} T cell infiltration into EG.7-Ova tumors as well as uncontrolled tumor growth in *Hdac7^{ko}* mice.

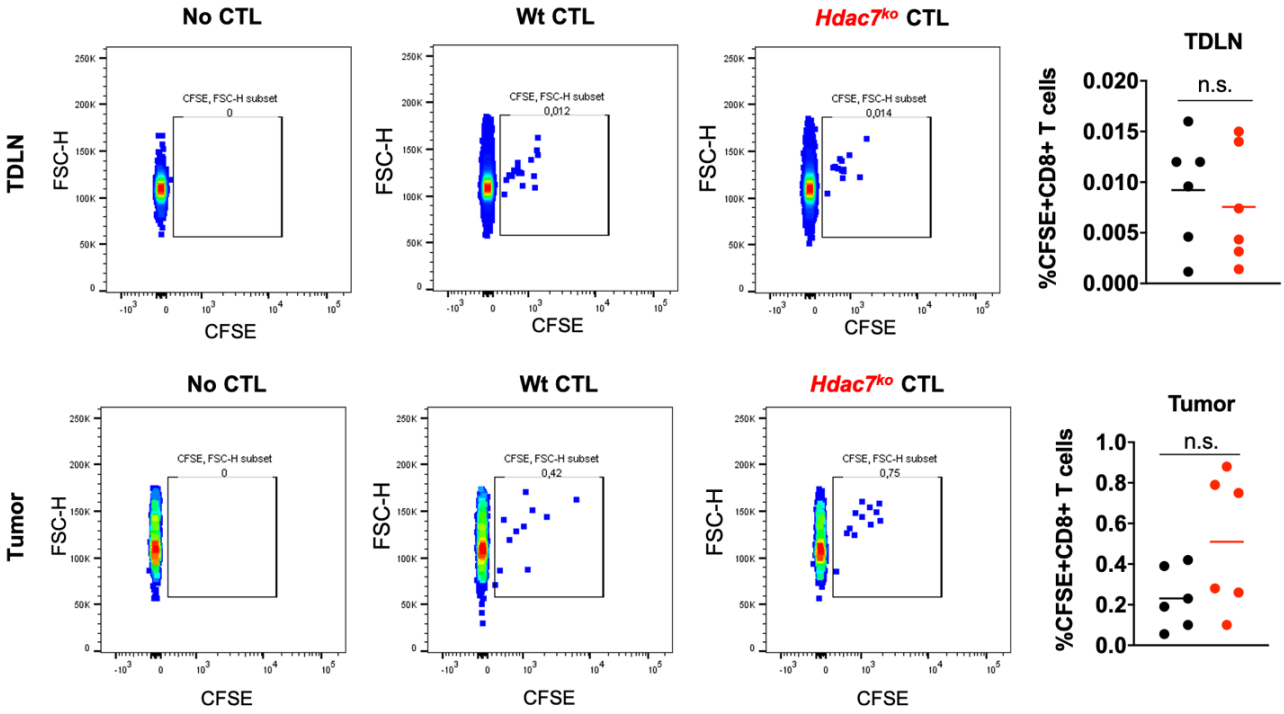

Figure 4-15 Hdac7-deficiency does not interfere with the homing capacity of CTLs*. B16-Ova bearing wild type (wt) mice were intravenously (i.v.) injected with carboxyfluorescein diacetate succinimidyl ester (CFSE)-labeled wt-Ot1 or Hdac7^{ko}-Ot1 cytotoxic T lymphocytes (CTLs) and sacrificed after 90 min. The frequencies of CFSE-high CD8^{+} T cells in tumor draining lymph nodes (TDLN) (upper panel) and tumors (lower panel) were assessed by flow cytometry (right). (n=6 mice per group). Multiple t test, n.s. p>0.05*

Given that the lack of *Hdac7* does not affect the homing capacities of CTLs, we hypothesized that the reduced numbers of infiltrating CTLs within tumors mice could be a reflection of a general decrease in the numbers of *Hdac7*-deficient CD8^{+} T cells in *Hdac7^{ko}* mice. To test this hypothesis, *Hdac7^{ko}* mice were transferred with *in vitro* differentiated wt-OT1-Thy1.1^{+} or *Hdac7^{ko}*-OT1-Thy1.1^{+} CTLs at equal numbers along with the intradermal injection of EG.7-Ova cells on the same day. This experimental setup allowed us to track the frequencies of transferred OVA-specific CTLs in case of their antigen encounter provided by OVA-expressing EG.7-Ova cells. On day-5 after transfer, blood samples were collected from all mice and the frequencies of Thy1.1 wt or *Hdac7^{ko}* mice to validate the successful adoptive transfer procedure **(Figure 4-16)**. In the blood samples, a significant difference was observed between the frequencies of wt-OT1-Thy1.1 and *Hdac7^{ko}*-OT1-Thy1.1 CTLs suggesting that the *Hdac7^{ko}*-CTLs have decreased cell numbers even at early timepoints after the transfer **(Figure 4-16)**. We then sacrificed all the mice on day 7 and collected spleens and lymph nodes to compare the frequencies of transferred wt-OT1-Thy1.1^{+} or *Hdac7^{ko}*-OT1-Thy1.1 CTLs in the mice. There was a significant reduction in the frequencies of transferred *Hdac7^{ko}*-OT1-Thy1.1 CTLs compared to transferred wt CTLs suggesting a role of HDAC7 for the regulation of cell numbers

of CD8⁺ T cells *in vivo* **(Figure 4-16)**. Therefore, decreased cell numbers in *Hdac7*^{ko} mice could be one of mechanisms explaining impaired CD8⁺ T cell infiltration within tumors and deterred tumor growth control.

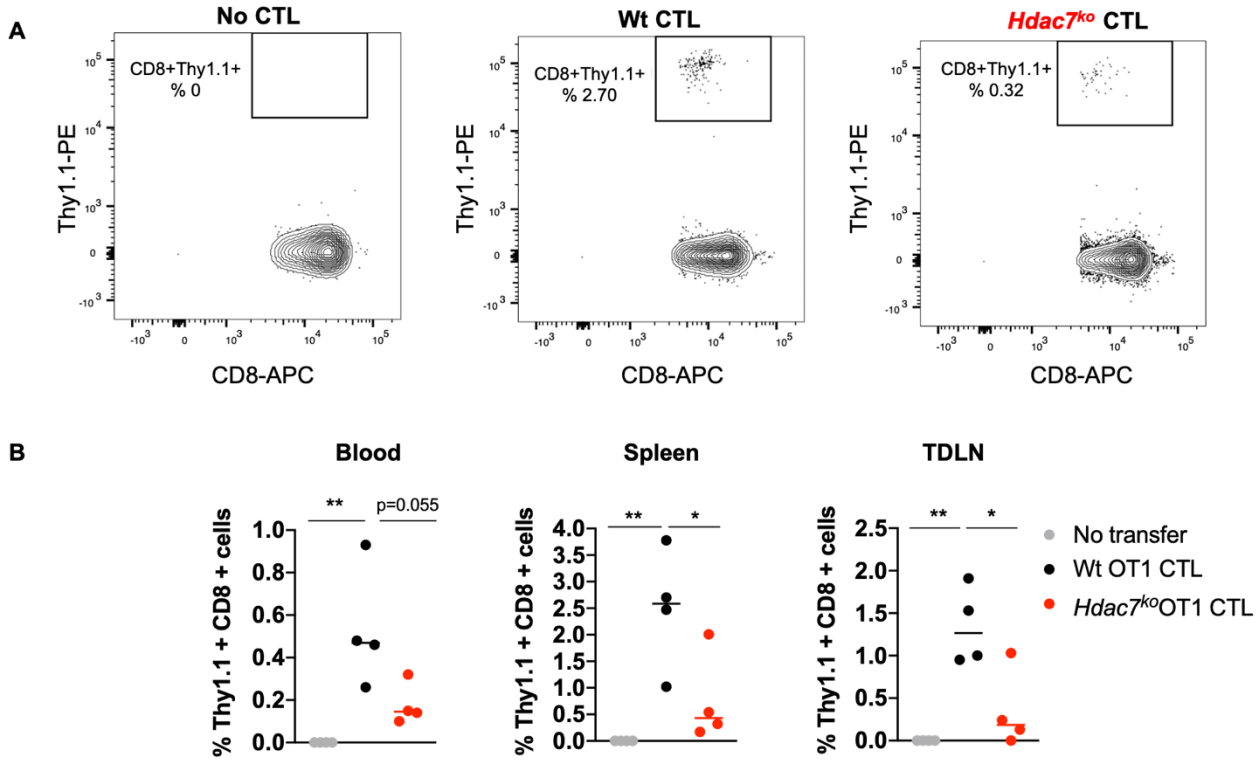

Figure 4-16 HDAC7 is important to maintain adequate cell numbers of CTLs in vivo (A) *Representative FACS plots showing the frequencies of adoptively transferred Thy1.1⁺ cytotoxic T lymphocytes (CTLs) in the spleens in mice without CTL transfer (no CTL), mice transferred with wild type (wt)-OT1 CTL and Hdac7*^{ko}*-OT1 CTL on day-7.* ***(B)*** *Dot plots showing the frequencies of transferred CD8⁺Thy1.1⁺ wt-OT1 and Hdac7*^{ko}*-OT1 CTLs in blood (day-5 after transfer), spleen (day-7 after transfer) and tumor draining lymph node (TDLN) (day-7 after transfer) of mice. n=4, multiple t test, *p<0.05, **p<0.01*

4.9 *Hdac7* deletion results in increased apoptosis and an exhausted phenotype in tumor infiltrating CD8⁺ T cells

We showed that *Hdac7* deletion in CTLs led to their decreased frequencies in blood, secondary lymphoid organs including TDLN and spleen during adoptive T cell transfer experiments if they were transferred simultaneously with antigen-expressing lymphoma cells. To be able to analyze how transferred antigen specific CTLs were affected by the lack of *Hdac7*, we performed so called “rescue” experiments in mice. Briefly, we first established EG.7-Ova tumors in *Hdac7*^{ko} mice by the intradermal injection of tumor cells. Seven days after the injection of tumor cells, mice were divided into three groups in a blinded manner and were transferred with either *in vitro* differentiated wt-OT1 or *Hdac7*^{ko}-OT1 CTLs intravenously, while another group of mice were not transferred to serve as controls. Via this experimental

set up, we were able to compare the anti-tumor responses of wt-OT1 and *Hdac7*^{ko}-OT1 by following the tumor growth. Similarly, we could isolate tumor infiltrating lymphocytes (TIL) as well as the TDLN and the spleens to analyze the cellular exhaustion and the survival of transferred wt-OT1 and *Hdac7*^{ko}-OT1 CTLs.

Over the course of the rescue experiment, we observed that the control mice which were only injected with the tumor cells developed tumors with higher volumes compared to wt-OT1 and *Hdac7*^{ko}-OT1 CTL transferred groups suggesting that the adoptive transfer as well as the tumor cell injections worked properly **(Figure 4-17)**. This observation was also reflected by the tumor weights at day seven after CTL transfer. However, we did not observe any difference between the tumor weights of wt-OT1 and *Hdac7*^{ko}-OT1 transferred mice suggesting that the lack of *Hdac7* in CTLs did not interfere with their ability to control the tumor growth during adoptive transfer experiments **(Figure 4-17)**. However, the frequency of annexin V^{+} *Hdac7*^{ko}-OT1 CTLs was slightly higher compared to wt-OT1 CTLs within tumors as well as TDLN suggesting a role of HDAC7 for the survival of TILs in tumor microenvironment **(Figure 4-17)**.

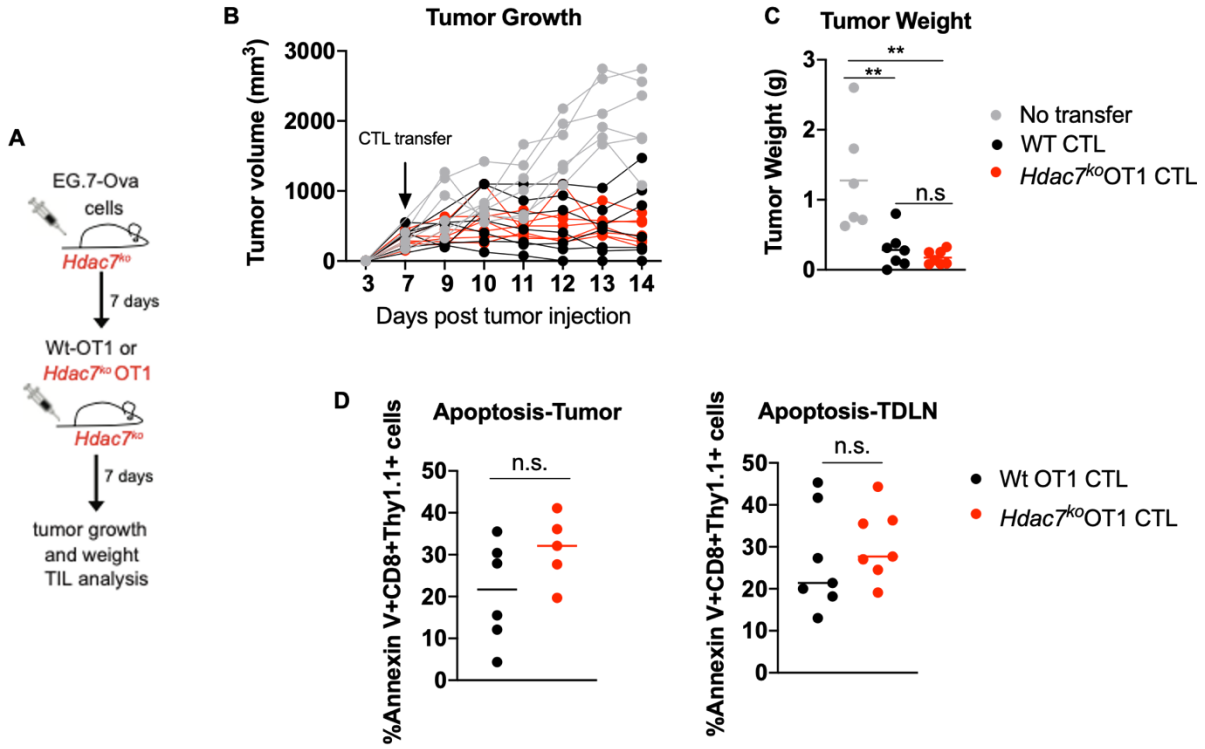

Figure 4-17 Adoptive transfer of antigen specific CTLs rescues the phenotype of Hdac7^{ko} mice. ***(A)*** *Experimental setup* ***(B)*** *Tumor growth over time and (**C**) tumor weights in tumor-bearing Hdac7^{ko} mice transferred with wild type (wt)-OT1 or Hdac7-OT1 cytotoxic T lymphocytes (CTLs) or no transfer. n=6-7 (**D**)The frequency of annexin V^{+}CD8^{+}Thy1.1^{+} wt-OT1 or Hdac7^{ko}-OT1 T cells in tumors (left) and tumor draining lymph nodes (TDLN) in Hdac7^{ko} mice. n=5-7, multiple t test, **p<0.01*

Chronic antigen stimulation in the tumor microenvironment drives tumor infiltrating CD8$^+$ T cells into so called "exhausted phenotype" resulting in immune evasion in tumors. To characterize whether HDAC7 has any role in this process, we analyzed the expression of the key T cell exhaustion markers PD-1 and Tim-3 in adoptively transferred Wt-OT1 and *Hdac7^{ko}*-OT1 CTLs during rescue experiments. We observed a significant increase in the frequency of PD1$^+$Tim-3$^+$ population in tumor infiltrating *Hdac7^{ko}*-OT1 CTLs compared to wt-OT1 CTLs suggesting that the lack of *Hdac7* resulted in an exhausted phenotype of CTLs within tumors where they are exposed to chronic antigen stimulation **(Figure 4-18)**. In line with this observation, within spleens and TDLN, no significant difference was detected in the frequencies of PD1$^+$Tim-3$^+$ populations of transferred Wt-OT1 and *Hdac7^{ko}*-OT1 cells **(Figure 4-18)**.

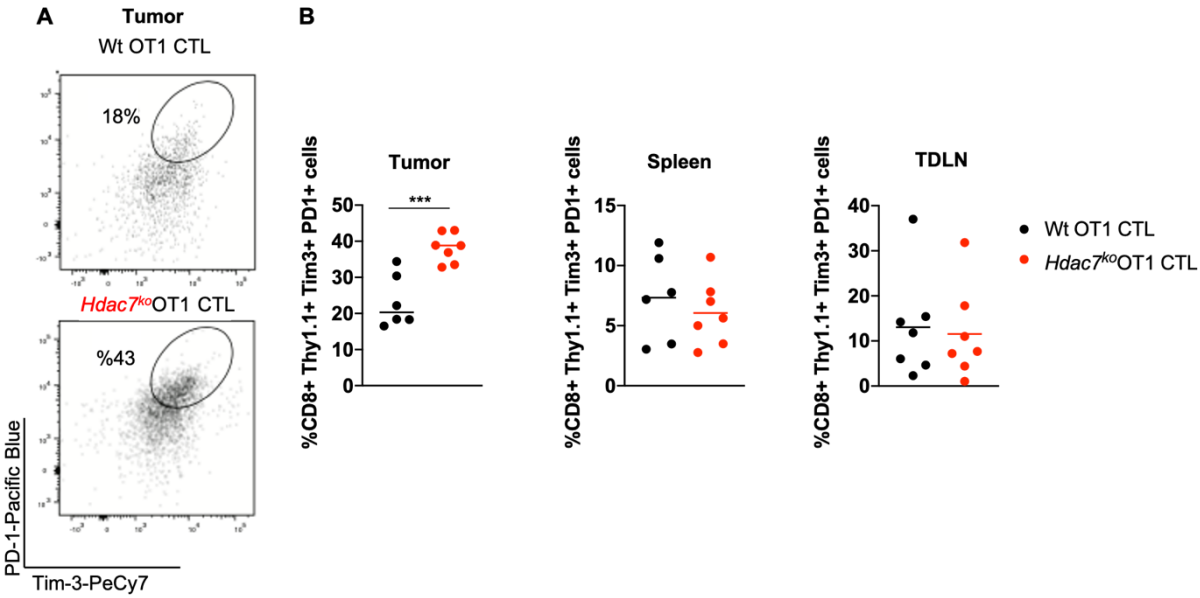

***Figure 4-18 Hdac7 deletion in TILs results in their cellular exhaustion**. **(A)** Representative FACS plots showing the frequencies of PD1$^+$Tim-3$^+$ populations within transferred wild type (wt) OT1 or Hdac7^{ko}OT1 cytotoxic T lymphocytes (CTLs) within tumors. **(B)** Dots plots showing the frequencies of PD1$^+$Tim-3$^+$ populations within transferred wt OT1 and Hdac7^{ko} CTLs within tumors, spleen or tumor draining lymph node (TDLN). Representative of 2 independent experiments. n=6-7, multiple t test, ***p<0.001*

4.10 Transcriptomic analysis characterizes HDAC7 as a regulator of CD8$^+$ T cell exhaustion during anti-tumor immunity

In vivo rescue experiments performed by the adoptive T cell transfers in *Hdac7^{ko}* mice suggested that the lack of *Hdac7* in tumor infiltrating CD8$^+$ T cells results in an increased frequency of PD1$^+$Tim3$^+$ population, which could mark their cellular exhaustion. To gain more insights on the role of HDAC7 in CD8$^+$ T cell exhaustion, we analyzed RNA-sequencing data derived from wt and *Hdac7^{ko}* CD8$^+$ T cells which were isolated from *Hdac7^{ko}* mice and wt

littermates and subsequently activated with anti-CD3 and anti-CD28 antibodies for 48 h. According to RNA-seq, activated *Hdac7*^{ko} CD8^{+} T cells displayed upregulation of several cellular exhaustion related genes **(Figure 4-19)**. For example, in addition to PD-1 and Tim-3 which had increased expression during *in vivo* rescue experiments in TILs, other key checkpoint molecules including Lag-3, Ctla-4, Tigit as well as Eomes were upregulated in *in vitro* activated *Hdac7*^{ko} CD8^{+} T cells compared to wt CD8^{+} T cells. To confirm RNA-seq data at the protein level, we analyzed the protein expression of some of these markers by flow cytometry. According to flow cytometry analysis, PD-1, Tim-3 and Tigit had increased protein expression in anti-CD3 and anti-CD28 activated *Hdac7*^{ko} CD8^{+} T cells compared to wt cells, while no significant difference was observed in Lag-3 and Ctla-4 expressions **(Figure 4-19)**.

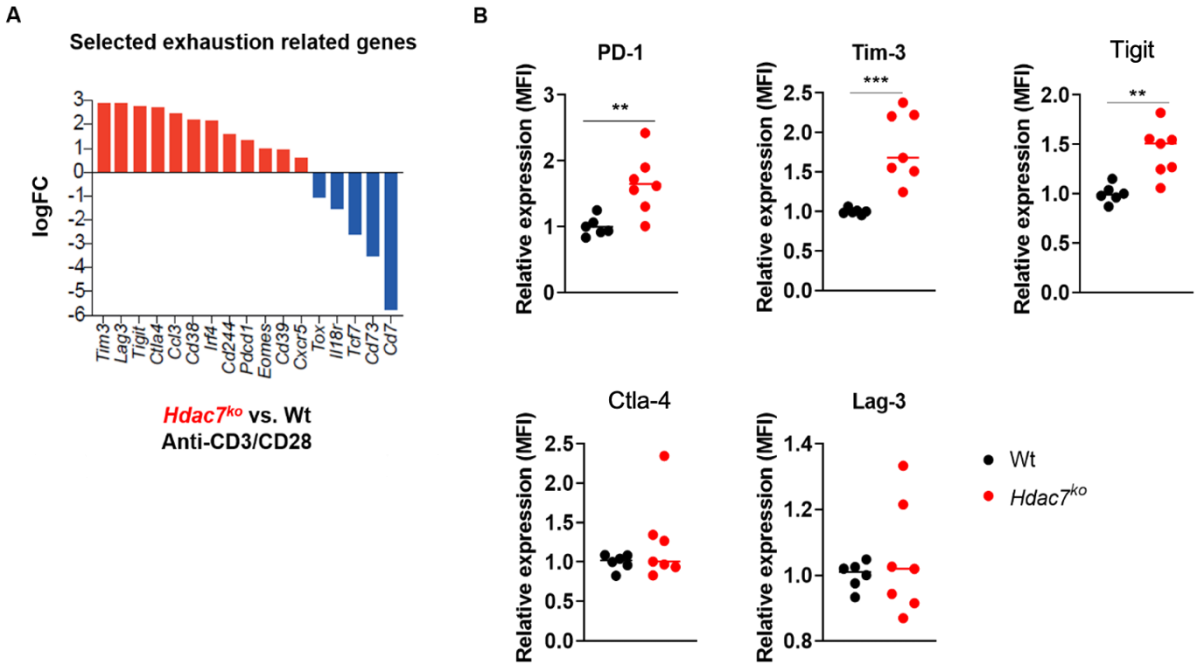

Figure 4-19 In vitro activated Hdac7^{ko} CD8^{+} T cells have increased expression of exhaustion markers. (A) *Fold change expression of selected exhaustion related genes in in vitro activated Hdac7^{ko} CD8^{+} T cells from comparative RNA-sequencing, p<0.05, independent samples n=3.* ***(B)*** *Dot plots showing the protein expression of programmed cell death protein 1 (PD-1), T cell immunoglobulin and mucin domain-containing-3 (Tim-3), T cell immunoreceptor with Ig and ITIM domain (Tigit), cytotoxic T-lymphocyte associated protein 4 (Ctla-4) and lymphocyte activation gene 3 (Lag-3) in in vitro activated wt and Hdac7^{ko}CD8^{+} T cells. Mean fluorescent intensity (MFI) values were determined by flow cytometry. Three independent experiments, n=6-7. Multiple t test, **p<0.01, ***p<0.001.*

Since our transcriptome data is derived from *in vitro* activated CD8^{+} T cells which can be considered as artificial, we also analyzed published single cell RNA sequencing (scRNA-seq) datasets which derived from tumor infiltrating CD8^{+} T cells within B16-Ova tumors in wt mice (Carmona et al., 2020). We first performed uniform manifold approximation and projection (UMAP) algorithm to visualize the clustering of different TIL subsets isolated from B16-Ova

tumors **(Figure 4-20)**. UMAP analysis revealed four different TIL clusters as naïve, memory like, effector memory (EM) like as well as exhausted CD8⁺ T cells. Gene signatures specific to each cell cluster were then derived and subsequently their enrichment in the transcriptome of different subsets of *Hdac7*^{ko} CD8⁺ T cells was analyzed **(Figure 4-20)**. Interestingly, exhaustion and memory like gene signatures were significantly enriched in *in vitro* anti-CD3 and anti-CD28 activated *Hdac7*^{ko} CD8⁺ T cells. Exhaustion-related gene signature was even enriched in naïve *Hdac7*^{ko} CD8⁺ T cells, but most importantly, LCMV-specific *Hdac7*^{ko} CD8⁺ T cells displayed the enrichment of exhaustion related gene signature in their transcriptome further claiming that *Hdac7*^{ko} CD8⁺ T cells are more prone to cellular exhaustion in the presence of continuous antigen stimulations during chronic infections as well as in tumor microenvironment **(Figure 4-20)**.

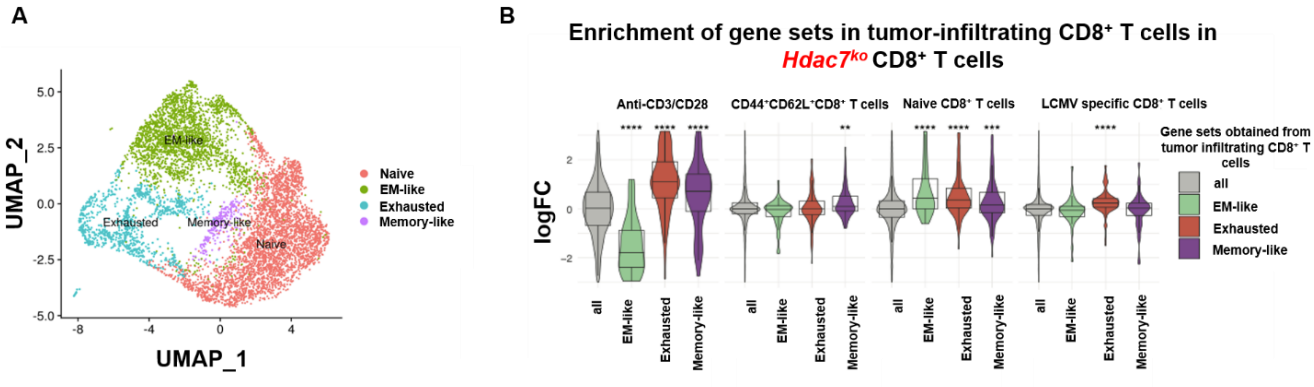

Figure 4-20 Exhaustion-related gene signature of tumor infiltrating CD8⁺ T cells is enriched in Hdac7^{ko} CD8⁺T cells. (A) *Unifold manifold approximation and projection (UMAP) analysis showing the clustering of tumor infiltrating CD8⁺ T cells in B16-Ova tumors.* ***(B)*** *Exhausted, effector memory (EM) like, memory-like and naïve CD8⁺ T cell gene signatures derived from published scRNA-seq data from tumor-infiltrating CD8⁺ T cells. Volcano plots show in silico enrichment analysis of these gene signatures in different subsets of CD8⁺ T cells isolated from Hdac7^{ko} mice when compared to the respective wt counterparts.*

4.11 *In vitro* T cell exhaustion model confirms impaired survival and exhausted phenotype of *Hdac7*^{ko} CD8⁺ T cells

To further investigate if *Hdac7*-deficiency results in the cellular exhaustion in CD8⁺ T cells, we established an *in vitro* T cell exhaustion method. For this purpose, CD8⁺ T cells were isolated from wt mice and activated for 48 h with anti-CD3 and anti-CD28 antibodies in the presence of recombinant IL-2. On day-2, cells were divided into two groups. While the experimental group was exposed to chronic antigen stimulation every two days to mimic repeated and chronic antigen stimulation, cells in the control group were grown in the presence of IL-2 only **(Figure 4-21)**. qPCR experiments confirmed the upregulation of T cell exhaustion markers

Pdcd1, *Havcr2* and *Tigit*, while the expression of *Ctla4* and *Lag3* were not changed **(Figure 4-22)**.

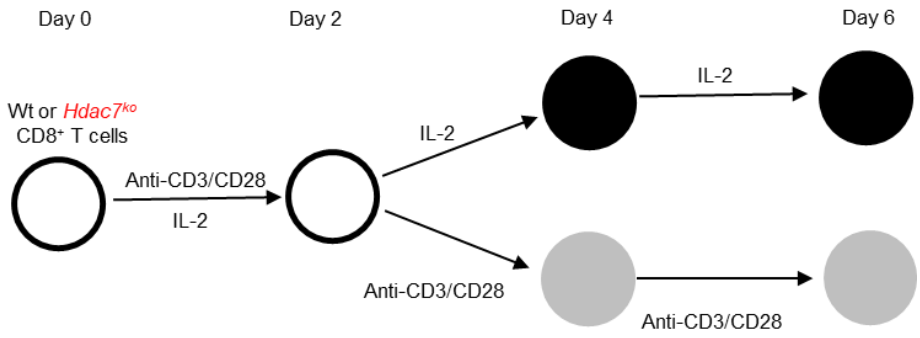

Figure 4-21 Experimental set up for in vitro T cell exhaustion assay. *CD8⁺ T cells isolated from wild type (wt) and Hdac7^{ko} mice were in vitro activated with anti-CD3 and anti-CD28 antibodies in the presence of recombinant IL-2 (20 ng/ml) for 48 hours. On day-2, cells were divided into two groups. One group was grown in the presence of IL-2 (20 ng/ml) only to serve as controls. The second group was repeatedly stimulated with anti-CD3 and anti-CD28 antibodies every 48 h.*

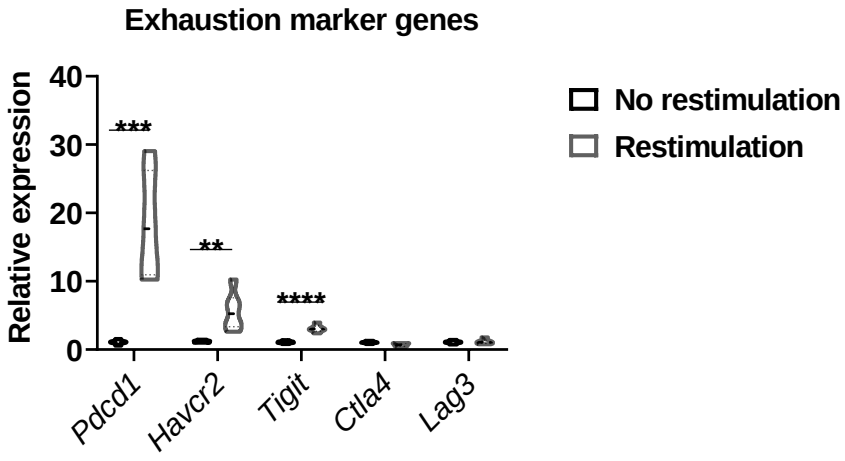

Figure 4-22 Expression of exhaustion marker genes is induced upon in vitro restimulation. *Wild type (wt) CD8⁺ T cells were isolated and stimulated with anti-CD3 and anti-CD28 antibodies in the presence of IL-2 on day 0. After 48 h, cells were divided into two groups and either restimulated with anti-CD3 and anti-CD28 antibodies without IL-2 or they were cultured with IL-2 supplementation as unstimulated controls. On day-4, RNA was collected. cDNAs were synthesized as described and qPCR was performed. Expression of target genes were normalized to 36b4 gene. Three independent experiments, n=6. Multiple t test, **p<0.01, ***p<0.001, ****p<0.0001*

To investigate whether the expression of *Hdac7* and the other class II *Hdac* genes are affected by chronic stimulation and the induction of cellular exhaustion in CD8⁺ T cells, qPCR experiments were performed. Interestingly, the expression of *Hdac7* significantly decreases upon restimulation and the induction of cellular exhaustion **(Figure 4-23)**. Similarly, the expressions of *Hdac4* and *Hdac10* were significantly lower under restimulation and exhaustion conditions, although they are expressed at very low levels in wt CD8⁺ T cells in the absence of restimulation compared to *Hdac7* **(Figure 4-23)**.

Next, we analyzed how *Hdac7* expression is correlated with the gene expression of exhaustion markers. Significant negative correlations were observed between *Hdac7* expression and *Pdcd1*, *Havcr2* and *Tigit* which were upregulated in wt CD8$^+$ T cells upon restimulation with anti-CD3 and anti-CD28 antibodies **(Figure 4-23)**. These results suggest that HDAC7 might be a repressor of CD8$^+$ T cell exhaustion under chronic and repeated antigen stimulation.

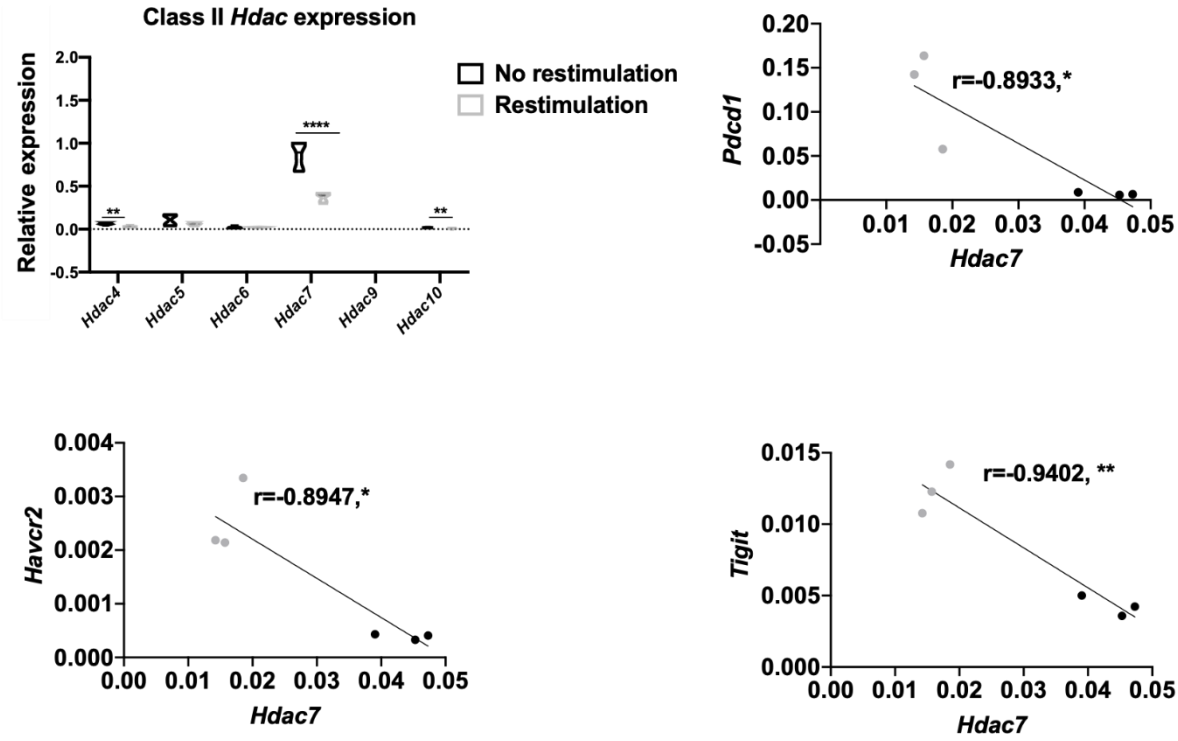

Figure 4-23 The expression of Hdac7 is negatively correlated with T cell exhaustion related marker expression. *Wild type (wt) CD8$^+$ T cells were restimulated as described and class II Hdac expression was determined by qPCR. $2^{-\Delta Ct}$values of Hdac7 and Pdcd1, Havcr2 and Tigit were plotted against each other by using Graphpad Prism software. R values were calculated by correlation analysis. For class II Hdac expression, three independent experiments, n=6, multiple t test **p<0.01, ****p<0.0001. Spearman correlation analysis, representative of three independent experiments, n=6, *p<0.05, **p<0.01*

In the next step, we applied our established *in vitro* T cell exhaustion protocol to both wt and *Hdac7^{ko}* CD8$^+$ T cells. Firstly, cell viability and apoptosis in wt and *Hdac7^{ko}* CD8$^+$ T cells with or without restimulation were analyzed by annexin V and PI staining and subsequent flow cytometry **(Figure 4-24)**. We observed that *Hdac7^{ko}* CD8$^+$ T cells had higher apoptosis on day 2 before restimulation which is consistent with bulk RNA-seq data derived from *in vitro* anti-CD3 and anti-CD28 activated wt and *Hdac7^{ko}* CD8$^+$ T cells. *Hdac7^{ko}* CD8$^+$ T cells were more prone to activation-induced apoptosis than wt CD8$^+$ T cells if they are restimulated with anti-CD3 and anti-CD28 antibodies. Consistently, *Hdac7^{ko}* CD8$^+$ T cells were always more apoptotic than wt CD8$^+$ T cells for all timepoints regardless of the restimulation conditions **(Figure 4-24)**.

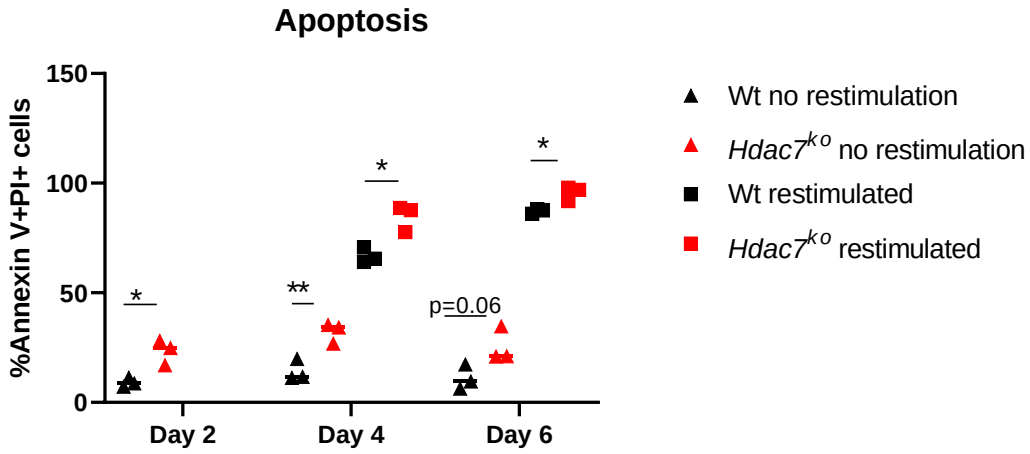

Figure 4-24 Hdac7^{ko} CD8^{+} T cells feature increased apoptosis during continuous antigen stimulation in vitro. *CD8^{+} T cells isolated from wild type (wt) and Hdac7^{ko} mice were in vitro activated with anti-CD3 and anti-CD28 antibodies in the presence of recombinant IL-2 (20 ng/ml) for 48 h. On day 2, cells were divided into two groups. One group was grown in the presence of IL-2 (20 ng/ml) to serve as controls. The second group was repeatedly stimulated with anti-CD3 and anti-CD28 antibodies every 48 h. The frequency of annexin V^{+}PI^{+} CD8^{+} T cells during with or without restimulation with anti-CD3 and anti-CD28 antibodies at different timepoints was determined by flow cytometry. n=3, multiple t test, *p<0.05, **p<0.01*

We also analyzed the protein expression of cellular exhaustion markers in wt and *Hdac7^{ko}* CD8^{+} T cells by flow cytometry **(Figure 4-25)**. However, we excluded the second and third restimulations since most of the *Hdac7^{ko}* CD8^{+} T cells were apoptotic on these timepoints. Flow cytometry analysis showed that protein expression of PD-1, Tim-3 and Tigit can be induced in wt CD8^{+} T cells upon restimulation with anti-CD3 and anti-CD28 antibodies compared to IL-2 control cells. Interestingly, the protein expression of these markers was significantly upregulated in *Hdac7^{ko}* CD8^{+} T cells suggesting that HDAC7 is needed to suppress the exhaustion of CD8^{+} T cells during chronic antigen stimulation **(Figure 4-25)**.

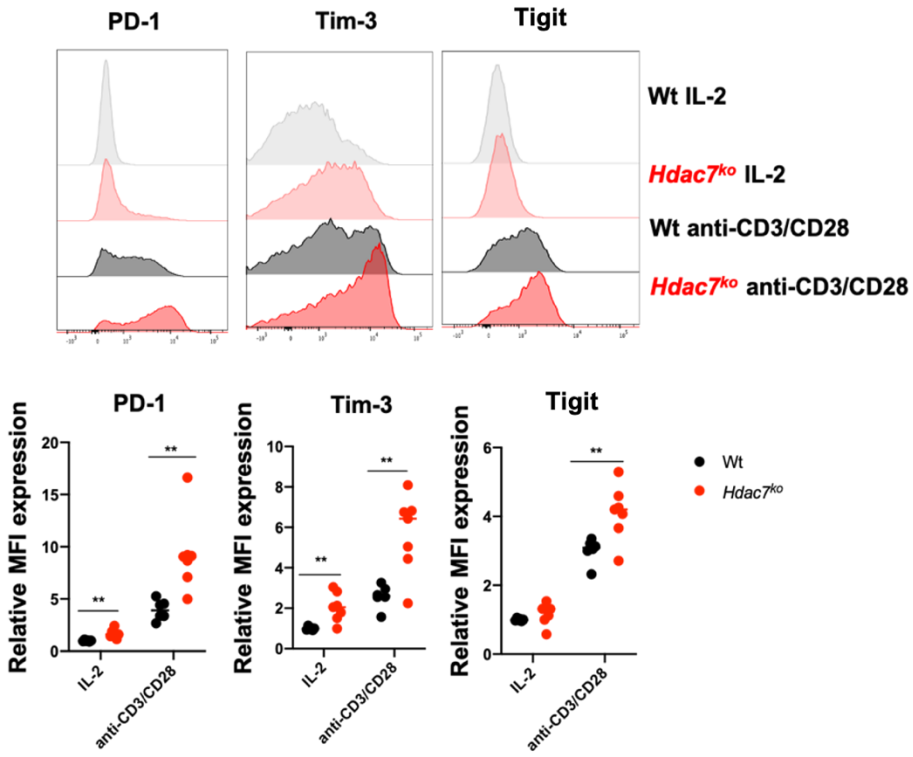

Figure 4-25 Hdac7^{ko} CD8^{+} T cells are more prone to cellular exhaustion during chronic antigen stimulation. *Wt and Hdac7^{ko} CD8^{+} T cells were restimulated with anti-CD3 and anti-CD28 antibodies to induce their exhaustion in vitro. Protein expression of indicated exhaustion markers were measured by flow cytometry. Upper histogram panels indicate representative primary FACS plots showing mean fluorescence intensity (MFI) of PD-1, Tim-3 and Tigit. Lower panels indicate relative MFI expressions in CD8^{+} T cells with restimulation (anti-CD3/CD28) and without restimulation (IL-2) conditions. MFI values were normalized to the mean of wt cells. Representative of three independent experiments, n=6-7. Multiple t test, **p<0.01*

4.12 Pan-HDAC inhibitor treatment results in impaired survival and reduced HDAC7 protein expression in CD8^{+} T cells

To investigate whether HDACi treatment affects the functions of CD8^{+} T cells, wt CD8^{+} T cells were treated with pan-HDACi vorinostat, also known as SAHA. Briefly, CD8^{+} T cells were isolated from the splenocytes of wt mice and in vitro activated with anti-CD3 and anti-CD28 antibodies for 48 h in the presence of different concentrations of vorinostat or dimethyl sulfoxide (DMSO) as the vehicle control. After 48 h, the apoptosis in CD8^{+} T cells was analyzed by annexin V PI staining **(Figure 4-26)**. We observed that vorinostat treatment induced apoptosis and impaired the survival of CD8^{+} T cells in a dose-dependent manner **(Figure 4-26)**.

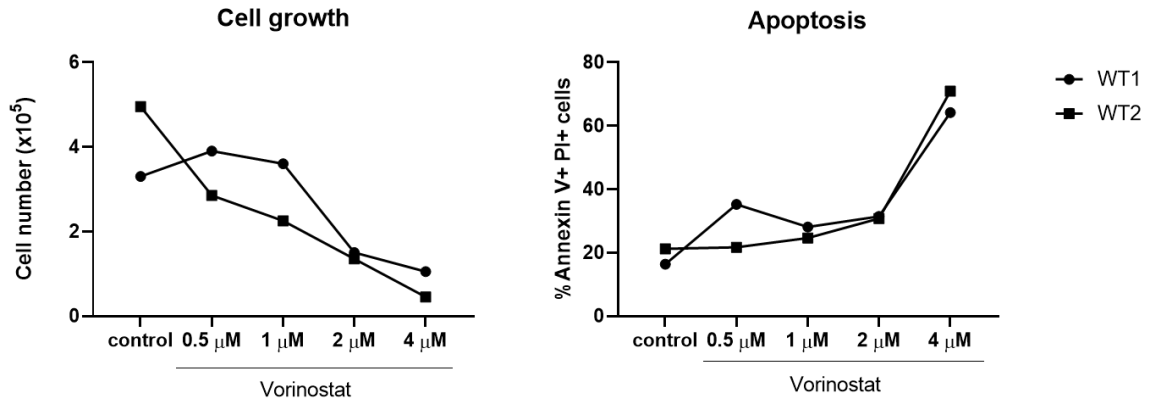

Figure 4-26 Vorinostat treatment results in increased apoptosis in CD8⁺ T cells. *Cell numbers (left) and the frequency of annexin V⁺PI⁺ wild type (wt) CD8⁺ T cells (right) treated with the indicated concentrations of vorinostat for 24 h.*

Next, the protein expression of HDAC7 upon vorinostat treatment was analyzed **(Figure 4-27)**. Similarly, wt CD8⁺ T cells were in vitro activated with anti-CD3 and anti-CD28 antibodies for 48 h in the presence of 0.5 µM vorinostat or the vehicle control. After 48 h, protein samples were collected, and western blot was performed to detect HDAC7 protein expression. As controls, we also included protein samples from *Hdac7^{ko}* CD8⁺ T cells to determine the specificity of anti-HDAC7 antibody. As a positive control for vorinostat treatment, immunoblotting with anti-acetyl-H3K9/K14 antibody was performed, since vorinostat inhibits the acetylase activities of HDACs. Interestingly, we observed that wt CD8⁺ T cells treated with vorinostat displayed significantly lower HDAC7 protein. Importantly, by western blot we did not observe any protein band for *Hdac7^{ko}* CD8⁺ T cells, suggesting that the anti-HDAC7 antibody was specific for HDAC7 **(Figure 4-27)**. We also confirmed that vorinostat treatment worked, since wt CD8⁺ T cells treated with the inhibitor had significantly higher levels of acetylated H3K9/K14. Moreover, untreated *Hdac7^{ko}* CD8⁺ T cells had significantly more acetylated H3K9/K14 than untreated wt CD8⁺ T cells **(Figure 4-27)**. Therefore, vorinostat treatment leads to increased apoptosis and impaired survival of CD8⁺ T cells during their activation by decreasing HDAC7 at the protein level. Regardless of vorinostat treatment, the deletion of HDAC7 in CD8⁺ T cells prompts a global increase in acetyl-H3K9/K14, suggesting that the deletion of *Hdac7* also interferes with the gene expression and the transcriptome of CD8⁺ T cells by deregulating the chromatin accessibility **(Figure 4-27)**.

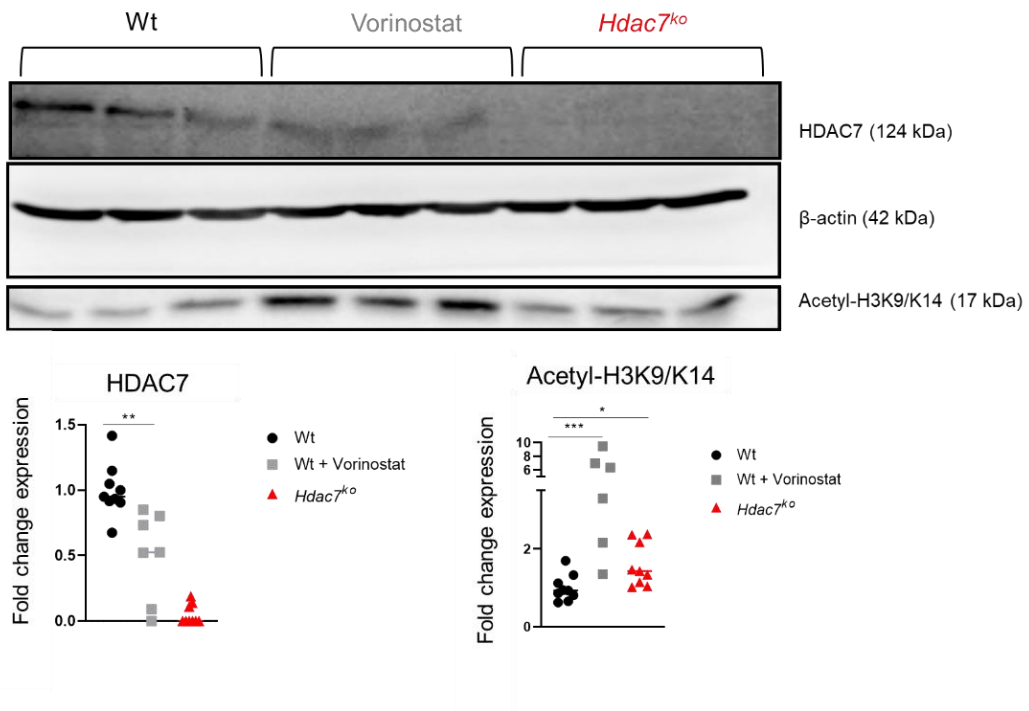

Figure 4-27 Vorinostat treatment results in decreased HDAC7 protein expression in wt CD8⁺ T cells. *Immunoblot analysis of HDAC7, β-actin and acetylated H3 at K9 and K14 (acetyl-H3K9/K14) in wild type (wt) cells with or without vorinostat treatment (5 μM) for 24 h or untreated Hdac7ko CD8⁺ T cells (upper panel). Dot plots showing the normalized protein expression of HDAC7 (lower left) and acetyl-H3K9/K14 (lower right). Values were normalized to the intensity of β-actin bands. n=6-9, multiple t test, *p<0.05, **p<0.01, ***p<0.001*

4.13 HDAC7 regulates transcription of its target genes through MEF2D in CD8⁺ T cells

It was previously reported that HDAC7 is a member of a transcriptional corepressor complex and it acts as a scaffold protein for the recruitment of other transcriptional regulators within this complex (Di Giorgio and Brancolini, 2016). HDAC7 suppresses the expression of its target genes by binding to MEF2D in T cells. In order to characterize the downstream targets of HDAC7 in CD8⁺ T cells, we aimed to establish ChIP experiments with anti-MEF2D antibody. *Nur77* was previously reported as a direct target of HDAC7 in T cells (Dequiedt et al., 2003). The stimulation of thymocytes cells results in the shuttling of HDAC7 into the cytoplasm, thus it cannot sequester MEF2D in the nucleus anymore, and MEF2D can bind to the promoter of *Nur77* and activate its expression (Dequiedt et al., 2003) . Therefore, we used this system as a positive control for our anti-MEF2D ChIP protocol. Briefly, wt CTLs were either stimulated with PMA/ionomycin for 2 h or left untreated and they were subjected to ChIP protocol with anti-MEF2D antibody as described, followed by ChIP-qPCR with primers to amplify the regions that contains MEF2D binding sites for the *Nur77* promoter. An enrichment of MEF2D on the promoter of *Nur77* was observed upon stimulation with PMA/ionomycin suggesting that the ChIP protocol worked **(Figure 4-28)**.

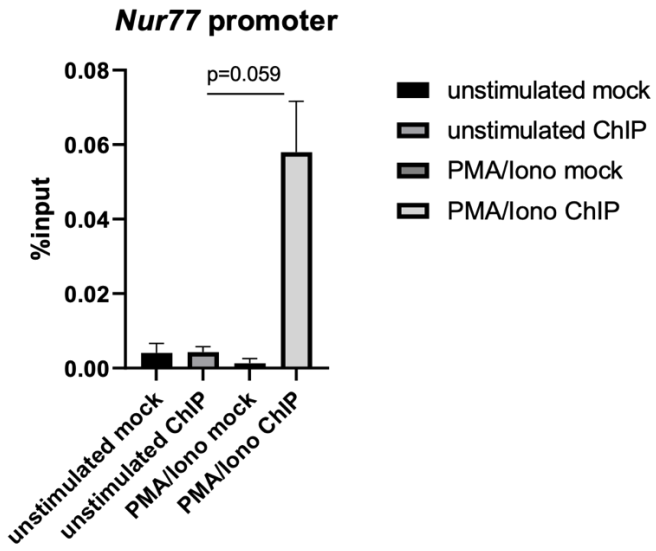

Figure 4-28 MEF2D binds to the promoter of Nur77 upon PMA/ionomycin stimulation in wt CTLs*. Wild type (wt) cytotoxic T lymphocytes (CTLs) were subjected to PMA/ionomycin stimulation for 2 h and subjected to chromatin immunoprecipitation (ChIP) by using anti-myocyte enhancer factor 2 D (MEF2D) antibody followed by ChIP-qPCR targeting MEF2D binding sites on the promoter of Nur77. % input was calculated as described. Representative of two independent experiments, multiple t test.*

Bulk RNA-seq data derived from *in vitro* activated wt and *Hdac7*^{ko} CD8^{+} T cells showed that several proapoptotic genes were upregulated in *Hdac7*^{ko} CD8^{+} T cells, and *Fasl* was the top hit in this gene cluster. To investigate if the upregulation of *Fasl* in *Hdac7*^{ko} CD8^{+} T cells is MEF2D-dependent, ChIP-qPCR experiments were performed. Firstly, three putative MEF2D binding sites were identified on *Fasl* promoter by in silico analysis named R1, R2 and R3 **(Figure 4-29)**. *In vitro* activated wt and *Hdac7*^{ko} CD8^{+} T cells were subjected to ChIP with anti-MEF2D antibody and ChIP-qPCR was performed to determine whether MEF2D binds to any of these putative binding sites on *Fasl* promoter. Interestingly, MEF2D was enriched on all three putative binding sites on *Fasl* promoter in *Hdac7*^{ko} CD8^{+} T cells, while no enrichment was detected in wt CD8^{+} T cells **(Figure 4-29)**. This observation suggested that the deletion of *Hdac7* in CD8^{+} T cells might allow MEF2D-binding to the promoter of *Fasl* driving its upregulation and contributing to the increased apoptosis in *Hdac7*^{ko} CD8^{+} T cells.

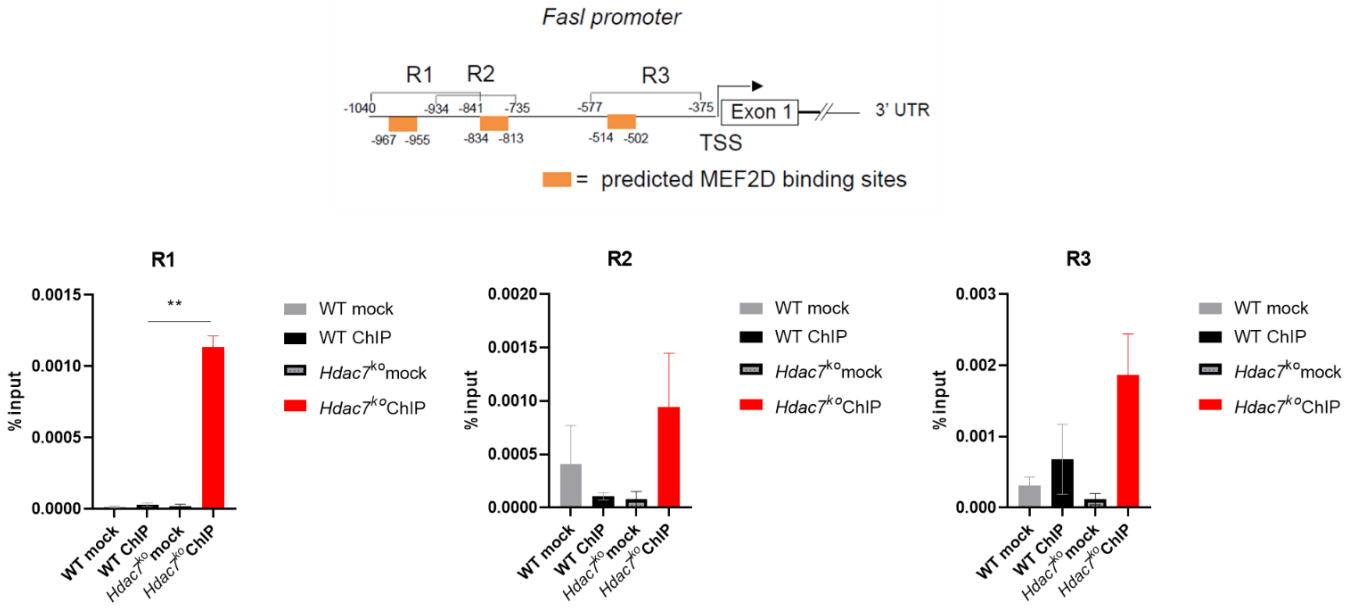

Figure 4-29 MEF2D binds to the promoter of FasL in the absence of Hdac7. *Three putative binding sites (R1-R3) were identified on the promoter of murine Fasl gene at the upstream of its transcription start site (TSS) by in silico analysis. In vitro anti-CD3 and anti-CD28 activated wild type (wt) and Hdac7^{ko}CD8^{+} T cells were subjected to chromatin immunoprecipitation (ChIP) by using anti-myocyte enhancer factor 2 D (MEF2D) antibody followed by ChIP-qPCR to amplify regions containing putative MEF2D binding sites. % input was calculated as described. Two independent experiments, wt and Hdac7^{ko} CD8^{+} T cells were pooled from several mice. multiple t test, **p<0.01*

5 DISCUSSION

$CD8^+$ T cells are essential components of adaptive immunity and immunological memory against viral infections as well as tumor cells. Since the anti-tumor immune responses of $CD8^+$ T cells are compromised due to the immune surveillance within the immunosuppressive tumor microenvironment resulting in uncontrolled tumor growth, novel approaches in cancer immunotherapy have been an active research area in recent years. Although novel cancer immunotherapy methods including CAR T cell and adoptive T cell therapies were developed, they are still challenged by the cellular exhaustion induced by the immunosuppressive tumors. Checkpoint blockade therapies which target co-inhibitory molecules including PD-1 and CTLA-4 expressed by $CD8^+$ T cells have been more effective against tumors. Thus, more knowledge on the regulators of co-inhibitory molecules is needed to improve current checkpoint blockade therapies as well as to develop novel cancer immunotherapy approaches.

Given that we still lack the complete knowledge on the epigenetic regulators of anti-tumor immune functions of $CD8^+$ T cells as well as their role in $CD8^+$ T cell exhaustion, in this PhD project we aimed to characterize the role of HDAC7 in the anti-tumor immune responses and homeostasis of $CD8^+$ T cells. Thereby, we showed that the lack of *Hdac7* in $CD8^+$ T cells results in uncontrolled tumor growth in the murine models since HDAC7 is essential for the survival and the fitness of $CD8^+$ T cells both *in vitro* and *in vivo*. Similarly, we identified HDAC7 as a crucial regulator of $CD8^+$ T cell exhaustion during chronic antigen stimulation contributing to the impairment of tumor growth control in conditional mice which lack *Hdac7* in T cells. Therefore, we propose that HDAC7 is a key regulator of proper anti-tumor immune responses of $CD8^+$ T cells.

5.1 Pre-activated phenotype of *Hdac7^{ko}* CD8+ T cells

We investigated the homeostasis of $CD8^+$ T cells in *Hdac7$^{fl/fl}$E8I-Cre* mice under steady state conditions. Unexpectedly, we observed that the frequency of $CD44^-CD62L^+CD8^+$ T cells were dramatically reduced in *Hdac7$^{fl/fl}$E8I-Cre* mice coupled with an increase in the frequency of $CD44^+CD62L^+CD8^+$ central memory cells suggesting that the deletion of *Hdac7* in $CD8^+$ T cells results in their pre-activated phenotype **(Figure 4-3)**. Previously, we also observed a similar pre-activated phenotype of $CD8^+$ T cells in *Hdac7$^{fl/fl}$CD4-Cre* mice under steady state conditions by using both mass and flow cytometry (Keye, 2018). Previous literature suggests

an important role of HDAC7 for thymocyte development and both negative and positive selection during the developmental process (Dequiedt et al., 2003; Kasler et al., 2012; Kasler and Verdin, 2007). HDAC7 regulates the expression of genes that are differentially expressed during positive and negative selection of thymocytes. HDAC7 target genes are mainly important for the coupling between TCR engagement and its subsequent downstream signaling cascades (Kasler and Verdin, 2007). Therefore, HDAC7 was characterized as a key player for the regulation of thymocyte survival and their positive and negative selection. Therefore, this pre-activated phenotype of $CD8^+$ T cells from *Hdac7*^{ko} mice under steady state conditions might be resulting from a defect during their thymic development. Similarly, we also observed that the number and the frequency of $CD8^+$ T cells are lower in both *Hdac7*$^{fl/fl}$*CD4-Cre* and *Hdac7*$^{fl/fl}$*E8I-Cre* mice compared to wt littermates under steady state conditions **(Figure 4-3)**. Moreover, this reduced frequency is coupled with an increased apoptosis in the presence of *in vitro* stimulation **(Figure 4-7)**. These observations are in line with previous findings from other groups showing that a nucleus-trapped inactive mutant form of HDAC7 resulted in the apoptosis of thymocytes and thus interfering with their development, which is induced by the pro-apoptotic factor *Nur77* expression in a MEF2D-dependent manner (Dequiedt et al., 2005, 2003). Therefore, deregulated apoptosis during the development of T cells in *Hdac7*^{ko} mice can also contribute to the decreased numbers of $CD8^+$ T cells under steady state conditions.

In this project, we neither investigated how our conditional mouse model for *Hdac7* deletion was affected in terms of the thymic development of T cells nor how this possible defect in the development of T cells contributes to the phenotypes that we observed in *Hdac7*^{ko} mice. Thus, the thymic content as well as positive and negative selection of T cells in *Hdac7*^{ko} mice should be investigated in more detail. As a future work, *Hdac7*$^{fl/fl}$*CD4-Cre* mice can be backcrossed to *Ert2-Cre* mice, which will result in *Hdac7*$^{fl/fl}$*CD4-Ert2-Cre* mouse strain, in which *Cre* recombinase can be induced by tamoxifen treatment, thus allowing to delete *Hdac7* at any stage of the T cell development as well as specifically in the peripheral adult T cells at later timepoints. This conditional mouse model can be useful to discriminate the phenotypes that result from defects during thymic development in *Hdac7*^{ko} mice.

5.2 CD8$^+$ T cell intrinsic effects of HDAC7

During this project, we focused on the role of HDAC7 in CD8$^+$ T cells. However, CD4$^+$ T cells are similarly crucial players of anti-tumor immunity (Tay et al., 2020). Depending on the cytokine milieu and the TCR activation, CD4$^+$ T cells upregulate the expression of key transcription factors which are necessary for their differentiation into different subtypes. CD4$^+$ T cells are similarly key regulators of anti-tumor immunity since they support the anti-tumor immune responses of CD8$^+$ T cells by facilitating their activation and effector responses. For example, CD4$^+$ T cells secrete IL-2, which subsequently induces the activation, effector function and the proliferation of CD8$^+$ T cells and thus the development of proper CTL responses (Dequiedt et al., 2003). Similarly, CD4$^+$ T cells are needed for the maintenance of cross-presenting pro-inflammatory DCs, which subsequently provide activating signals for CD8$^+$ T cells. This mechanism is essential for the direct killing capacities of CD8$^+$ T cells such as the release of pro-inflammatory and anti-tumoricidal cytokine IFNγ as well as their effector functions and memory differentiation. In addition, CD4$^+$ T cells can also produce IFNγ and TNFα themselves which allows them to possess cytotoxicity against tumor cells (Tay et al., 2020).

Since *Hdac7* is conditionally deleted in both the CD4$^+$ and the CD8$^+$ T cell compartment of the *Hdac7$^{fl/fl}$CD4-Cre* (*Hdac7^{ko}*) mouse strain **(Figure 4-2)**, we should also clarify whether the uncontrolled tumor growth in *Hdac7^{ko}* mice is originating solely from the intrinsic effects of HDAC7 in CD8$^+$ T cells or whether HDAC7-deficient CD4$^+$ T cells also contribute to this phenotype. To answer this question, we repeated tumor challenge experiments in *Hdac7$^{fl/fl}$E8I-Cre* mice, in which *Hdac7* was exclusively deleted in the CD8$^+$ T cell compartment **(Figure 4-2)**. Similar to *Hdac7^{ko}* mice, *Hdac7$^{fl/fl}$E8I-Cre* mice have impaired tumor growth control when challenged with EG.7-Ova lymphoma cells suggesting that the phenotypes that we have observed in *Hdac7^{ko}* mice are resulting from CD8$^+$ T cell intrinsic effects of *Hdac7* deletion **(Figure 4-13)**.

Previous data from our group also support that the effector functions of CD4$^+$ T cells are not affected by *Hdac7* deletion. For instance, the CD4$^+$ T cell compartment of LCMV-infected *Hdac7^{ko}* mice was largely normal and their cytokine production capacities were unchanged compared to wt littermates. Furthermore, *Hdac7*-deficient CD4$^+$ T cells did not display disturbances in their colitogenic potential during T cell transfer models in colitis (Keye, 2018).

Therefore, we conclude that in *Hdac7$^{fl/fl}$CD4-Cre* mice, CD4$^+$ T cells can function properly and might provide sufficient help to CD8$^+$ T cells for their anti-tumor immune responses.

5.3 The role of HDAC7 in CD8$^+$ T cell metabolism

The metabolism of CD8$^+$ T cells is tightly regulated during differentiation (Buck et al., 2015b, 2016; Windt et al., 2011). Their activation leads to the induction of glycolysis, whereas they mainly switch to fatty acid metabolism, if they acquire a memory phenotype (Buck et al., 2016; Windt et al., 2011). The analysis of RNA-seq data from *in vitro* anti-CD3/anti-CD28 activated wt and *Hdac7^{ko}* CD8$^+$ T cells did not reveal any differences in the pathways related to glycolysis and FAO in *Hdac7^{ko}* CD8$^+$ T cells **(Figure 4-5)**. In line with the transcriptome data, *Hdac7^{ko}* CTLs did not display any disturbances in these pathways during Seahorse analysis **(Figure 4-9)**. However, Seahorse analysis revealed that *Hdac7^{ko}* CTLs have augmented glutamine uptake compared to wt CTLs **(Figure 4-9)**. Indeed, cellular amino acid metabolic process was the only metabolic pathway that was enriched in the transcriptome of *Hdac7^{ko}* CD8$^+$ T cells according to RNA-seq **(Figure 4-5)**.

The role of glycolysis and the mitochondrial metabolism in CD8$^+$ T cell has been mostly clarified. Glycolysis is essential for the proper activation of CD8$^+$ T cells, whereas a switch to mitochondrial metabolism drives their memory differentiation (Buck et al., 2015b, 2016; Chang et al., 2013). However, the knowledge about the role of amino acid metabolism in T cell fate decisions is limited. Some studies suggested that amino acid transporters are important for peripheral naïve T cell homeostasis, activation and differentiation of T cells as well as their memory differentiation and function (Ren et al., 2017). However, these studies mainly focus on certain amino acid transporters such as ASCT2 and LAT1 and the roles of other amino acid transporters are still unknown. ASCT2 and LAT1 transporters are coupled with the leucine transport, which is an activator of mTORC1 signaling, and the effects of amino acid transporters in T cell function are thought to depend on mTOR (Ren et al., 2017). mTOR signaling is a central pathway for the regulation of survival and metabolism of T cells, and it is also closely related to activation and differentiation of CD8$^+$ T cells. We also observed disturbed mTOR signaling in *Hdac7^{ko}* CTLs **(Figure 4-10)**, which might be related to the deregulated amino acid metabolism in these cells, subsequently contributing to the phenotype of *Hdac7^{ko}* CD8$^+$ T cells with impaired survival and exhaustion and ultimately

impaired anti-tumor immune functions. However, more research is needed to highlight this crosstalk between amino acid metabolism, mTOR signaling and HDAC7 in $CD8^+$ T cells.

5.4 The role of HDAC7 in the calcium homeostasis of $CD8^+$ T cells

We observed a diminished signaling strength of SOCE and thus a disturbed calcium homeostasis in *Hdac7^{ko}* CTLs **(Figure 4-11)**. RNA-sequencing of in vitro activated wt and *Hdac7^{ko}* $CD8^+$ T cells also confirmed impaired SOCE signaling in these cells, since several key components of SOCE signaling including calcium channel protein *Orai2*, the adaptor molecule *Stim1* and the sarco/endoplasmic reticulum Ca^{+2}-ATPase (SERCA) pump *Atp2a2* was significantly downregulated in *Hdac7^{ko}* $CD8^+$ T cells **(Figure 4-11)**.

SOCE has been shown to play a crucial role in several aspects of T cell function, including their metabolic regulation and proper memory response by $CD8^+$ T cells (Bergmeier et al., 2013; Feske, 2011). Interestingly, *Stim1$^{fl/fl}$Stim2$^{fl/fl}$CD4-Cre* mice display a very similar phenotype to *Hdac7^{ko}* mice since SOCE-deficient $CD8^+$ T cells feature increased exhaustion with high Pd-1 and Tim-3 expression paralleled by an impaired production of pro-inflammatory cytokines including IFNγ and TNFα despite an increased Eomes expression that is the master regulator of memory differentiation of $CD8^+$ T cells. Eomes is dispensable for the fitness of memory $CD8^+$ T cells and promotes the persistence of cells with the long-lived memory phenotype against the terminally differentiated effector phenotype (Shaw et al., 2014; Banerjee et al., 2010). $CD8^+$ T cells from *Stim1$^{fl/fl}$Stim2$^{fl/fl}$CD4-Cre* mice featured defective functional memory recall responses upon secondary infections with LCMV (Shaw et al., 2014). Similarly, SOCE-deficient $CD8^+$ T cells had severe defects in their anti-tumor immune responses in mouse models of melanoma as well as lymphoma (Weidinger et al., 2013).

SOCE controls the clonal expansion of T cells by regulating their metabolism through NFAT-regulated transcription and PI3K/AKT/mTOR pathway. Thus, it is an upstream regulator of the central mTOR pathway (Vaeth et al., 2017). Therefore, the downregulated mTOR signaling in *Hdac7^{ko}* CTLs can be partially explained by the impaired SOCE signaling. These observations also suggest that HDAC7 might be a regulator of SOCE signaling and the calcium homeostasis in $CD8^+$ T cells. However, our data is limited, and more mechanistic research is required to investigate this possible role of HDAC7 in the role of calcium homeostasis in $CD8^+$ T cells. For example, it should be investigated whether HDAC7 regulates the key SOCE-related genes such as *Stim1*, *Stim 2* and *Orai1* directly or indirectly. To answer this question, anti-MEF2D ChIP-

qPCR experiments can be performed in wt and *Hdac7*^{ko} CD8^{+} T cells. If MEF2D is enriched on the promoters of these genes in *Hdac7*^{ko} CD8^{+} T cells, one can claim that HDAC7 directly controls the expression of SOCE related genes and directly contributes to the signaling strength of SOCE in CD8^{+} T cells.

5.5 The role of HDAC7 in the anti-tumor immune responses and the exhaustion of CD8^{+} T cells

Here, we showed that the lack of *Hdac7* in CD8^{+} T cells resulted in impaired tumor growth control in both *Hdac7*$^{fl/fl}$*CD4-Cre* and *Hdac7*$^{fl/fl}$*E8I-Cre* mice which were challenged with EG.7-Ova cells **(Figure 4-13)**. The histologic analysis of EG.7-Ova tumors from *Hdac7*^{ko} mice displayed reduced CD8^{+} T cell infiltration into EG.7-Ova tumors **(Figure 4-14)**. Moreover, *Hdac7*-deficient CD8^{+} T cells had an impaired expansion *in vivo*, resulting in reduced CD8^{+} T cell infiltration into tumors in *Hdac7*$^{fl/fl}$*CD4-Cre* mice **(Figure 4-16)**, which explains the outgrowth of EG.7-Ova tumors. The exclusion of CD8^{+} T cells from the tumor microenvironment represents one of the mechanisms that contribute to the immune evasion in solid tumors (Anderson et al., 2017). T cell exclusion from the tumors can be driven by different mechanisms including the modulation of adhesion and chemokine molecules by tumor cells and the endothelial cells needed for T cell arrest and extravasation (Anderson et al., 2017). For instance, C-X-C chemokine motif ligand (CXCL) 9 and CXCL10 which are T cell attracting chemokines are epigenetically silenced in ovarian tumor cells (Peng et al., 2015). Moreover, the nitration of reactive oxygen species present in the tumors interferes with the CXCL11-mediated attraction of T cells into tumors (Molon et al., 2011). In our case, we did not observe any alteration in the homing capacities of tumor-specific CD8^{+} T cells into EG.7-Ova tumors in the absence of HDAC7 **(Figure 4-15)**. However, we attribute the reduced infiltration of CD8^{+} T cells in the EG.7-Ova tumors in *Hdac7*^{ko} mice to a general decrease in the numbers of CD8^{+} T cells in the periphery **(Figure 4-3)**. In line with this observation, our *in vitro* CTL differentiation experiments also confirm the defective expansion of *Hdac7*^{ko} CD8^{+} T cells as assessed by their decreased cell numbers **(Figure 4-6)**. We also showed that the decreased cell numbers of *Hdac7*^{ko} CD8^{+} T cells results from their increased apoptosis and impaired survival **(Figure 4-7)**. Clinical studies showed that the success of checkpoint blockade therapies strongly depends on the presence of a sufficient T cell infiltrate within tumors (Zhang et al., 2019). For example, melanoma patients with TIL infiltration in tumors responded better to

anti-PD-1 and anti-CTLA-4 blockade compared to patients without TIL infiltration (Ayers et al., 2017). Consistently, enhanced infiltration of $CD4^+$ and $CD8^+$ T cells in tumors could be associated with good prognosis in triple-negative breast cancer as well as non-small cell lung cancers (Matsumoto et al., 2016; So et al., 2020). Therefore, our findings suggest that the downregulation or the functional inhibition of HDAC7 results in a reduction in $CD8^+$ T cell infiltration into tumors, which is one of the main obstacles in cancer immunotherapy.

We also performed an in vivo rescue experiment in EG.7-Ova tumor bearing mice by the adoptive transfer of tumor antigen specific wt or *Hdac7*^{ko} CTLs **(Figure 4-17)**. We could successfully rescue the uncontrolled tumor growth in *Hdac7*^{ko} mice by the adoptive transfer of wt CTLs further proving that provision of adequate number of $CD8^+$ T cells is sufficient to control tumor growth in *Hdac7*^{ko} mice **(Figure 4-17)**. However, the transfer of wt and *Hdac7*^{ko} CTLs were equally effective for the control of tumor growth in *Hdac7*^{ko} mice which is not in line with our previous observations that *Hdac7*^{ko} $CD8^+$ T cells have impaired anti-tumor immune responses **(Figure 4-17)**. One explanation might be that our setup in this rescue experiment has not been appropriate enough to test the anti-tumor immune functions of CTLs due to the presence of an unaffected $CD4^+$ T cell compartment in *Hdac7*^{ko} mice. Although *Hdac7*^{ko} mice have a reduced $CD8^+$ T cell compartment, the $CD4^+$ T cell compartment is largely normal in terms of their numbers and functional capacities as assessed by cytokine production **(Figure 4-5)**. Therefore, it is not T-cell deficient. Hence, it is difficult to discriminate the effects of transferred CTLs with the already present T cells in *Hdac7*^{ko} mice. In the future, this experiment should be repeated in EG.7-Ova tumor bearing *Rag1*-deficient mice which do not have any mature T and B cells (Mombaerts et al., 1992).

Nevertheless, the analysis of tumor infiltrating $CD8^+$ T cells revealed that *Hdac7*^{ko} CTLs have increased co-expression of PD-1 and Tim-3. $CD8^+$ TILs that co-express PD-1 and Tim-3 are the main population of TILs. Moreover, this population is also the most dysfunctional and exhausted subset of $CD8^+$ T cells within solid tumors due to their impaired proliferation as well as the loss of the production of IFNγ, TNFα and IL-2 (Sakuishi et al., 2010). Accordingly, combined targeting of PD-1 and Tim-3 by antibody-mediated blockade is more effective than their single targeting for the control of tumor growth (Sakuishi et al., 2010). Thus, our data suggested that HDAC7 is needed to counteract the exhaustion of $CD8^+$ T cells during chronic antigen exposure within tumors **(Figure 4-18)**. In line with these observations, previous data

from our group showed that virus-specific CD8$^+$ T cells in *Hdac7^{ko}* mice could not expand properly during the secondary infection with LCMV-clone13 after the acute phase of LCMV infection. Similarly, these cells had elevated expression of the exhaustion marker PD-1, which was paralleled by increased viral load compared to wt littermates (Keye, 2018).

T cell exhaustion is characterized by the concurrent expression of several exhaustion markers and the loss of cytokine production capacity (Schietinger and Greenberg, 2014). For example, simultaneous co-expression of multiple co-inhibitory receptors such as PD-1, Lag-3, CD244 and CD160 was elevated in virus-specific CD8$^+$ T cells paralleled by their loss of function resulting in increased viral load during LCMV infection in mice (Blackburn et al., 2009). Simultaneous expression of these co-inhibitory receptors also correlated with the severity of the LCMV infection (Blackburn et al., 2009). Furthermore, different co-inhibitory receptors can act via independent pathways to regulate T cell exhaustion. Thus, co-targeting PD-1 and Lag-3 by antibody blockade resulted in better control of LCMV infection in mice compared to single blockade of PD-1 and Lag-3 (Blackburn et al., 2009). Therefore, our results obtained from the rescue experiment are limited to prove that the lack of *Hdac7* drives the exhaustion of CD8$^+$ T cells in case of tumor challenge. This experiment should be repeated and the expression of additional exhaustion markers such as Lag-3, Ctla-4 and Tigit as well as IFNγ, TNFα and IL-2 production of the transferred CTLs should be analyzed (Blackburn et al., 2009). As an alternative, the co-expression of exhaustion markers can be characterized by the histologic staining of EG.7-Ova tumor tissues isolated from wt and *Hdac7^{ko}* mice.

Our RNA-sequencing data **(Figure 4-19)** as well as the published scRNA-sequencing data of tumor infiltrating CD8$^+$ T cells confirm the role of HDAC7 in the exhaustion of CD8$^+$ T cells **(Figure 4-20).** We analyzed published scRNA-seq data obtained from murine melanoma-infiltrating CD8$^+$ T cells and we derived gene signatures specific for each subset of CD8$^+$ T cells within these tumors (Carmona et al., 2020) The comparison of the published scRNA-seq data and our bulk RNA-seq revealed that exhaustion-related gene signature was significantly enriched in naïve, *in vitro* activated as well as LCMV-specific *Hdac7^{ko}* CD8$^+$ T cells (Figure 4-20). Moreover, our *in vitro* T cell exhaustion protocol also validated that the lack of *Hdac7* leads to the upregulation of exhaustion markers in CD8$^+$ T cells compared to wt controls during chronic antigen stimulation **(Figure 4-25)**. We should also note that our *in vitro* T cell exhaustion assay is limited, since we could not induce the expression of some exhaustion

markers including Ctla-4 and Lag-3 by repeated antigen stimulation. Although the concurrent expression of multiple co-inhibitory receptors is necessary to define T cell exhaustion (Blackburn et al., 2009), we could not observe this phenotype during our *in vitro* T cell exhaustion assay. **(Figure 4-22)**. The commitment of $CD8^+$ T cells to exhaustion occurs in a progressive manner *in vivo* as well as during *in vitro* T cell exhaustion models (Angelosanto et al., 2012). Therefore, at least three restimulations of $CD8^+$ T cells are needed to mimic this progress *in vitro* (Liu et al., 2020). However, in our set up $CD8^+$ T cells could not survive the second and the third restimulations which are needed to mimic the progressive exhaustion and the loss of anti-tumor immune functions of $CD8^+$ T cells **(Figure 4-24)**.

5.6 Genome-wide mapping of HDAC7 gene targets by ChIP-seq

Since we characterized HDAC7 as a crucial regulator of proper anti-tumor immune function in $CD8^+$ T cells, we aimed to understand the underlying molecular mechanism of the phenotypes that we observed in the absence of HDAC7. For this purpose, we aimed to identify the genes that were directly controlled by HDAC7 in $CD8^+$ T cells. Since HDAC7 suppresses the expression of its target genes through MEF2D in T cells (Dequiedt et al., 2003), we established chromatin immunoprecipitations by using anti-MEF2D antibody to isolate MEF2D-interacting DNA. By using ChIP-qPCR experiments, we could validate that MEF2D binds to the promoter of *Nur77* upon stimulation **(Figure 4-28)**. The transcription of *Nur77* is induced by the binding of MEF2D to its promoter upon PMA/ionomycin stimulation in thymocytes, subsequently inducing their apoptosis (Dequiedt et al., 2003). Thus, we could replicate this finding in CTLs and proved that our protocol for anti-MEF2D ChIP-qPCR worked. We could also show that in *in vitro* activated *Hdac7*^{ko} $CD8^+$ T cells, MEF2D binds to the promoter of *Fasl* gene, which is one of the top hits from our RNA-seq, on the three putative MEF2 binding sites that we identified by in silico analysis **(Figure 4-29)**. FasL-mediated apoptosis of T cells is a well characterized mechanism that prevents immunopathology by inducing AICD that results from repeated antigen stimulation of $CD8^+$ T cells, thus, it represents an immune checkpoint mechanism (Zhu et al., 2019). Similarly, increased FasL expression on $CD8^+$ T cells can also diminish the numbers of $CD8^+$ TILs. The lack of $CD8^+$ T cell accumulation within tumors also interferes with the response to cancer immunotherapies (Zhu et al., 2019). Therefore, MEF2D-driven FasL expression in *Hdac7*^{ko} $CD8^+$ T cells contributed to the reduced numbers of $CD8^+$ T cells in EG.7-Ova tumors **(Figure 4-14)**. Paralleled by the increased expression of co-inhibitory molecules PD-1 and Tim-

3, increased expression of FasL could also induce tumor formation in *Hdac7*^{ko} mice by the elimination of antigen-specific CD8^{+} T cells within tumors.

Since we could successfully establish this method, we also aimed to perform anti-MEF2D ChIP-seq by using *in vitro*-activated wt and *Hdac7*^{ko} CD8^{+} T cells. However, our ChIP-seq experiment failed due to the presence of high percentage of PCR duplicates in the sequencing libraries (Furey, 2012). Although the anti-MEF2D antibody worked properly for ChIP-qPCR experiments, it was not specific enough for a successful ChIP-seq resulting in a low number of reads that can be uniquely mapped to the genome (Furey, 2012). Therefore, MEF2D ChIP-seq should be repeated by using another anti-MEF2D antibody.

As another approach, genome-wide targets of HDAC7 can be characterized by acetylated histone 3 ChIP-seq. We already observed that *Hdac7*^{ko} CD8^{+} T cells are characterized by an increased expression of acetylated histone 3 at lysine 9 and lysine 14 residues (acetyl-H3K9/K14), which is a mark for transcriptionally active genes (Azagra et al., 2016) **(Figure 4-27)**. However, it is also known that class II HDACs do not have catalytic activity due to their mutated HDAC domain, suggesting that these differences that we have observed in acetyl-H3K9/K14 expression might not be the direct effects of HDAC7 deletion in CD8^{+} T cells. Nevertheless, this experiment will help us to characterize the chromatin regions in *Hdac7*^{ko} CD8^{+} T cells which are more accessible for transcriptional machinery due to increased acetyl-H3K9/K14 as well as genes residing in these regions. The results of acetyl-H3K9/K14 ChIP-seq can also be compared to our RNA-seq data from *in vitro* activated wt and *Hdac7*^{ko} CD8^{+} T cells and help us understand the changes in the transcriptome of CD8^{+} T cells in the absence of HDAC7. Moreover, other distal regulatory regions such as enhancers that are important for the phenotype of *Hdac7*^{ko} CD8^{+} T cells can be discovered by acetyl-H3K9/K14 ChIP-seq since this specific acetylation of H3 also marks enhancers along with the transcription start sites and the promoters of genes (Azagra et al., 2016). Although performing an anti-acetyl-H3K9/K14 ChIP-seq will be useful to highlight the underlying molecular mechanisms of the phenotypes in *Hdac7*^{ko} mice at the transcriptional level, the results of this experiment should be carefully analyzed due to the minimal catalytic activity of HDAC7.

5.7 Clinical relevance of HDAC7 and HDAC inhibitors

We observed that the treatment of wt CD8^{+} T cells with the pan-HDACi vorinostat resulted in significantly reduced protein expression of HDAC7 **(Figure 4-27)** and the induction of apoptosis

(Figure 4-26). Our results are consistent with the previous findings, since pan-HDAC inhibitor vorinostat showed anti-inflammatory effects at low doses by suppressing pro-inflammatory cytokine production (Leoni et al., 2002), and the subsequent inhibition of graft-versus-host disease (GvHD) (Reddy et al., 2004). Similarly, oral administration of vorinostat to mice diminished the production of anti-inflammatory cytokines including IFNγ, TNFα, IL-1β and IL-6 that were induced by lipopolysaccharide (LPS) treatment (Leoni et al., 2002). Moreover, vorinostat and panobinostat were shown to decrease IFNγ production, the survival as well as the cytotoxic capacity of human HIV-specific $CD8^+$ T cells (Jones et al., 2014). Interestingly, HDACi do not block the deacetylase activity of HDAC7, but rather have been shown to suppress the expression of HDAC7 in several cell types including epithelial cells, bladder and prostate cancer cells as well as myeloma cells (Dokmanovic et al., 2007).

In line with the increasing number of HDACi which are currently used or being tested for the treatment of cancer (Hontecillas-Prieto et al., 2020) as well as autoimmune diseases including type I diabetes, multiple sclerosis and inflammatory bowel disease (IBD) (Christensen et al., 2011; Glauben and Siegmund, 2011; Lopresti, 2019), we propose that the inhibition of HDAC7 might impair proper anti-tumor immune responses by resulting in increased exhaustion of $CD8^+$ T cells **(Figure 5-1)**. T cell exhaustion is one of the key drivers of immune evasion in tumors since it results in dysfunctional $CD8^+$ T cells with defective proliferation paralleled by impaired pro-inflammatory cytokine production necessary for their cytotoxicity against tumor cells (Zhang et al., 2020). Furthermore, the inhibition of HDAC7 expression might also interfere with the development of proper memory responses by $CD8^+$ T cells, thus alter the function, the metabolic fitness and the calcium homeostasis as well as the survival of $CD8^+$ T cells during immune responses against viral infections and tumors **(Figure 5-1)**.

In this project, we investigated the role of HDAC7 in murine $CD8^+$ T cells. To understand, if our findings have any potential for clinical translation, the phenotypes that we observed in *Hdac7*^{ko} mice should also be tested in human cells. In case HDAC7 plays a similar role in human $CD8^+$ T cells, our results point to potential side effects of HDACi during cancer treatment. The functional inhibition of HDAC7 by HDACi might cause a disturbance in the calcium homeostasis and survival of $CD8^+$ T cells in the periphery as well as in the tumors reducing in decreased $CD8^+$ T cell infiltration in tumors. Furthermore, the inhibition of the function of HDAC7 can lead to the exhaustion of tumor-specific $CD8^+$ T cells within tumors by the upregulation of co-

inhibitory receptors such as PD-1 and TIM-3 contributing to impaired tumor control. Furthermore, our results are equally important for the design and the development of novel HDACi which are more specifically capable of targeting single class II HDACs.

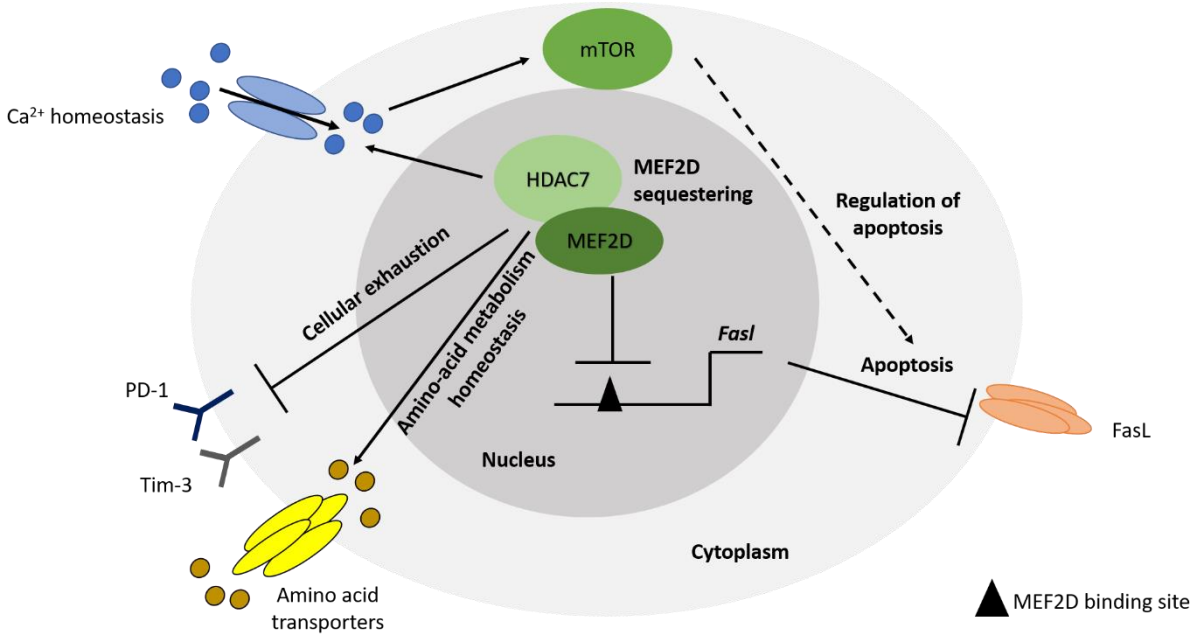

Figure 5-1 The role of HDAC7 in CD8⁺ T cells. *HDAC7 regulates multiple pathways in CD8⁺ T cells. HDAC7 is a central regulator of calcium homeostasis and amino acid metabolism in CD8⁺ T cells. The deletion of Hdac7 results in impaired mammalian target of rapamycin (mTOR) signaling. Disturbed mTOR signaling and myocyte enhancer factor 2 D (MEF2D)-driven Fas ligand (FasL) expression contribute to the apoptotic phenotype of CD8⁺ T cells in the absence of Hdac7. The lack of Hdac7 also results in the exhaustion of CD8⁺ T cells in the presence of chronic antigen exposure by upregulating co-inhibitory receptors including programmed cell death protein 1 (PD-1) and T cell immunoglobulin and mucin domain-containing-3 (Tim-3). Therefore, the deletion or the functional inhibition of HDAC7 in CD8⁺ T cells interferes with their anti-tumor immune responses*

6 REFERENCES

Adcock, I.M., 2007. HDAC inhibitors as anti-inflammatory agents. Br. J. Pharmacol. 150, 829–831. https://doi.org/10.1038/sj.bjp.0707166

Ali, I., Conrad, R.J., Verdin, E., Ott, M., 2018. Lysine Acetylation Goes Global: From Epigenetics to Metabolism and Therapeutics. Chem. Rev. 118, 1216–1252. https://doi.org/10.1021/acs.chemrev.7b00181

Anderson, K.G., Stromnes, I.M., Greenberg, P.D., 2017. Obstacles Posed by the Tumor Microenvironment to T cell Activity: A Case for Synergistic Therapies. Cancer Cell 31, 311–325. https://doi.org/10.1016/j.ccell.2017.02.008

Angelosanto, J.M., Blackburn, S.D., Crawford, A., Wherry, E.J., 2012. Progressive Loss of Memory T Cell Potential and Commitment to Exhaustion during Chronic Viral Infection. J. Virol. 86, 8161–8170. https://doi.org/10.1128/jvi.00889-12

Ayers, M., Lunceford, J., Nebozhyn, M., Murphy, E., Loboda, A., Kaufman, D.R., Albright, A., Cheng, J.D., Kang, S.P., Shankaran, V., Piha-Paul, S.A., Yearley, J., Seiwert, T.Y., Ribas, A., McClanahan, T.K., 2017. IFN-γ-related mRNA profile predicts clinical response to PD-1 blockade. J. Clin. Invest. 127, 2930–2940. https://doi.org/10.1172/JCI91190

Azagra, A., Román-gonzález, L., Collazo, O., Rodríguez-ubreva, J., De Yébenes, V.G., Barneda-zahonero, B., Rodríguez, J., De Moura, M.C., Grego-Bessa, J., Fernández-duran, I., Islam, A.B.M.M.K., Esteller, M., Ramiro, A.R., Ballestar, E., Parra, M., 2016. In vivo conditional deletion of Hdac7 reveals its requirement to establish proper b lymphocyte identity and development. J. Exp. Med. 213, 2591–2601. https://doi.org/10.1084/jem.20150821

Backs, J., Backs, T., Bezprozvannaya, S., McKinsey, T.A., Olson, E.N., 2008. Histone Deacetylase 5 Acquires Calcium/Calmodulin-Dependent Kinase II Responsiveness by Oligomerization with Histone Deacetylase 4. Mol. Cell. Biol. 28, 3437–3445. https://doi.org/10.1128/mcb.01611-07

Banerjee, A., Gordon, S.M., Intlekofer, A.M., Paley, M.A., Mooney, E.C., Lindsten, T., Wherry, E.J., Reiner, S.L., 2010. Cutting Edge: The Transcription Factor Eomesodermin Enables CD8 + T Cells To Compete for the Memory Cell Niche. J. Immunol. 185, 4988–4992. https://doi.org/10.4049/jimmunol.1002042

Barneda-Zahonero, B., Román-González, L., Collazo, O., Rafati, H., Islam, A.B.M.M.K.,

References

Bussmann, L.H., di Tullio, A., de Andres, L., Graf, T., López-Bigas, N., Mahmoudi, T., Parra, M., 2013. HDAC7 Is a Repressor of Myeloid Genes Whose Downregulation Is Required for Transdifferentiation of Pre-B Cells into Macrophages. PLoS Genet. 9. https://doi.org/10.1371/journal.pgen.1003503

Bergmeier, W., Weidinger, C., Zee, I., Feske, S., 2013. Emerging roles of store-operated Ca2+ entry through STIM and ORAI proteins in immunity, hemostasis and cancer. Channels 7, 379–391. https://doi.org/10.4161/chan.24302

Best, J.A., Blair, D.A., Knell, J., Yang, E., Mayya, V., Doedens, A., Dustin, M.L., Goldrath, A.W., Monach, P., Shinton, S.A., Hardy, R.R., Jianu, R., Koller, David, Collins, J., Gazit, R., Garrison, B.S., Rossi, D.J., Narayan, K., Sylvia, K., Kang, J., Fletcher, A., Elpek, K., Bellemare-Pelletier, A., Malhotra, D., Turley, S., Best, J.A., Jojic, V., Koller, Daphne, Shay, T., Regev, A., Cohen, N., Brennan, P., Brenner, M., Kreslavsky, T., Bezman, N.A., Sun, J.C., Kim, C.C., Lanier, L.L., Miller, J., Brown, B., Merad, M., Gautier, E.L., Jakubzick, C., Randolph, G.J., Kim, F., Rao, T.N., Wagers, A., Heng, T., Painter, M., Ericson, J., Davis, S., Ergun, A., Mingueneau, M., Mathis, D., Benoist, C., 2013. Transcriptional insights into the CD8+ T cell response to infection and memory T cell formation. Nat. Immunol. 14, 404–412. https://doi.org/10.1038/ni.2536

Blackburn, S.D., Shin, H., Haining, W.N., Zou, T., Workman, C.J., Polley, A., Betts, M.R., Freeman, G.J., Vignali, D.A.A., Wherry, E.J., 2009. Coregulation of CD8+ T cell exhaustion by multiple inhibitory receptors during chronic viral infection. Nat. Immunol. 10, 29–37. https://doi.org/10.1038/ni.1679

Boija, A., Mahat, D.B., Zare, A., Holmqvist, P.H., Philip, P., Meyers, D.J., Cole, P.A., Lis, J.T., Stenberg, P., Mannervik, M., 2017. CBP Regulates Recruitment and Release of Promoter-Proximal RNA Polymerase II. Mol. Cell 68, 491-503.e5. https://doi.org/10.1016/j.molcel.2017.09.031

Boyault, C., Sadoul, K., Pabion, M., Khochbin, S., 2007. HDAC6, at the crossroads between cytoskeleton and cell signaling by acetylation and ubiquitination. Oncogene 26, 5468–5476. https://doi.org/10.1038/sj.onc.1210614

Bradley, E.W., Carpio, L.R., Olson, E.N., Westendorf, J.J., 2015. Histone deacetylase 7 (Hdac7) suppresses chondrocyte proliferation and β-catenin activity during endochondral ossification. J. Biol. Chem. 290, 118–126. https://doi.org/10.1074/jbc.M114.596247

References

Brandman, O., Liou, J., Park, W.S., Meyer, T., 2007. STIM2 is a feedback regulator that stabilizes basal cytosolic and endoplasmic reticulum $Ca2^{+}$ levels. Cell 131, 1327–1339. https://doi.org/10.1016/j.cell.2007.11.039

Brooks, C.L., Gu, W., 2011. The impact of acetylation and deacetylation on the p53 pathway. Protein Cell 2, 456–462. https://doi.org/10.1007/s13238-011-1063-9

Brown, L.E., Kelso, A., 2009. Prospects for an influenza vaccine that induces cross-protective cytotoxic T lymphocytes. Immunol. Cell Biol. 87, 300–308. https://doi.org/10.1038/icb.2009.16

Buck, M.D., Sullivan, D.O., Geltink, R.I.K., Huber, T.B., Rambold, A.S., Pearce, E.L., Buck, M.D., Sullivan, D.O., Geltink, R.I.K., Curtis, J.D., Chang, C., Sanin, D.E., Qiu, J., Kretz, O., Braas, D., Windt, G.J.W. Van Der, Chen, Q., Huang, S.C., 2016. Mitochondrial dynamics controls T cell fate through metabolic programming. Cell 166, 63–76. https://doi: 10.1016/j.cell.2016.05.035.

Buck, M.D., Sullivan, D.O., Pearce, E.L., 2015. T cell metabolism drives immunity. Cell 212, 1345–1360. https://doi.org/10.1084/jem.20151159

Byun, M., Abhyankar, A., Lelarge, V., Plancoulaine, S., Palanduz, A., Telhan, L., Boisson, B., Picard, C., Dewell, S., Zhao, C., Jouanguy, E., Feske, S., Abel, L., Casanova, J., 2010. Whole-exome sequencing-based discovery of STIM1 deficiency in a child with fatal classic Kaposi sarcoma. J. Exp. Med. 207, 2307–2312. https://doi.org/10.1084/jem.20101597

Cantley, M.D., Fairlie, D.P., Bartold, P.M., Marino, V., Gupta, P.K., Haynes, D.R., 2015. Inhibiting histone deacetylase 1 suppresses both inflammation and bone loss in arthritis. Rheumatol. U. K. 54, 1713–1723. https://doi.org/10.1093/rheumatology/kev022

Carmona, S.J., Siddiqui, I., Bilous, M., Held, W., Gfeller, D., 2020. Deciphering the transcriptomic landscape of tumor-infiltrating CD8 lymphocytes in B16 melanoma tumors with single-cell RNA-Seq. OncoImmunology 9, 1–15. https://doi.org/10.1080/2162402X.2020.1737369

Chang, C., Curtis, J.D., Maggi, L.B., Faubert, B., Villarino, A.V., Sullivan, D.O., Huang, S.C., Windt, G.J.W.V.D., Blagih, J., Qiu, J., Weber, J.D., Pearce, E.J., Jones, R.G., Pearce, E.L., 2013a. Posttranscriptional Control of T Cell Effector Function by Aerobic Glycolysis. Cell 1239–1251.

References

Chen, L.F., Fischle, W., Verdin, E., Greene, W.C., 2001. Duration of nuclear NF-κB action regulated by reversible acetylation. Science 293, 1653–1657. https://doi.org/10.1126/science.1062374

Chen, Y., Zander, R., Khatun, A., Schauder, D.M., Cui, W., 2018. Transcriptional and Epigenetic Regulation of Effector and Memory CD8 T Cell Differentiation. Front. Immunol. 9, 2826. https://doi.org/10.3389/fimmu.2018.02826

Choudhary, C., Kumar, C., Gnad, F., Nielsen, M.L., Rehman, M., Walther, T.C., Olsen, J. V., Mann, M., 2009. Lysine acetylation targets protein complexes and co-regulates major cellular functions. Science 325, 834–840. https://doi.org/10.1126/science.1175371

Choudhary, C., Weinert, B.T., Nishida, Y., Verdin, E., Mann, M., 2014. The growing landscape of lysine acetylation links metabolism and cell signalling. Nat. Rev. Mol. Cell Biol. 15, 536–550. https://doi.org/10.1038/nrm3841

Christensen, D.P., Dahllöf, M., Lundh, M., Rasmussen, D.N., Nielsen, M.D., Billestrup, N., Grunnet, L.G., Mandrup-Poulsen, T., 2011. Histone deacetylase (HDAC) inhibition as a novel treatment for diabetes mellitus. Mol. Med. 17, 378–390. https://doi.org/10.2119/molmed.2011.00021

Chung, Y.L., Lee, M.Y., Wang, A.J., Yao, L.F., 2003. A therapeutic strategy uses histone deacetylase inhibitors to modulate the expression of genes involved in the pathogenesis of rheumatoid arthritis. Mol. Ther. 8, 707–717. https://doi.org/10.1016/S1525-0016(03)00235-1

Clocchiatti, A., Di Giorgio, E., Ingrao, S., Meyer-Almes, F.J., Tripodo, C., Brancolini, C., 2013. Class IIa HDACs repressive activities on MEF2-depedent transcription are associated with poor prognosis of ER+ breast tumors. FASEB J. 27, 942–954. https://doi.org/10.1096/fj.12-209346

Clocchiatti, A., Di Giorgio, E., Viviani, G., Streuli, C., Sgorbissa, A., Picco, R., Cutano, V., Brancolini, C., 2015. The MEF2-HDAC axis controls proliferation of mammary epithelial cells and acini formation in vitro. J. Cell Sci. 128, 3961–3976. https://doi.org/10.1242/jcs.170357

Cohen, I., Poręba, E., Kamieniarz, K., Schneider, R., 2011. Histone modifiers in cancer: Friends or foes? Genes Cancer 2, 631–647. https://doi.org/10.1177/1947601911417176

Cornel, A.M., Mimpen, I.L., Nierkens, S., 2020. MHC Class I Downregulation in Cancer:

Underlying Mechanisms and Potential Targets for Cancer Immunotherapy. Cancers 12, 1760. https://doi.org/10.3390/cancers12071760

Cosma, G., Eisenlohr, L., 2018. CD8 (+) T-cell responses in vaccination: reconsidering targets and function in the context of chronic antigen stimulation. F1000Research 7, F1000 Faculty Rev-508. https://doi.org/10.12688/f1000research.14115.1

Cox, D.M., Du, M., Marback, M., Yang, E.C.C., Chan, J., Siu, K.W.M., Mcdermott, J.C., 2003. Phosphorylation Motifs Regulating the Stability and Function of Myocyte Enhancer Factor 2A. J. Biol. Chem. 278, 15297–15303. https://doi.org/10.1074/jbc.M211312200

Day, J.A., Cohen, S.M., 2013. Investigating the selectivity of metalloenzyme inhibitors. J. Med. Chem. 56, 7997–8007. https://doi.org/10.1021/jm401053m

De Ruijter, A.J.M., Van Gennip, A.H., Caron, H.N., Kemp, S., Van Kuilenburg, A.B.P., 2003. Histone deacetylases (HDACs): Characterization of the classical HDAC family. Biochem. J. 370, 737–749. https://doi.org/10.1042/BJ20021321

Dequiedt, F., Kasler, H., Fischle, W., Kiermer, V., Weinstein, M., Herndier, B.G., Verdin, E., 2003. HDAC7, a thymus-specific class II histone deacetylase, regulates Nur77 transcription and TCR-mediated apoptosis. Immunity 18, 687–698. https://doi.org/10.1016/S1074-7613(03)00109-2

Dequiedt, F., Van Lint, J., Lecomte, E., Van Duppen, V., Seufferlein, T., Vandenheede, J.R., Wattiez, R., Kettmann, R., 2005. Phosphorylation of histone deacetylase 7 by protein kinase D mediates T cell receptor-induced Nur77 expression and apoptosis. J. Exp. Med. 201, 793–804. https://doi.org/10.1084/jem.20042034

Desvignes, L., Weidinger, C., Shaw, P., Vaeth, M., Ribierre, T., Liu, M., Fergus, T., Kozhaya, L., Mcvoy, L., Unutmaz, D., Ernst, J.D., Feske, S., 2015. STIM1 controls T cell – mediated immune regulation and inflammation in chronic infection. J. Clin. Invest. 125, 2347–2362. https://doi.org/10.1172/JCI80273.functions.

Di Giorgio, E., Brancolini, C., 2016. Regulation of class IIa HDAC activities: It is not only matter of subcellular localization. Epigenomics 8, 251–269. https://doi.org/10.2217/epi.15.106

Dokmanovic, M., Perez, G., Xu, W., Ngo, L., Clarke, C., Parmigiani, R.B., Marks, P.A., 2007. Histone deacetylase inhibitors selectively suppress expression of HDAC7. Mol. Cancer Ther. 6,

2525–2534. https://doi.org/10.1158/1535-7163.MCT-07-0251

Dougan, M., Dranoff, G., Dougan, S.K., 2019. Cancer Immunotherapy: Beyond Checkpoint Blockade. Annu. Rev. Cancer Biol. 3, 55–75. https://doi.org/10.1146/annurev-cancerbio-030518-055552

Du, M., Perry, R.L.S., Nowacki, N.B., Gordon, J.W., Salma, J., Zhao, J., Aziz, A., Chan, J., Siu, K.W.M., Mcdermott, J.C., 2008. Protein Kinase A Represses Skeletal Myogenesis by Targeting Myocyte Enhancer Factor 2D. Mol. Cell Biol. 28, 2952–2970. https://doi.org/10.1128/MCB.00248-08

Duan, G., Walther, D., 2015. The Roles of Post-translational Modifications in the Context of Protein Interaction Networks. PLoS Comput. Biol. 11, 1–23. https://doi.org/10.1371/journal.pcbi.1004049

Engelhard, V.H., Rodriguez, A.B., Ileana, S., Woods, A.N., Peske, J.D., Craig, L., 2020. Immune Cell Infiltration and Tertiary Lymphoid Structures as Determinants of Antitumor Immunity. J. Immunol. 200, 430-442. https://doi.org/10.4049/jimmunol.1701269

Estrella, N.L., Desjardins, C.A., Nocco, S.E., Clark, A.L., Maksimenko, Y., Naya, F.J., 2015. MEF2 Transcription Factors Regulate Distinct Gene Programs in Mammalian Skeletal Muscle Differentiation. J. Biol. Chem. 290, 1256–1268. https://doi.org/10.1074/jbc.M114.589838

Fai, S., Huang, X., Mckercher, S.R., Zaidi, R., Okamoto, S., Nakanishi, N., Lipton, S.A., 2015. Genomics Data Transcriptional pro fi ling of MEF2-regulated genes in human neural progenitor cells derived from embryonic stem cells. GDATA 3, 24–27. https://doi.org/10.1016/j.gdata.2014.10.022

Faraco, G., Cavone, L., Chiarugi, A., 2011. The therapeutic potential of HDAC inhibitors in the treatment of multiple sclerosis. Mol. Med. 17, 442–447. https://doi.org/10.2119/molmed.2011.00077

Feske, S., 2011. Immunodeficiency due to defects in store-operated calcium entry. Ann N. Y. Acad. Sci. 1238, 74–90. https://doi.org/10.1111/j.1749-6632.2011.06240.x

Feske, S., 2009. ORAI1 and STIM1 deficiency in human and mice : roles of store-operated Ca 2 + entry in the immune system and beyond. Immunol. Rev. 231, 189–209. https:// doi: 10.1111/j.1600-065X.2009.00818.x.

References

Fiorino, A.S., Zvibel, I., 1996. Disruption of cell-cell adhesion in the presence of sodium butyrate activates expression of the 92 kDa type IV collagenase in MDCK cells. Cell Biol. Int. 20, 489–499. https://doi.org/10.1006/cbir.1996.0064

Fischle, W., Dequiedt, F., Hendzel, M.J., Guenther, M.G., Lazar, M.A., Voelter, W., Verdin, E., 2002. Enzymatic activity associated with class II HDACs is dependent on a multiprotein complex containing HDAC3 and SMRT/N-CoR. Mol. Cell 9, 45–57. https://doi.org/10.1016/S1097-2765(01)00429-4

Flavell, S.W., Kim, T., Gray, J.M., Harmin, D.A., Hemberg, M., Hong, E.J., Markenscoff-papadimitriou, E., Bear, D.M., Greenberg, M.E., 2008. Genome-Wide Analysis of MEF2 Transcriptional Program Reveals Synaptic Target Genes and Neuronal Activity-Dependent Polyadenylation Site Selection. Neuron 60, 1022-1038. https://doi.org/10.1016/j.neuron.2008.11.029

Furey, T.S., 2012. ChIP-seq and beyond: New and improved methodologies to detect and characterize protein-DNA interactions. Nat. Rev. Genet. 13, 840–852. https://doi.org/10.1038/nrg3306

Gao, Y., Hubbert, C.C., Lu, J., Lee, Y.-S., Lee, J.-Y., Yao, T.-P., 2007. Histone Deacetylase 6 Regulates Growth Factor-Induced Actin Remodeling and Endocytosis. Mol. Cell. Biol. 27, 8637–8647. https://doi.org/10.1128/mcb.00393-07

Giorgio, E. Di, Gagliostro, E., Clocchiatti, A., Brancolini, C., 2015. The Control Operated by the Cell Cycle Machinery on MEF2 Stability Contributes to the Downregulation of CDKN1A and Entry into S Phase. Mol. Cell Biol. 35, 1633–1647. https://doi.org/10.1128/MCB.01461-14

Giraldo, N.A., Sanchez-salas, R., Peske, J.D., Vano, Y., Becht, E., Petitprez, F., Validire, P., Ingels, A., Cathelineau, X., Fridman, W.H., Sautès-fridman, C., 2019. The clinical role of the TME in solid cancer. Br. J. Cancer 120, 45-53. https://doi.org/10.1038/s41416-018-0327-z

Glauben, R., Batra, A., Fedke, I., Zeitz, M., Lehr, H.A., Leoni, F., Mascagni, P., Fantuzzi, G., Dinarello, C.A., Siegmund, B., 2006. Histone Hyperacetylation Is Associated with Amelioration of Experimental Colitis in Mice. J. Immunol. 176, 5015. https://doi.org/10.4049/jimmunol.176.8.5015

Glauben, R., Siegmund, B., 2011. Inhibition of histone deacetylases in inflammatory bowel diseases. Mol. Med. 17, 426–433. https://doi.org/10.2119/molmed.2011.00069

Gonzalez, H., Hagerling, C., Werb, Z., 2018. Roles of the immune system in cancer: from tumor initiation to metastatic progression. Genes Dev. 32, 1267–1284. https://doi.org/10.1101/gad.314617.118.tissue

Greenwood, B., 2014. The contribution of vaccination to global health: past, present and future. Philos. Trans. R. Soc. Lond. B. Biol. Sci. 369, 20130433–20130433. https://doi.org/10.1098/rstb.2013.0433

Grozinger, C.M., Schreiber, S.L., 2002. Deacetylase enzymes: Biological functions and the use of small-molecule inhibitors. Chem. Biol. 9, 3–16. https://doi.org/10.1016/S1074-5521(02)00092-3

Grozinger, C.M., Schreiber, S.L., 2000. Regulation of histone deacetylase 4 and 5 and transcriptional activity by 14-3-3-dependent cellular localization. Proc. Natl. Acad. Sci. U. S. A. 97, 7835–7840. https://doi.org/10.1073/pnas.140199597

Haberland, M., Arnold, M.A., McAnally, J., Phan, D., Kim, Y., Olson, E.N., 2007. Regulation of HDAC9 Gene Expression by MEF2 Establishes a Negative-Feedback Loop in the Transcriptional Circuitry of Muscle Differentiation. Mol. Cell. Biol. 27, 518–525. https://doi.org/10.1128/mcb.01415-06

Han, A., Pan, F., Stroud, J.C., Youn, H.D., Liu, J.O., Chen, L., 2003. Sequence-specific recruitment of transcriptional co-repressor Cabin1 by myocyte enhancer factor-2. Nature 422, 730–734. https://doi.org/10.1038/nature01555

Hayashi, M., Kim, S.-W., Imanaka-Yoshida, K., Yoshida, T., Abel, E.D., Eliceiri, B., Yang, Y., Ulevitch, R.J., Lee, J.-D., 2004. Targeted deletion of BMK1/ERK5 in adult mice perturbs vascular integrity and leads to endothelial failure. J. Clin. Invest. 113, 1138–1148. https://doi.org/10.1172/JCI19890

He, J., Ye, J., Cai, Y., Riquelme, C., Liu, J.O., Liu, X., Han, A., Chen, L., 2011. Structure of p300 bound to MEF2 on DNA reveals a mechanism of enhanceosome assembly. Nucleic Acids Res. 39, 4464–4474. https://doi.org/10.1093/nar/gkr030

Hontecillas-Prieto, L., Flores-Campos, R., Silver, A., de Álava, E., Hajji, N., García-Domínguez,

D.J., 2020. Synergistic Enhancement of Cancer Therapy Using HDAC Inhibitors: Opportunity for Clinical Trials. Front. Genet. 11. https://doi.org/10.3389/fgene.2020.578011

Howie, D., Waldmann, H., Cobbold, S.P., 2014. Nutrient sensing via mTOR in T cells maintains a tolerogenic microenvironment. Front. Immunol. 5, 1–14. https://doi.org/10.3389/fimmu.2014.00409

Hubbert, C., Guardiola, A., Shao, R., Kawaguchi, Y., Ito, A., Nixon, A., Yoshida, M., Wang, X.F., Yao, T.P., 2002. HDAC6 is a microtubule-associated deacetylase. Nature 417, 455–458. https://doi.org/10.1038/417455a

Hull, E.E., Montgomery, M.R., Leyva, K.J., 2016. HDAC Inhibitors as Epigenetic Regulators of the Immune System: Impacts on Cancer Therapy and Inflammatory Diseases. BioMed Res. Int. 2016. https://doi.org/10.1155/2016/8797206

Intlekofer A. M., Takemoto N. J., Wherry E.J., Longworth S.A., Northrup J.T., Palanivel V.R., Mullen A.C., Gasink C.R., Kaech S.M., Miller J.D., Gapin L., Ryan K., Russ A.P., Lindsten T., Orange J.S., Goldrath A.W., Ahmed R., Reiner S.L., 2005. Effector and memory CD8 + T cell fate coupled T-bet and eomesodermin. Nat. Immunol. 6, 1236-1244. https://doi: 10.1038/ni1268.

Itakura, E., Huang, R.-R., Wen, D.-R., Paul, E., Wünsch, P.H., Cochran, A.J., 2011. IL-10 expression by primary tumor cells correlates with melanoma progression from radial to vertical growth phase and development of metastatic competence. Mod. Pathol. 24, 801–809. https://doi.org/10.1038/modpathol.2011.5

Jang, H., Choi, D.E., Kim, H., Cho, E.J., Youn, H.D., 2007. Cabin1 represses MEF2 transcriptional activity by association with a methyltransferase, SUV39H1. J. Biol. Chem. 282, 11172–11179. https://doi.org/10.1074/jbc.M611199200

Jiménez-Canino, R., Lorenzo-Díaz, F., Jaisser, F., Farman, N., Giraldez, T., De La Rosa, D.A., 2016. Histone deacetylase 6-controlled Hsp90 acetylation significantly alters mineralocorticoid receptor subcellular dynamics but not its transcriptional activity. Endocrinology 157, 2515–2532. https://doi.org/10.1210/en.2015-2055

Jin, M., Klionsky, D.J., Jin, M., Klionsky, D.J., 2015. The amino acid transporter SLC38A9 regulates The amino acid transporter SLC38A9 regulates MTORC1 and autophagy. Autophagy 8627, 9–11. https://doi.org/10.1080/15548627.2015.1084461

Johnson, M.E., Deliard, S., Zhu, F., Xia, Q., Wells, A.D., Hankenson, K.D., Grant, S.F.A., 2014. A ChIP-seq-Defined Genome-Wide Map of MEF2C Binding Reveals Inflammatory Pathways Associated with Its Role in Bone Density Determination. Calcif. Tissue. Int. 94, 396–402. https://doi.org/10.1007/s00223-013-9824-5

Jones, R.B., O'Connor, R., Mueller, S., Foley, M., Szeto, G.L., Karel, D., Lichterfeld, M., Kovacs, C., Ostrowski, M.A., Trocha, A., Irvine, D.J., Walker, B.D., 2014. Histone deacetylase inhibitors impair the elimination of hiv-infected cells by cytotoxic t-lymphocytes. PLoS Pathog. 10. https://doi.org/10.1371/journal.ppat.1004287

Jones, R.G., Pearce, E.J., 2017. MenTORing Immunity: mTOR Signaling in the Development and Function of Tissue-Resident Immune Cells. Immunity 46, 730–742. https://doi.org/10.1016/j.immuni.2017.04.028

Joshi, N.S., Cui, W., Chandele, A., Lee, H.K., Urso, D.R., Hagman, J., Gapin, L., Kaech, S.M., 2007. Inflammation Directs Memory Precursor and Short-Lived Effector CD8 + T Cell Fates via the Graded Expression of T-bet Transcription Factor. Immunity 27, 281–295. https://doi.org/10.1016/j.immuni.2007.07.010

Kasler, H.G., Lee, I.S., Lim, H.W., Verdin, E., 2018. Histone Deacetylase 7 mediates tissue-specific autoimmunity via control of innate effector function in invariant Natural Killer T Cells. eLife 7, e32109. https://doi.org/10.7554/eLife.32109

Kasler, H.G., Lim, H.W., Mottet, D., Collins, A.M., Lee, I.S., Verdin, E., 2012. Nuclear export of histone deacetylase 7 during thymic selection is required for immune EMBO J. 31, 4453–4465. https://doi.org/10.1038/emboj.2012.295

Kasler, H.G., Verdin, E., 2007. Histone Deacetylase 7 Functions as a Key Regulator of Genes Involved in both Positive and Negative Selection of Thymocytes. Mol. Cell. Biol. 27, 5184–5200. https://doi.org/10.1128/MCB.02091-06

Kasler, H.G., Young, B.D., Mottet, D., Lim, W., Collins, A.M., Olson, E.N., Verdin, E., 2011. Histone Deacetylase 7 Regulates Cell Survival and TCR Signaling in CD4/CD8 Double-Positive Thymocytes. J. Immunol. 186, 4782-4793. https://doi.org/10.4049/jimmunol.1001179

Kato, Y., Zhao, M., Morikawa, A., Sugiyama, T., Chakravortty, D., Koide, N., Yoshida, T., Tapping, R.I., Yang, Y., Yokochi, T., Lee, J., 2000. Big Mitogen-activated Kinase Regulates Multiple Members of the MEF2 Protein Family. J. Biol. Chem. 275, 18534–18540.

https://doi.org/10.1074/jbc.M001573200

Kawaguchi, Y., Kovacs, J.J., McLaurin, A., Vance, J.M., Ito, A., Yao, T.P., 2003. The deacetylase HDAC6 regulates aggresome formation and cell viability in response to misfolded protein stress. Cell 115, 727–738. https://doi.org/10.1016/S0092-8674(03)00939-5

Keye J., 2018. Die funktionelle Rolle von Histondeacetylase 7 in peripheren T Zellen. Doctoral dissertation. Freie Universität Berlin

Knudson, K.M., Pritzl, C.J., Saxena, V., Altman, A., Daniels, M.A., Teixeiro, E., 2017. NF κ B – Pim-1 – Eomesodermin axis is critical for maintaining CD8 T-cell memory quality. Proc. Natl. Acad. Sci. U. S. A. 114, 1659-1667. https://doi.org/10.1073/pnas.1608448114

Kohlmeier, J.E., Ely, K.H., Roberts, A.D., Blackman, M.A., Woodland, D.L., 2006. T-cell memory and recall responses to respiratory virus infections. Immunol. Rev. 211, 119–132. https:// doi: 10.1111/j.0105-2896.2006.00385.x.

Kovacs, J.J., Murphy, P.J.M., Gaillard, S., Zhao, X., Wu, J.T., Nicchitta, C. V., Yoshida, M., Toft, D.O., Pratt, W.B., Yao, T.P., 2005. HDAC6 regulates Hsp90 acetylation and chaperone-dependent activation of glucocorticoid receptor. Mol. Cell 18, 601–607. https://doi.org/10.1016/j.molcel.2005.04.021

Kozhemyakina, E., Cohen, T., Yao, T.-P., Lassar, A.B., 2009. Parathyroid Hormone-Related Peptide Represses Chondrocyte Hypertrophy through a Protein Phosphatase 2A/Histone Deacetylase 4/MEF2 Pathway. Mol. Cell. Biol. 29, 5751–5762. https://doi.org/10.1128/mcb.00415-09

Lahm, A., Paolini, C., Pallaoro, M., Nardi, M.C., Jones, P., Neddermann, P., Sambucini, S., Bottomley, M.J., Surdo, P. Lo, Koch, U., Francesco, R. De, Steinku, C., Gallinari, P., 2007. Unraveling the hidden catalytic activity of vertebrate class IIa histone deacetylases. Proc. Natl. Acad. Sci. U. S. A. 104, 17335–17340. https://doi.org/10.1073/pnas.0706487104

Larsen, L., Tonnesen, M., Ronn, S.G., Størling, J., Jørgensen, S., Mascagni, P., Dinarello, C.A., Billestrup, N., Mandrup-Poulsen, T., 2007. Inhibition of histone deacetylases prevents cytokine-induced toxicity in beta cells. Diabetologia 50, 779–789. https://doi.org/10.1007/s00125-006-0562-3

Lee, H., Rezai-Zadeh, N., Seto, E., 2004. Negative Regulation of Histone Deacetylase 8 Activity

by Cyclic AMP-Dependent Protein Kinase A. Mol. Cell. Biol. 24, 765–773. https://doi.org/10.1128/mcb.24.2.765-773.2004

Leoni, F., Zaliani, A., Bertolini, G., Porro, G., Pagani, P., Pozzi, P., Donà, G., Fossati, G., Sozzani, S., Azam, T., Bufler, P., Fantuzzi, G., Goncharov, I., Kim, S.H., Pomerantz, B.J., Reznikov, L.L., Siegmund, B., Dinarello, C.A., Mascagni, P., 2002. The antitumor histone deacetylase inhibitor suberoylanilide hydroxamic acid exhibits antiinflammatory properties via suppression of cytokines. Proc. Natl. Acad. Sci. U. S. A. 99, 2995–3000. https://doi.org/10.1073/pnas.052702999

Li, M., Linseman, D.A., Allen, M.P., Meintzer, M.K., Wang, X., Laessig, T., Wierman, M.E., Heidenreich, K.A., 2001. Myocyte enhancer factor 2A and 2D undergo phosphorylation and caspase-mediated degradation during apoptosis of rat cerebellar granule neurons. J. Neurosci. 21, 6544–6552. https://doi.org/10.1523/jneurosci.21-17-06544.2001

Li, X., Song, S., Liu, Y., Ko, S., Kao, H., 2004. Phosphorylation of the Histone Deacetylase 7 Modulates Its Stability and Association with 14-3-3 Proteins. J. Biol. Chem. 279, 34201–34208. https://doi.org/10.1074/jbc.M405179200

Liou, J., Kim, M.L., Heo, W. Do, Jones, J.T., Myers, J.W., Ferrell, J.E., Meyer, T., 2005. STIM Is a Ca 2 + Sensor Essential for Ca 2 + -Store-Depletion-Triggered Ca 2 + Influx. Curr. Biol. 15, 1235–1241. https://doi.org/10.1016/j.cub.2005.05.055

Liu, C., Somasundaram, A., Manne, S., Gocher, A.M., Szymczak-workman, A.L., Vignali, K.M., Scott, E.N., Normolle, D.P., Wherry, E.J., Lipson, E.J., Ferris, R.L., Bruno, T.C., Workman, C.J., Vignali, D.A.A., 2020. Neuropilin-1 is a T cell memoty checkpoint limiting long-term antitumor immunity. Nat. Immunol. 21, 1010-1021. https://doi: 10.1038/s41590-020-0733-2.

Lopresti, P., 2019. The selective HDAC6 inhibitor ACY-738 sneaks into memory and disease regulation in an animal model of multiple sclerosis. Front. Neurol. 10. https://doi.org/10.3389/fneur.2019.00519

Luik, R.M., Wu, M.M., Buchanan, J., Lewis, R.S., 2006. The elementary unit of store-operated Ca 2 + entry: local activation of CRAC channels by STIM1 at ER–plasma membrane junctions. J. Cell. Biol. 174, 815–825. https://doi.org/10.1083/jcb.200604015

Lundblad, J.R., Kwok, R.P.S., Laurance, M.E., Harter, M.L., Goodman, R.H., 1995. Adenoviral ElA-associated protein p300 as a functional homologue of the transcriptional co-activator CBP.

Nature 374, 85–88. https://doi.org/10.1038/374085a0

Ma, K., Chan, J.K.L., Zhu, G., Wu, Z., 2005. Myocyte Enhancer Factor 2 Acetylation by p300 Enhances Its DNA Binding Activity, Transcriptional Activity, and Myogenic Differentiation. Mol. Cell. Biol. 25, 3575–3582. https://doi.org/10.1128/mcb.25.9.3575-3582.2005

Mao, Z., Bonni, A., Xia, F., Nadal-Vicens, M., Greenberg, M.E., 1999. Neuronal activity-dependent cell survival mediated by transcription factor MEF2. Science 286, 785–790. https://doi.org/10.1126/science.286.5440.785

Margariti, A., Xiao, Q., Zampetaki, A., Zhang, Z., Li, H., Martin, D., Hu, Y., Zeng, L., Xu, Q., 2009. Splicing of HDAC7 modulates the SRF-myocardin complex during stem-cell differentiation towards smooth muscle cells. J. Cell Sci. 122, 460–470. https://doi.org/10.1242/jcs.034850

Marmorstein, R., Zhou, M.M., 2014. Writers and readers of histone acetylation: Structure, mechanism, and inhibition. Cold Spring Harb. Perspect. Biol. 6, 1–25. https://doi.org/10.1101/cshperspect.a018762

Martin, M., Kettmann, R., Dequiedt, F., 2007. Class IIa histone deacetylases: Regulating the regulators. Oncogene 26, 5450–5467. https://doi.org/10.1038/sj.onc.1210613

Martin, M., Potente, M., Janssens, V., Vertommen, D., Twizere, J.C., Rider, M.H., Goris, J., Dimmeler, S., Kettmann, R., Dequiedt, F., 2008. Protein phosphatase 2A controls the activity of histone deacetylase 7 during T cell apoptosis and angiogenesis. Proc. Natl. Acad. Sci. U. S. A. 105, 4727–4732. https://doi.org/10.1073/pnas.0708455105

Martin, M.D., Badovinac, V.P., 2018. Defining Memory CD8 T Cell. Front. Immunol. 9, 1–10. https://doi.org/10.3389/fimmu.2018.02692

Masopust, D., 2008. Developing an HIV cytotoxic T-lymphocyte vaccine: issues of CD8 T-cell quantity, quality and location. J. Intern. Med. 265, 125–137. https://doi.org/10.1111/j.1365-2796.2008.02054.x

Matsumoto, H., Thike, A.A., Li, H., Yeong, J., Koo, S., Dent, R.A., Tan, P.H., Iqbal, J., 2016. Increased CD4 and CD8-positive T cell infiltrate signifies good prognosis in a subset of triple-negative breast cancer. Breast Cancer Res. Treat. 156, 237–247. https://doi.org/10.1007/s10549-016-3743-x

Matthews, S.A., Liu, P., Spitaler, M., Olson, E.N., McKinsey, T.A., Cantrell, D.A., Scharenberg,

A.M., 2006. Essential Role for Protein Kinase D Family Kinases in the Regulation of Class II Histone Deacetylases in B Lymphocytes. Mol. Cell. Biol. 26, 1569–1577. https://doi.org/10.1128/mcb.26.4.1569-1577.2006

McKinsey, T.A., Zhang, C.L., Lu, J., Olson, E.N., 2000. Signal-dependent nuclear export of a histone deacetylase regulates muscle differentiation. Nature 408, 106–111. https://doi.org/10.1038/35040593

Metallo, C.M., Heiden, M.G. Vander, 2013. Understanding Metabolic Regulation and Its Influence on Cell Physiology. Mol. Cell. 49, 388-398. https://doi.org/: 10.1016/j.molcel.2013.01.018.

Mihaylova, M.M., Vasquez, D.S., Ravnskjaer, K., Denechaud, P.D., Yu, R.T., Alvarez, J.G., Downes, M., Evans, R.M., Montminy, M., Shaw, R.J., 2011. Class IIa histone deacetylases are hormone-activated regulators of FOXO and mammalian glucose homeostasis. Cell 145, 607–621. https://doi.org/10.1016/j.cell.2011.03.043

Mishra, N., Brown, D.R., Olorenshaw, I.M., Kammer, G.M., 2001. Trichostatin A reverses skewed expression of CD154, interleukin-10, and interferon-γ gene and protein expression in lupus T cells. Proc. Natl. Acad. Sci. U. S. A. 98, 2628–2633. https://doi.org/10.1073/pnas.051507098

Mishra, N., Reilly, C.M., Brown, D.R., Ruiz, P., Gilkeson, G.S., 2003. Histone deacetylase inhibitors modulate renal disease in the MRL-lpr/lpr mouse. J. Clin. Invest. 111, 539–552. https://doi.org/10.1172/JCI16153

Miska, E.A., Karlsson, C., Langley, E., Nielsen, S.J., Pines, J., Kouzarides, T., 1999. HDAC4 deacetylase associates with and represses the MEF2 transcription factor. EMBO J. 18, 5099–5107. https://doi.org/10.1093/emboj/18.18.5099

Molkentin, J.D., Black, B.L., Martin, J.F., Olson, E.N., 1996. Mutational analysis of the DNA binding, dimerization, and transcriptional activation domains of MEF2C. Mol. Cell. Biol. 16, 2627–2636. https://doi.org/10.1128/mcb.16.6.2627

Molon, B., Ugel, S., Del Pozzo, F., Soldani, C., Zilio, S., Avella, D., De Palma, A., Mauri, P., Monegal, A., Rescigno, M., Savino, B., Colombo, P., Jonjic, N., Pecanic, S., Lazzarato, L., Fruttero, R., Gasco, A., Bronte, V., Viola, A., 2011. Chemokine nitration prevents intratumoral infiltration of antigen-specific T cells. J. Exp. Med. 208, 1949–1962.

https://doi.org/10.1084/jem.20101956

Mombaerts, P., Iacomini, J., Johnson, R.S., Herrup, K., Tonegawa, S., Papaioannou, V.E., 1992. RAG-1-deficient mice have no mature B and T lymphocytes. Cell 68, 869–877. https://doi.org/10.1016/0092-8674(92)90030-G

Moreth, K., Riester, D., Hildmann, C., Hempel, R., Wegener, D., Schober, A., Schwienhorst, A., 2007. An active site tyrosine residue is essential for amidohydrolase but not for esterase activity of a class 2 histone deacetylase-like bacterial enzyme. Biochem. J. 401, 659–665. https://doi.org/10.1042/BJ20061239

Müller, M.R., Rao, A., 2010. NFAT, immunity and cancer: a transcription factor comes of age. Nat. Rev. Immunol. 10, 645-656. https://doi.org/10.1038/nri2818

Murciano-Goroff, Y.R., Warner, A.B., Wolchok, J.D., 2020. The future of cancer immunotherapy: microenvironment-targeting combinations. Cell Res. 30, 507–519. https://doi.org/10.1038/s41422-020-0337-2

Muth, V., Nadaud, S., Grummt, I., Voit, R., 2001. Acetylation of TAFI68, a subunit of TIF-IB/SL1, activates RNA polymerase I transcription. EMBO J. 20, 1353–1362. https://doi.org/10.1093/emboj/20.6.1353

Nabel, G.J., 2007. Mapping the future of HIV vaccines. Nat. Rev. Microbiol. 5, 482-484. https://doi: 10.1038/nrmicro1713.

Nakaya, M., Xiao, Y., Zhou, X., Chang, J., Chang, M., Cheng, X., Blonska, M., Lin, X., Sun, S., 2014. Inflammatory T Cell Responses Rely on Amino Acid Transporter ASCT2 Facilitation of Glutamine Uptake and mTORC1 Kinase Activation. Immunity 5, 692-705. https://doi: 10.1016/j.immuni.2014.04.007.

Navarro, M.N., Goebel, J., Feijoo-carnero, C., Morrice, N., Cantrell, D.A., 2011. resource Phosphoproteomic analysis reveals an intrinsic pathway for the regulation of histone deacetylase 7 that controls the function of cytotoxic T lymphocytes. Nat. Immunol. 12. https://doi.org/10.1038/ni.2008

Nishida, K., Komiyama, T., Miyazawa, S.I., Shen, Z.N., Furumatsu, T., Doi, H., Yoshida, A., Yamana, J., Yamamura, M., Ninomiya, Y., Inoue, H., Asahara, H., 2004. Histone deacetylase inhibitor suppression of autoantibody-mediated arthritis in mice via regulation of p16INK4a

and p21 WAF1/Cip1 expression. Arthritis Rheum. 50, 3365–3376. https://doi.org/10.1002/art.20709

Nishino, T.G., Miyazaki, M., Hoshino, H., Miwa, Y., Horinouchi, S., Yoshida, M., 2008. 14-3-3 regulates the nuclear import of class IIa histone deacetylases. Biochem. Biophys. Res. Commun. 377, 852–856. https://doi.org/10.1016/j.bbrc.2008.10.079

North, B.J., Marshall, B.L., Borra, M.T., Denu, J.M., Verdin, E., 2003. The human Sir2 ortholog, SIRT2, is an NAD+-dependent tubulin deacetylase. Mol. Cell 11, 437–444. https://doi.org/10.1016/S1097-2765(03)00038-8

Khochbin, Verdel, Lemercier, Seigneurin-Berny, 2001. Functional significance of histone deacetylase diversity. Curr. Opin. Genet. Dev. 11, 162–166. https:// doi: 10.1016/s0959-437x(00)00174-x.

Olson and Schutz, 1995. Regulation of muscle differentiation by the MEF2 family of MADS box transcription factors. Dev Biol. 14, 2–14. https:// doi: 10.1006/dbio.1995.0002.

Park, S.Y., Kim, J.S., 2020. A short guide to histone deacetylases including recent progress on class II enzymes. Exp. Mol. Med. 52, 204–212. https://doi.org/10.1038/s12276-020-0382-4

Paroni, G., Mizzau, M., Henderson, C., Sal, G. Del, Schneider, C., Brancolini, C., Biomediche, T., Biologia-universita, S., 2004. Caspase-dependent Regulation of Histone Deacetylase 4 Nuclear-Cytoplasmic Shuttling Promotes Apoptosis. Mol. Biol. Cell. 15, 2804–2818. https://doi.org/10.1091/mbc.E03

Parra, M., Kasler, H., McKinsey, T.A., Olson, E.N., Verdin, E., 2005. Protein kinase D1 phosphorylates HDAC7 and induces its nuclear export after T-cell receptor activation. J. Biol. Chem. 280, 13762–13770. https://doi.org/10.1074/jbc.M413396200

Pearce, E.L., Mullen, A.C., Martins, A., Krawczyk, C.M., Hutchins, A.S., Zediak, V.P., Banica, M., Dicioccio, C.B., Gross, D.A., Mao, C., Shen, H., Cereb, N., Yang, S.Y., Lindsten, T., Rossant, J., Hunter, C.A., Reiner, S.L., 2004. Control of Effector $CD8^+$ T Cell Function by the Transcription Factor Eomesodermin. Science 302, 1041-1043. https://doi: 10.1126/science.1090148.

Pearce, E.L., Walsh, M.C., Cejas, P.J., Harms, G.M., Shen, H., Wang, L., Jones, R.G., Choi, Y., 2009. Enhancing CD8 T-cell memory by modulating fatty acid metabolism. Nature 460, 103–108. https://doi.org/10.1038/nature08097

Peng, D., Kryczek, I., Nagarsheth, N., Zhao, L., Wei, S., Wang, W., Sun, Y., Zhao, E., Vatan, L., Szeliga, W., Kotarski, J., Tarkowski, R., Dou, Y., Cho, K., Hensley-Alford, S., Munkarah, A., Liu, R., Zou, W., 2015. Epigenetic silencing of TH1-type chemokines shapes tumour immunity and immunotherapy. Nature 527, 249–253. https://doi.org/10.1038/nature15520

Pietrocola, F., Galluzzi, L., Bravo-San Pedro, J.M., Madeo, F., Kroemer, G., 2015. Acetyl coenzyme A: A central metabolite and second messenger. Cell Metab. 21, 805–821. https://doi.org/10.1016/j.cmet.2015.05.014

Plitas, G., Rudensky, A.Y., 2020. Regulatory T Cells in Cancer. Annu. Rev. Cancer Biol. 4, 459–477. https://doi.org/10.1146/annurev-cancerbio-030419-033428

Pluhar, G.E., Pennell, C.A., Olin, M.R., 2015. $CD8^+$ T Cell-Independent Immune-Mediated Mechanisms of Anti-Tumor Activity. Crit. Rev. Immunol. 35, 153–172. https://doi.org/10.1615/critrevimmunol.2015013607

Poligone, B., 2011. Romidepsin: evidence for its potential use to manage previously treated cutaneous T cell lymphoma. Core Evid. 6, 1–12. https://doi.org/10.2147/CE.S9084

Pollizzi, K.N., Delgoffe, G.M., Powell, J.D., Pollizzi, K.N., Patel, C.H., Sun, I., Oh, M., Waickman, A.T., Wen, J., Delgoffe, G.M., 2015. mTORC1 and mTORC2 selectively regulate CD8 + T cell differentiation. J. Clin. Invest. 125, 2090–2108. https://doi.org/10.1172/JCI77746DS1

Pollizzi, K.N., Powell, J.D., 2015. Regulation of T cells by mTOR: The known knowns and the known unknowns. Trends Immunol. 36, 13–20. https://doi.org/10.1016/j.it.2014.11.005

Pon, J.R., Marra, M.A., 2016. MEF2 transcription factors: Developmental regulators and emerging cancer genes. Oncotarget 7, 2297–2312. https://doi.org/10.18632/oncotarget.6223

Potthoff, M.J., Olson, E.N., 2007. MEF2: A central regulator of diverse developmental programs. Development 134, 4131–4140. https://doi.org/10.1242/dev.008367

Prakriya, M., Feske, S., Gwack, Y., Srikanth, S., Rao, A., Hogan, P.G., 2006. Orai1 is an essential pore subunit of the CRAC channel. Nature 443, 10–13. https://doi.org/10.1038/nature05122

Raf, R., 2013. Dense genotyping of immune-related disease regions identifies nine new risk loci for primary sclerosing cholangitis. Nat. Genet. 6, 670-675. https://doi.org/10.1038/ng.2616

Rebsamen, M., Superti-furga, G., Manuele, F., 2016. SLC38A9: A lysosomal amino acid

transporter at the core of the amino acid-sensing machinery that controls MTORC1. Autophagy 12, 1061–1062. https://doi.org/10.1080/15548627.2015.1091143

Reddy, P., Maeda, Y., Hotary, K., Liu, C., Reznikov, L.L., Dinarello, C.A., Ferrara, J.L.M., 2004. Histone deacetylase inhibitor suberoylanilide hydroxamic acid reduces acute graft-versus-host disease and preserves graft-versus-leukemia effect. Proc. Natl. Acad. Sci. U. S. A. 101, 3921–3926. https://doi.org/10.1073/pnas.0400380101

Ren, W., Liu, G., Yin, J., Tan, B., Wu, G., Bazer, F.W., Peng, Y., Yin, Y., 2017. Amino-acid transporters in T-cell activation and differentiation. Cell Death Dis. 1–9. https://doi.org/10.1038/cddis.2016.222

Roos, J., Digregorio, P.J., Yeromin, A. V, Ohlsen, K., Lioudyno, M., Zhang, S., Safrina, O., Kozak, J.A., Wagner, S.L., Cahalan, M.D., Veliçelebi, G., Stauderman, K.A., 2004. STIM1, an essential and conserved component of store-operated Ca^{2+} channel function. J. Cell Biol. 6, 435–445. https://doi.org/10.1083/jcb.200502019

Roy, S., Packman, K., Jeffrey, R., Tenniswood, M., 2005. Histone deacetylase inhibitors differentially stabilize acetylated p53 and induce cell cycle arrest or apoptosis in prostate cancer cells. Cell Death Differ. 12, 482–491. https://doi.org/10.1038/sj.cdd.4401581

Ryan, K., Russ, A.P., Lindsten, T., Orange, J.S., Goldrath, A.W., Ahmed, R., Reiner, S.L., 2005. Effector and memory CD8+ T cell fate coupled by T-bet and eomesodermin. Nat. Immunol. 6, 1236–1244. https://doi.org/10.1038/ni1268

Sakuishi, K., Apetoh, L., Sullivan, J.M., Blazar, B.R., Kuchroo, V.K., Anderson, A.C., 2010. Targeting Tim-3 and PD-1 pathways to reverse T cell exhaustion and restore anti-tumor immunity. J. Exp. Med. 207, 2187–2194. https://doi.org/10.1084/jem.20100643

Santo-Domingo, J., Demaurex, N., 2012. Perspectives on: SGP Symposium on Mitochondrial Physiology and Medicine: The renaissance of mitochondrial pH. J. Gen. Physiol. 139, 415–423. https://doi.org/10.1085/jgp.201110767

Schietinger, A., Greenberg, P.D., 2014. Tolerance and exhaustion: Defining mechanisms of T cell dysfunction. Trends Immunol. 35, 51–60. https://doi.org/10.1016/j.it.2013.10.001

Eckschlager T, Plch J, Stiborova M, Hrabeta J. Histone Deacetylase Inhibitors as Anticancer Drugs., 2017. Histone Deacetylase Inhibitors as Anticancer Drugs. Int J Mol Sci. 18, 1–25.

https://doi.org/10.3390/ijms18071414

Scott, F.L., Fuchs, G.J., Boyd, S.E., Denault, J., Hawkins, C.J., Dequiedt, F., Salvesen, G.S., 2008. Caspase-8 Cleaves Histone Deacetylase 7 and Abolishes Its Transcription Repressor Function. J. Biol. Chem. 283, 19499–19510. https://doi.org/10.1074/jbc.M800331200

Sengupta, N., Seto, E., 2004. Regulation of histone deacetylase activities. J. Cell. Biochem. 93, 57–67. https://doi.org/10.1002/jcb.20179

Shaw, P.J., Kaech, S.M., Feske, S., Shaw, P.J., Weidinger, C., Vaeth, M., Luethy, K., Kaech, S.M., Feske, S., 2014. CD4 + and CD8 + T cell – dependent antiviral immunity requires STIM1 and STIM2. J. Clin. Invest. 124, 4549–4563. https://doi.org/10.1172/JCI76602.

Shore, P., Sharrocks, A.D., 1995. The MADS-Box Family of Transcription Factors. Eur. J. Biochem. 229, 1–13. https://doi.org/10.1111/j.1432-1033.1995.tb20430.x

Shrikant, P.A., Rao, R., Li, Q., Kesterson, J., Eppolito, C., Mischo, A., Singhal, P., 2010. Regulating functional cell fates in CD8 T cells. Immunol. Res. 46, 12–22. https://doi.org/10.1007/s12026-009-8130-9

Sleiman, S.F., Langley, B.C., Basso, M., Berlin, J., Xia, L., Payappilly, J.B., Kharel, M.K., Guo, H., Marsh, J.L., Thompson, L.M., Mahishi, L., Ahuja, P., Maclellan, W.R., Geschwind, D.H., Coppola, G., Rohr, J., Ratan, R.R., 2011. Mithramycin is a gene-selective sp1 inhibitor that identifies a biological intersection between cancer and neurodegeneration. J. Neurosci. 31, 6858–6870. https://doi.org/10.1523/jneurosci.0710-11.2011

Slepak, T.I., Webster, K.A., Zang, J., Prentice, H., O'Dowd, A., Hicks, M.N., Bishopric, N.H., 2001. Control of Cardiac-specific Transcription by p300 through Myocyte Enhancer Factor-2D. J. Biol. Chem. 276, 7575–7585. https://doi.org/10.1074/jbc.M004625200

Smith, K.A., 2011. Edward jenner and the small pox vaccine. Front. Immunol. 2, 21–21. https://doi.org/10.3389/fimmu.2011.00021

So, Y.K., Byeon, S.-J., Ku, B.M., Ko, Y.H., Ahn, M.-J., Son, Y.-I., Chung, M.K., 2020. An increase of CD8+ T cell infiltration following recurrence is a good prognosticator in HNSCC. Sci. Rep. 10, 20059. https://doi.org/10.1038/s41598-020-77036-8

Strahl, B.D., Allis, C.D., 2000. The language of covalent histone modifications. Nature 403, 41–45. https://doi.org/10.1038/47412

Struhl, K., 1998. Histone acetylation and transcriptional regulatory mechanisms. Genes Dev. 12, 599–606. https://doi.org/10.1101/gad.12.5.599

Suraweera, A., Byrne, K.J.O., Richard, D.J., Chen, S., 2018a. Combination Therapy With Histone Deacetylase Inhibitors (HDACi) for the Treatment of Cancer : Achieving the Full Therapeutic Potential of HDACi. Front. Oncol., 8, 1–15. https://doi.org/10.3389/fonc.2018.00092

Szabo, S.J., Sullivan, B.M., Stemmann, C., Satoskar, A.R., Sleckman, B.P., Glimcher, L.H., 2002. Distinct Effects of T-bet in Th1 Lineage Commitment and IFNγ Production in CD4 and CD8 T Cells. Science 295, 338–343. https://doi: 10.1126/science.1065543.

Takemoto, N., Intlekofer, A.M., John, T., Wherry, E.J., Reiner, S.L., 2020. Cutting Edge: IL-12 Inversely Regulates T-bet and Eomesodermin Expression during Pathogen-Induced CD8 + T Cell Differentiation. J. Ommunol. 177, 7515-7519. https://doi.org/10.4049/jimmunol.177.11.7515

Taube, R., Lin, X., Irwin, D., Fujinaga, K., Peterlin, B.M., 2002. Interaction between P-TEFb and the C-Terminal Domain of RNA Polymerase II Activates Transcriptional Elongation from Sites Upstream or Downstream of Target Genes. Mol. Cell Biol. 22, 321–331. https://doi.org/10.1128/MCB.22.1.321

Tay, R.E., Richardson, E.K., Toh, H.C., 2020. Revisiting the role of CD4+ T cells in cancer immunotherapy—new insights into old paradigms. Cancer Gene Ther. 28, 5–17. https://doi.org/10.1038/s41417-020-0183-x

Theos, A.C., Martina, A., Hurbain, I., Peden, A.A., Sviderskaya, E. V, Stewart, A., Robinson, M.S., Bennett, D.C., Cutler, D.F., Bonifacino, J.S., Marks, M.S., 2005. Functions of adaptor protein (AP)-3 and AP-1 in tyrosinase sorting from endosomes to melanosomes. Mol. Biol. Cell 16, 5356–5372. https://doi.org/10.1091/mbc.E05

Todryk, S.M., Hill, A.V.S., 2007. Malaria vaccines: the stage we are at. Nat. Rev. Microbiol 5, 487–489. https://doi.org/10.1038/nrmicro1712

Vaeth, M., Maus, M., Klein-Hessling, S., Freinkman, E., Yang, J., Eckstein, M., Cameron, S., Turvey, S.E., Serfling, E., Berberich-Siebelt, F., Possemato, R., Feske, S., 2017. Store-Operated Ca 2+ Entry Controls Clonal Expansion of T Cells through Metabolic Reprogramming. Immunity 47, 664-679.e6. https://doi.org/10.1016/j.immuni.2017.09.003

Vannini, A., Volpari, C., Filocamo, G., Casavola, E.C., Brunetti, M., Renzoni, D., Chakravarty, P., Paolini, C., De Francesco, R., Gallinari, P., Steinkühler, C., Di Marco, S., 2004. Crystal structure of a eukaryotic zinc-dependent histone deacetylase, human HDAC8, complexed with a hydroxamic acid inhibitor. Proc. Natl. Acad. Sci. U. S. A. 101, 15064–15069. https://doi.org/10.1073/pnas.0404603101

Vella, P., Barozzi, I., Cuomo, A., Bonaldi, T., Pasini, D., 2012. Yin Yang 1 extends the Myc-related transcription factors network in embryonic stem cells. Nucleic Acids Res. 40, 3403–3418. https://doi.org/10.1093/nar/gkr1290

Verdin, E., Dequiedt, F., Kasler, H.G., 2003. Class II histone deacetylases: Versatile regulators. Trends Genet. 19, 286–293. https://doi.org/10.1016/S0168-9525(03)00073-8

Villagra, A., Cheng, F., Wang, H.W., Suarez, I., Glozak, M., Maurin, M., Nguyen, D., Wright, K.L., Atadja, P.W., Bhalla, K., Pinilla-Ibarz, J., Seto, E., Sotomayor, E.M., 2009. The histone deacetylase HDAC11 regulates the expression of interleukin 10 and immune tolerance. Nat. Immunol. 10, 92–100. https://doi.org/10.1038/ni.1673

Walkinshaw, D.R., Weist, R., Kim, G.W., You, L., Xiao, L., Nie, J., Li, C.S., Zhao, S., Xu, M., Yang, X.J., 2013. The tumor suppressor kinase LKB1 activates the downstream kinases SIK2 and SIK3 to stimulate nuclear export of class IIa histone deacetylases. J. Biol. Chem. 288, 9345–9362. https://doi.org/10.1074/jbc.M113.456996

Wang, Z., Yu, T., Huang, P., 2016. Post-translational modifications of FOXO family proteins. Mol. Med. Rep. 14, 4931–4941. https://doi.org/10.3892/mmr.2016.5867

Weidinger, C., Shaw, P.J., Feske, S., 2013. STIM1 and STIM2-mediated Ca2+ influx regulates antitumour immunity by CD8+ T cells. EMBO Mol. Med. 5, 1311–1321. https://doi.org/10.1002/emmm.201302989

Windt, G.J.W. Van Der, Everts, B., Chang, C., Curtis, J.D., Freitas, T.C., Amiel, E., Pearce, E.J., Pearce, E.L., 2011. Mitochondrial Respiratory Capacity Is a Critical Regulator of CD8 + T Cell Memory Development. Immunity 36, 68-78. https://doi.org/10.1016/j.immuni.2011.12.007

Xu, X., Araki, K., Li, S., Han, J., Ye, L., Tan, W.G., Konieczny, B.T., Bruinsma, M.W., Martinez, J., Pearce, E.L., Green, D.R., Jones, D.P., Virgin, H.W., Ahmed, R., 2014. Autophagy is essential for effector CD8 + T cell survival and memory formation 15. https://doi.org/10.1038/ni.3025

Yang, X.J., Seto, E., 2008. The Rpd3/Hda1 family of lysine deacetylases: From bacteria and yeast to mice and men. Nat. Rev. Mol. Cell Biol. 9, 206–218. https://doi.org/10.1038/nrm2346

Yerinde, C., Siegmund, B., Glauben, R., Weidinger, C., 2019. Metabolic Control of Epigenetics and Its Role in CD8 + T Cell Differentiation and Function. Front. Immunol. 10, 1–9. https://doi.org/10.3389/fimmu.2019.02718

Yeromin, A. V, Zhang, S.L., Jiang, W., Yu, Y., Safrina, O., Cahalan, M.D., 2006. Molecular identification of the CRAC channel by altered ion selectivity in a mutant of Orai. Nature 443, 2–5. https://doi.org/10.1038/nature05108

Youn, H., Jun, O.L., 2000. Cabin1 Represses MEF2 -Dependent Nur 77 Expression and T Cell Apoptosis by Controlling Association of Histone Deacetylases and Acetylases with MEF2. Immunity 13, 85–94. https://doi: 10.1016/s1074-7613(00)00010-8

Youn, H.-D., 2000. Integration of calcineurin and MEF2 signals by the coactivator p300 during T-cell apoptosis. EMBO J. 15, 4323-4331. https://doi.org/10.1093/emboj/19.16.4323

Youn, H.D., Grozinger, C.M., Liu, J.O., 2000. Calcium regulates transcriptional repression of myocyte enhancer factor 2 by histone deacetylase 4. J. Biol. Chem. 275, 22563–22567. https://doi.org/10.1074/jbc.C000304200

Zhang, C.L., McKinsey, T.A., Lu, J.R., Olson, E.N., 2001. Association of COOH-terminal-binding protein (CtBP) and MEF2-interacting transcription repressor (MITR) contributes to transcriptional repression of the MEF2 transcription factor. J. Biol. Chem. 276, 35–39. https://doi.org/10.1074/jbc.M007364200

Zhang, L., Jin, M., Margariti, A., Wang, G., Luo, Z., Zampetaki, A., Zeng, L., Ye, S., Zhu, J., Xiao, Q., 2010. Sp1-dependent activation of HDAC7 is required for platelet-derived growth factor-BB-induced smooth muscle cell differentiation from stem cells. J. Biol. Chem. 285, 38463–38472. https://doi.org/10.1074/jbc.M110.153999

Zhang, Ozawa, Lee, Wen, Tan, Wadzinski, Seto, 2005. Is Regulated By Interaction With Protein Serine / Threonine Phosphatase 4. Genes Dev. 3, 827–839. https://doi.org/10.1101/gad.1286005.HDAC3

Zhang, Z., Liu, S., Zhang, B., Qiao, L., Zhang, Y., Zhang, Y., 2020. T Cell Dysfunction and Exhaustion in Cancer. Front. Cell Dev. Biol. 8, 1–13. https://doi.org/10.3389/fcell.2020.00017

References

Zhao, M., New, L., Kravchenko, V. V, Kato, Y., Gram, H., Padova, F.D.I., Olson, E.N., Ulevitch, R.J., Han, J., 1999. Regulation of the MEF2 Family of Transcription Factors by p38. Mol. Cell Biol. 19, 21–30. https://doi: 10.1128/mcb.19.1.21.

Zhao, X., Sternsdorf, T., Bolger, T.A., Evans, R.M., Yao, T.-P., 2005. Regulation of MEF2 by Histone Deacetylase 4- and SIRT1 Deacetylase-Mediated Lysine Modifications. Mol. Cell. Biol. 25, 8456–8464. https://doi.org/10.1128/mcb.25.19.8456-8464.2005

Zhou, B., Margariti, A., Zeng, L., Habi, O., Xiao, Q., Martin, D., Wang, G., Hu, Y., Wang, X., Xu, Q., 2011. Splicing of histone deacetylase 7 modulates smooth muscle cell proliferation and neointima formation through nuclear β-catenin translocation. Arterioscler. Thromb. Vasc. Biol. 31, 2676–2684. https://doi.org/10.1161/ATVBAHA.111.230888

Zhu, J., Petit, P.F., Van den Eynde, B.J., 2019. Apoptosis of tumor-infiltrating T lymphocytes: a new immune checkpoint mechanism. Cancer Immunol. Immunother. 68, 835–847. https://doi.org/10.1007/s00262-018-2269-y

Zhuang, S., 2013. Regulation of STAT signaling by acetylation. Cell. Signal. 25, 1924–1931. https://doi.org/10.1016/j.cellsig.2013.05.007

Zoncu, R., Efeyan, A., Sabatini, D.M., 2011. mTOR: from growth signal integration to cancer, diabetes and ageing. Nat. Rev. Mol. Cell Biol. 12, 7–12. https://doi.org/10.1038/nrm3025

7 APPENDIX

7.1 List of abbreviations

2-DG	2-deoxy-D-glucose
acetyl-CoA	acetyl-coenzyme A
AICD	activation-induced cell death
AP	alkaline phosphatase
APS	ammonium persulfate
ATP	adenosine triphosphate
Bcl-2	B-cell lymphoma-2
BCR	B cell receptor
BSA	bovine serum albumin
CABIN1	calcineurin binding protein 1
CaMk	calcium/calmodulin-dependent kinase
CAR T-cell	chimeric-antigen receptor-engineered T cell
CCR	CC-chemokine receptor
CFSE	carboxyfluorescein diacetate succinimidyl ester
ChIP	chromatin immunoprecipitation
CHK1	checkpoint kinase-1
CK2	casein kinase 2
CMV	cytomegalovirus
Co-IP	Co-immunoprecipitation
CoREST	corepressor of RE-1 silencing transcription factor
CPT1A	carnitine palmitoyltransferase 1a
CRAC	calcium release-activated channels
CRM1	chromosomal maintenance 1

CtBP	C-terminal binding protein 1
CTL	cytotoxic T lymphocyte
CTLA-4	cytotoxic T-lymphocyte associated protein 4
CXCL	C-X-C chemokine motif ligand
DAB	diaminobenzidine
DCs	dendritic cells
DKO	double knockout
DMSO	dimethyl sulfoxide
EBV	Epstein Barr virus
ECAR	extracellular acidification rate
EDTA	ethylenediamine tetraacetic acid
EM	effector memory
EMSA	electro mobility shift assay
Eomes	Eomesodermin
ER	endoplasmic reticulum
FAK	focal adhesion kinase
FAO	fatty acid oxidation
FCCP	fluorocarbonyl cyanide phenylhydrazone
FCS	fetal bovine serum
FOS	fos proto proto-oncogene
FOXO	forkhead box
GNAT	GCN5-related N-acetyltransferases
GvHD	graft-versus-host disease
GWAS	genome genome-wide association studies
h	hour

Appendix

HAT	histone acetyltransferase
HDAC	histone deacetylase
HDAC7-ΔP	triple mutant HDAC7-ΔP
HDACi	histone deacetylase inhibitor
HIV	human immunodeficiency virus
HP1	heterochromatin protein 1
hpf	high power field
HRP	horseradish peroxidase
HSP90	heat shock protein 90
i.d.	intradermal
i.v.	intravenous
IBD	inflammatory bowel disease
IFNγ	interferon γ
IL	interleukin
$InsP_3$	inositol-1-4-5-triphosphate
JUN	Jun proto proto-oncogene
KAT13D	circadian locomotor output cycles protein kaput CLOCK
$KLRG1^+$	killer cell lectin-like receptor subfamily G member 1
Lag-3	lymphocyte-activation gene 3
LCMV	lymphocytic choriomeningitis virus
LPS	lipopolysaccharide
MACS	magnetic-activated cell sorting
MAP	microtubule associated protein
MAPK	mitogen-activated protein kinase
MARK	MAP-microtubule affinity regulating kinase

MAX	Myc-associated factor X
MDSC	myeloid-derived suppressor cells
MEF2	myocyte enhancer factor 2
MFI	mean fluorescence intensity
MHC	major histocompatibility complex
MHC I	major histocompatibility complex class I
MHC II	major histocompatibility complex class II
min	minutes
MMP-9	matrix metalloproteinase 9
Mtb	*Mycobacterium tuberculosis*
mTOR	mammalian target of rapamycin
MYC	Myc proto proto-oncogene
MYPT	myosin phosphatase targeting protein
MYST	MOZ, Ybf2, Sas2 and Tip60
NCoA-1	nuclear receptor coactivator 1
NCoA-1	nuclear receptor coactivator 1
NF-κB	nuclear factor-κB
NFAT	nuclear factor of activated T-cells
NK	natural killer
NKT cells	natural killer T cells
NuRD	nucleosome remodeling deacetylase
OCR	cellular oxygen consumption rate
ORAI	Orai1 calcium release-activated calcium modulator 1
Ova	ovalbumin
P-TEFb	positive transcription elongation factor b

p300/CBP	p300/CREB binding protein
PBS	phosphate-buffered-saline
PCR	polymerase chain reaction
PD-1	programmed cell death protein 1
PDGF-BB	platelet platelet-defined growth factor BB monomer
PI	propidium iodide
PKA	protein kinase A
PKD	protein kinase D
PMA	phorbol myristate acetate
PP1	protein phosphatase 1
PP2A	protein phosphatase 2A
PSA	psoriatic arthritis
PSC	primary sclerosing cholangitis
PVDF	polyvinylidene fluoride
qPCR	quantitative polymerase chain reaction
Rheb	Ras homolog enriched in brain
RIPA	radioimmunoprecipitation assay
RotA/AA	rotenone/antimycin A
SAHA	suberoylanilide hydroxamic acid
scRNA-seq	single cell RNA sequencing
SDS	sodium dodecyl sulphate
SERCA	sarco/endoplasmic reticulum Ca^{+2}-ATPase
SIK	salt-inducible kinases
Sir	silent information regulator
siRNA	small interfering RNA

SLE	systemic lupus erythematosus
SOCE	Store-Operated Calcium Entry
Sp	specificity protein
SPF	specific pathogen free
STAT	signal transducer and activator of transcription
STIM	stromal interaction molecule
TAA	tumor-associated antigens
TAFII250	TBF associated factor 250 kd
TBS	Tris-buffered saline
TBST	Tris-buffered saline with tween20
TCA	tricarboxylic acid
T_{CM}	central memory T cells
TCR	T cell receptor
TDLN	tumor draining lymph nodes
T_E	effector T cells
T_{EM}	effector memory T cells
TEMED	tetramethylethylene-diamine
TGF-β	transforming growth factor β
Tigit	T cell immunoreceptor with Ig and ITIM domain
TIL	tumor infiltrating lymphocytes
Tim-3	T cell immunoglobulin and mucin domain-containing-3
TLS	tertiary lymphoid structures
T_{mem}	long-lived memory T cells
T_N	naïve T cells
TNF α	tumor necrosis factor α

Treg	regulatory T cells
TSA	trichostatin A
TSC2	tuberous sclerosis 2
UMAP	uniform manifold approximation and projection
UPS	ubiquitin proteasome system
wt	wild type
YY1	yin and yang 1
ZnF	Zn-finger binding domain
αTAT1	α-tubulin acetyltransferase

7.2 Summary

$CD8^+$ T cells represent an essential component of anti-tumor immune responses by mediating direct cytotoxicity against neoplastic cells as well as by providing immunological memory. The activation of $CD8^+$ T cells by tumor-specific or tumor-associated antigens results in their rapid expansion and differentiation into effector cytotoxic cells (CTL). Once target tumor cells are eradicated, the population of effector CTLs contracts and leaves behind a small population of long-lived memory cells. However, the immunosuppressive nature of the tumor microenvironment and sustained antigen exposure commonly drive tumor-infiltrating CTLs into a hypo-responsive and so called "exhausted" state which is characterized by defective cytotoxicity and impaired production of anti-neoplastic cytokines such as TNFα and IFNγ. This exhausted phenotype of tumor-specific $CD8^+$ T cells is furthermore marked by an increased expression of co-inhibitory molecules such as PD-1 and Tim-3, which deter the activation and function of $CD8^+$ T cells contributing to the immune evasion of tumor cells. The exhaustion of tumor-specific T cells thereby not only affects endogenous $CD8^+$ T cells but also compromises the success of immunotherapies such as the adoptive transfer of $CD8^+$ T cell or CAR T cell therapies as transferred T cells become frequently exhausted and dysfunctional. Therefore, it is crucial to better understand the molecular regulators of $CD8^+$ T cell function and exhaustion to overcome the limitations of current $CD8^+$ T cell-based immunotherapies. Similarly, we believe that a better characterization of new molecular regulators of $CD8^+$ T cell exhaustion will allow to develop more potent immunotherapies against human tumors that are so far not sufficiently treated by current adoptive T cell therapies.

HDACs are among the key epigenetic orchestrators of gene regulation. They catalyze the removal of acetyl groups from histone tails resulting in chromatin condensation and suppression of gene expression. As a class IIa HDAC, HDAC7 can shuttle from the nucleus to the cytoplasm depending on its phosphorylation status. Therefore, HDAC7 represents a regulator of both nuclear and cytoplasmic proteins with diverse functions and HDAC7 was found to play a critical role during the thymic development of T cells by regulating T cell apoptosis and their positive selection. Although the role of HDAC7 in T cell development is well understood, very little is known about its role in peripheral adult T cells, especially in the context of anti-tumor immunity. In this PhD project, we hypothesized that HDAC7 might also play a central role during $CD8^+$ T cell-mediated anti-tumor responses of $CD8^+$ T cells, in which

sustained exposure of $CD8^+$ T cells to TAA and TSA hamper the metabolic fitness and the functional capacity of $CD8^+$ T cells.

To investigate the role of HDAC7 in the anti-tumor immune responses of $CD8^+$ T cells, we used conditional mouse models with T cell specific deletion of *Hdac7*. In line with the previous findings from our group, we could show that *HDAC7$^{fl/fl}$E8I-Cre* mice display a pre-activated phenotype as there is a significant reduction in the frequency of naïve $CD8^+$ T cells compared to wild type (wt) littermates. We also observed that HDAC7 is the main class II HDAC expressed in $CD8^+$ T cells during their *in vitro* differentiation into CTL. In addition, the deletion of *Hdac7* in $CD8^+$ T cells led to a growth defect *in vitro* due to increased apoptosis. We showed that the increased apoptosis in *Hdac7*-deficient $CD8^+$ T cells was at least partially caused by increased MEF2D-driven FasL expression. Moreover, $CD8^+$ T cells lacking HDAC7 displayed deterred calcium homeostasis, mTOR signaling as well as augmented amino acid metabolism suggesting that they have an impaired anti-tumor immune response. Indeed, *Hdac7$^{fl/fl}$CD4-Cre* and *HDAC7$^{fl/fl}$E8I-Cre* mice could not control tumor growth upon challenge with lymphoma cells supporting that HDAC7 is a crucial factor for the proper anti-tumor immune functions of $CD8^+$ T cells. Moreover, tumors from *Hdac7$^{fl/fl}$CD4-Cre* mice had reduced infiltration of $CD8^+$ T cells which resulted from an impaired expansion of $CD8^+$ T cells *in vivo*, but not from a homing defect as assessed by adoptive T cell transfer experiments in mice. Interestingly, the adoptive transfer of *in vitro* differentiated tumor-antigen-specific CTLs could rescue the phenotype of *Hdac7$^{fl/fl}$CD4-Cre* mice. Furthermore, tumor infiltrating *Hdac7*-deficient CTLs had elevated frequency of $PD1^+Tim3^+$ population pointing to a role of HDAC7 in the exhaustion of $CD8^+$ T cells during chronic antigen exposure. Additionally, the analysis of our RNA-seq data, published scRNA-seq data as well as *in vitro* T cell exhaustion models that we have established confirmed the role of HDAC7 in the exhaustion of $CD8^+$ T cells.

In summary, we here identified HDAC7 as a key regulator of $CD8^+$ T cell-based anti-tumor immune responses since the lack of *Hdac7* impaired the survival, metabolism as well as the fitness of $CD8^+$ T cells by increased exhaustion within the immunosuppressive tumor microenvironment. We propose that our findings are not only clinically relevant to highlight the possible side effects of HDAC inhibitors, but are also important for the design and the development of novel HDAC inhibitors to treat inflammatory and neoplastic diseases.

7.3 Zusammenfassung

$CD8^+$ T-Zellen stellen eine essentielle Komponente der anti-Tumor-Immunantwort dar, indem sie sowohl direkte Zytotoxizität gegen neoplastische Zellen vermitteln, als auch ein immunologisches Gedächtnis bereitstellen. Die Aktivierung von $CD8^+$ T-Zellen durch tumorspezifische oder tumorassoziierte Antigene führt zu ihrer schnellen Expansion und Differenzierung in zytotoxische Effektorzellen (CTL). Sobald die Zieltumorzellen eliminiert sind, verkleinert sich die Population der Effektor-CTLs und hinterlässt eine kleine Population von langlebigen Gedächtniszellen. Die immunsuppressive Natur des Tumormilieus und die anhaltende Antigenexposition treiben die tumorinfiltrierenden CTLs jedoch häufig in einen hyporesponsiven und so genannten "erschöpften" Zustand, der durch defekte Zytotoxizität und beeinträchtigte Produktion von anti-neoplastischen Zytokinen wie TNFα und IFNγ gekennzeichnet ist. Dieser erschöpfte Phänotyp tumorspezifischer $CD8^+$ T-Zellen ist darüber hinaus durch eine erhöhte Expression ko-inhibitorischer Moleküle wie PD-1 und Tim-3 gekennzeichnet, die die Aktivierung und Funktion von $CD8^+$ T-Zellen verhindern und so zur Immunevasion von Tumorzellen beitragen. Die Erschöpfung tumorspezifischer T-Zellen beeinträchtigt dabei nicht nur die endogenen $CD8^+$ T-Zellen, sondern gefährdet auch den Erfolg von Immuntherapien wie dem adoptiven Transfer von $CD8^+$ T-Zellen oder CAR T-Zell-Therapien, da übertragene T-Zellen häufig erschöpft und dysfunktional werden. Daher ist es von entscheidender Bedeutung, die molekularen Regulatoren der $CD8^+$ T-Zell-Funktion und -Erschöpfung besser zu verstehen, um die Grenzen der derzeitigen $CD8^+$ T-Zell-basierten Immuntherapien zu überwinden. Daher kann nur eine bessere Charakterisierung neuer molekularer Regulatoren der $CD8^+$ T-Zell-Erschöpfung die Entwicklung potenterer Immuntherapien gegen humane Tumore ermöglichen, die bisher durch aktuelle adoptive T-Zell-Therapien nicht ausreichend behandelt werden.

Histondeacetylasen (HDAC) nehmen eine zentrale Funktion in der epigenetischen Genregulation ein. Sie katalysieren die Entfernung von Acetylgruppen von Histonen, was zur Chromatinkondensation und Unterdrückung der Genexpression führt. Als Klasse-IIa-HDAC kann HDAC7 je nach Phosphorylierungsstatus vom Zellkern ins Zytoplasma wandern. Daher stellt HDAC7 einen Regulator von sowohl nukleären als auch zytoplasmatischen Proteinen mit vielfältigen Funktionen dar. Es wurde festgestellt, dass HDAC7 eine kritische Rolle während der thymischen Entwicklung von T-Zellen spielt, indem es die Apoptose von T-Zellen und

deren positive Selektion reguliert. Obwohl die Rolle von HDAC7 in der T-Zell-Entwicklung gut verstanden ist, ist sehr wenig über seine Rolle in peripheren adulten T-Zellen bekannt, insbesondere im Kontext der anti-Tumor-Immunität. In diesem Promotionsprojekt stellten wir die Hypothese auf, dass HDAC7 eine zentrale Rolle während der $CD8^+$ T-Zell-vermittelten anti-Tumor-Antwort spielen könnte, bei der eine anhaltende Exposition von $CD8^+$ T-Zellen gegenüber Tumor-assoziierten Antigenen und Trichostatin A die metabolische Fitness und die funktionelle Kapazität von $CD8^+$ T-Zellen beeinträchtigt.

Um die Rolle von HDAC7 bei der anti-Tumor-Immunantwort von $CD8^+$ T-Zellen zu untersuchen, haben wir konditionale Mausmodelle mit T-Zell-spezifischer Deletion von HDAC7 verwendet. In Übereinstimmung mit den früheren Ergebnissen unserer Gruppe konnten wir zeigen, dass $HDAC7^{fl/flE8I\text{-}Cre}$-Mäuse einen voraktivierten Phänotyp aufweisen, da die Häufigkeit naiver $CD8^+$ T-Zellen im Vergleich zu Wildtypmäusen aus demselben Wurf signifikant reduziert ist. Wir beobachteten auch, dass HDAC7 die wichtigste Klasse-II-HDAC ist, die in $CD8^+$ T-Zellen während ihrer *in vitro*-Differenzierung zu CTL exprimiert wird, und dass die Deletion von HDAC7 in $CD8^+$ T-Zellen zu einem Wachstumsdefekt *in vitro* aufgrund von erhöhter Apoptose führt. Wir konnten zeigen, dass die erhöhte Apoptose in HDAC7-defizienten $CD8^+$ T-Zellen zumindest teilweise durch eine erhöhte MEF2D-getriebene FasL-Expression verursacht wurde. Darüber hinaus zeigten $CD8^+$ T-Zellen, denen HDAC7 fehlte sowohl eine gestörte Kalzium-Homöostase als auch mTOR-Signalweg sowie einen erhöhten Aminosäuren-Stoffwechsel, was darauf hindeutet, dass sie eine beeinträchtigte anti-Tumor-Immunantwort haben könnten. Tatsächlich konnten $Hdac7^{fl/flCD4\text{-}Cre}$- und $HDAC7^{fl/flE8I\text{-}Cre}$-Mäuse das Tumorwachstum nach einer Provokation mit Lymphomzellen nicht kontrollieren, was darauf hindeutet, dass HDAC7 ein entscheidender Faktor für die effektive anti-Tumor-Immunfunktionen von $CD8^+$ T-Zellen ist. Darüber hinaus wiesen Tumore von $Hdac7^{fl/flCD4\text{-}Cre}$-Mäusen eine reduzierte Infiltration von $CD8^+$ T-Zellen auf, was aus einer beeinträchtigten Expansion von $CD8^+$ T-Zellen *in vivo* resultierte, aber nicht aus einem Homing-Defekt, wie durch adoptive T-Zell-Transfer-Experimente in Mäusen festgestellt wurde. Interessanterweise konnte der adoptive Transfer von *in vitro* differenzierten tumorantigenspezifischen CTLs den Phänotyp von $Hdac7^{fl/flCD4\text{-}Cre}$-Mäusen retten. Darüber hinaus wiesen tumorinfiltrierende HDAC7-defiziente CTLs eine erhöhte Frequenz von $PD\text{-}1^+Tim\text{-}3^+$-Populationen auf, was auf eine Rolle von HDAC7 bei der Erschöpfung von $CD8^+$

T-Zellen während chronischer Antigenexposition hinweist. Darüber hinaus bestätigte die Analyse unserer RNA-seq-Daten, publizierte scRNA-seq-Daten sowie die von uns etablierten *in vitro* T-Zell-Erschöpfungsmodelle die Rolle von HDAC7 bei der Erschöpfung von $CD8^+$ T-Zellen.

Zusammenfassend haben wir hier HDAC7 als einen Schlüsselregulator von $CD8^+$ T-Zell-basierten anti-Tumor-Immunantworten identifiziert, da das Fehlen von HDAC7 das Überleben, den Stoffwechsel sowie die Fitness von $CD8^+$ T-Zellen beeinträchtigt. Wir schlagen vor, dass unsere Ergebnisse nicht nur klinisch relevant sind, da sie auf mögliche Nebenwirkungen von HDAC-Inhibitoren hinweisen, sondern auch wichtig für die Entwicklung von neuartigen HDAC-Inhibitoren zur Behandlung von entzündlichen und neoplastischen Erkrankungen.

7.4 Acknowledgements

First and foremost, I would like to thank my first supervisor Britta Siegmund for her continuous support during my PhD. She enabled me to follow my research interests by providing space in her lab and funding as well as supporting my attendance to international conferences to expand my scientific knowledge and network. I am grateful for the valuable discussions and her incredible support during the writing process of my doctoral thesis.

I would like to thank Gerhard Wolber for reviewing my thesis as well as his support during my university enrollment.

I cannot describe how thankful I am to Carl Weidinger, who closely supervised me during my PhD. I was always inspired by his never-ending enthusiasm and motivation. He was always there when I needed both technical and personal help. I am thankful to him for always believing in me and supporting me under every circumstance. He enabled me to develop as an independent researcher and to meet the exciting field of tumor immunology. His door has always been open to me whenever I needed help. I am grateful for the long discussions and new ideas. This PhD project would not be possible without him.

I am thankful to Rainer Glauben for his continuous support during my PhD. He always helped me with his deep knowledge of histone deacetylases. Besides my PhD, I appreciate his support for my personal life, establishing a life in Berlin and to get accustomed to German culture.

I am grateful to Gerald Willimsky for being a member of my committee in the graduate school. His valuable discussions and suggestions helped improving the quality of my research.

I have always been proud to be a member of Berlin School of Integrative Oncology (BSIO). I would like to thank BSIO and all scientific coordinators for giving me the chance to attend incredible lectures as well as for their financial support. During the final year of my PhD, I have been supported by Ruth Jeschke Scholarship for Tumor Immunology and Molecular Oncology. Thanks to scholarship commission for considering my scholarship application and their financial support. I was honored by their positive evaluation of my doctoral work.

I would like to thank Benedikt Obermayer for the analysis of published scRNA-seq data and his patience for answering my naïve questions related to the bioinformatic analysis that he performed.

I would like to express my deep gratitude to all past and current members of AG Siegmund for their warm friendship and creating a nice and collaborative working environment. I am thankful to Inka Freise for her incredible technical help. She has been always next door and had the patience to answer even the simplest questions that I had. I would like to thank Hsiang-Jung Hsiao for her technical help and inspiring discussions. Thanks to Adrian Huck for the bioinformatic analysis of my data. I am thankful to Jacqueline Keye since her PhD studies shaped my research interest and helped me to understand my data better. Thanks to Hao Wu for teaching me metabolic assays and his help during mouse experiments as well as the discussion of my data. Franziska Schmidt and Yasmina Rodriguez Sillke were very kind to teach me flow cytometry. I am also thankful to Marilena Letizia, Lorenz Gerbeth, Sophiya Siddiqui, Julia Hecker and Laura Golusda for their technical support, discussions as well as friendship. I am thankful to Annegret Sand and Anne-Kristin Fritsche for giving me the opportunity to supervise them. It was an honor to work closely with them.

My deepest thank and gratitude go to my husband Ahmet Bugra Tufan for his endless support and love before and during my PhD. I feel so lucky to have him in my life. He always believed in and encouraged me in every aspect of my life. He also contributed to my PhD project by his ideas, criticism, discussions as well as his technical help. Thanks to him from the bottom of my heart for establishing a life together in Berlin and being a family to me.

Finally, I owe my deepest gratitude to my family for their support and endless love throughout my life. My parents Ali Kaya Yerinde and Hakime Yerinde and my brothers Caner Yerinde and Cüneyt Yerinde always believed in me and supported every decision of me during both my education and personal life. Since my childhood, they always respected my scientific curiosity and supported me for becoming a well-educated independent woman despite all cultural circumstances. I would like to thank my little niece and nephew Defne and Yagiz Yerinde for bringing joy to my life and reducing my stress during my PhD life. Thanks to my mother- and father-in law Fatma Tufan and Mehmet Emin Tufan for being a second family to me and their endless support in every part of my life.

7.5 Selbständigkeitserklärung

Hiermit erkläre ich, dass ich diese Arbeit selbständig verfasst habe und keine anderen als die angegebenen Quellen und Hilfsmittel in Anspruch genommen habe. Ich versichere, dass diese Arbeit in dieser oder anderer Form keiner anderen Prüfungsbehörde vorgelegt wurde.

Cansu Yerinde Berlin, April 2021

7.6 Publications

Parts of this thesis will be published in:

HDAC7 controls anti-viral and anti-tumor immunity by CD8$^+$ T cells
Cansu Yerinde$^{\#}$, Jacqueline Keye$^{\#}$, Sibel Durlanik, Inka Freise, Franziska Schmidt, Stephan Schlickeiser, Marie Friedrich, Hao Wu, Désirée Kunkel, Anja A. Kühl, Sebastian Bauer, Andreas Thiel, Britta Siegmund, Rainer Glauben$^{\#}$ and Carl Weidinger$^{\#}$, $^{\#}$equal contribution, under preparation

Other publications during the period of the thesis:

Yerinde C, Siegmund B, Glauben R$^{\#}$ and Weidinger C.$^{\#}$, $^{\#}$equal contribution
Metabolic control of epigenetics and its role in CD8$^+$ T cell differentiation and functions. 2019 *Front. Immunol.* 10, 2718. https://doi.org/10.3389/fimmu.2019.02718.

Ziegler JF$^{\#}$, Böttcher C$^{\#}$, Letizia M, **Yerinde C**, Wu H, Freise I, Rodriguez-Sillke Y, Stoyanova AK, Kreis ME, Asbach P, Kunkel D, Priller J, Anagnostopoulos I, Kühl AA, Miehle K, Stumvoll M, Tran F, Fredrich B, Forster M, Franke A, Bojarski C, Glauben R, Löscher BS, Siegmund B$^{\#}$, Weidinger C$^{\#}$. $^{\#}$equal contribution. **Leptin induces TNFα-dependent inflammation in acquired generalized lipodystrophy and combined Crohn's disease**. 2019 *Nat. Commun.* 10, 5629. https://doi.org/10.1038/s41467-019-13559-7.

Wu H, Weidinger C, Schmidt F, Keye J, Friedrich M, **Yerinde C**, Willimsky G, Qin Z, Siegmund B, Glauben R. **Oleate but not stearate induces the regulatory phenotype of myeloid suppressor cells**. 2017 *Sci. Rep.* 8, 7498. https://doi.org/10.1038/s411598-017-07685-9.

Khalil M, Alliger K, Weidinger C, **Yerinde** C, Wirtz S, Becker C, & Engel, MA **Functional Role of Transient Receptor Potential Channels in Immune Cells and Epithelia**. 2018 *Front. Immunol. 9*, 174. https://doi.org/10.3389/fimmu.2018.00174

7.8 Conference presentations during the period of the thesis

2020 Poster presentation, Cold Spring Harbor Meeting on "The Gene Expression and Signaling in the Immune System", New York, The USA (poster title: HDAC7 controls anti-viral and anti-tumor immunity by $CD8^+$ T cells)

2019 Oral presentation, II Joint Meeting of the German Society of Immunology (DGFI) and the Italian Society of Immunology, Clinical Immunology and Allergology (SIICA), Munich, Germany (title: HDAC7 controls anti-viral and anti-tumor immunity by $CD8^+$ T cells)

2019 Oral presentation, "Learning from the Yins and Yangs of Cancer", International Conference organized by the Molecular Cancer Research Center (MKFZ) at the Charité and Berlin School of Integrative Oncology (BSIO), Berlin, Germany (Title: HDAC7 controls anti-viral and anti-tumor immunity by $CD8^+$ T cells)

2019 Poster presentation, Keystone Symposia, Uncovering Mechanisms of Immune Based Therapy in Cancer and Autoimmunity, Colorado, The USA (Title: HDAC7 controls anti-viral and anti-tumor immunity by $CD8^+$ T cells)

2018 Oral presentation, European Congress of Immunology (ECI) 2018, Amsterdam, the Netherlands (Title: HDAC7 controls anti-viral and anti-tumor immunity by $CD8^+$ T cells)

7.9 Curriculum Vitae

For reasons of data protection, the curriculum vitae is not published in the electronic version.

Appendix

For reasons of data protection, the curriculum vitae is not published in the electronic version.